Different treatment approaches to infectious diseases: from novel antimicrobials to T-cell therapy

Inauguraldissertation

zur

Erlangung der Würde eines Doktors der Philosophie

vorgelegt der

Philosophisch-Naturwissenschaftlichen Fakultät

der Universität Basel

von

Justyna Nowakowska

aus Łęki, Poland

Basel, 2015

Genehmigt von der Philosophisch-Naturwissenschaftlichen Fakultät
auf Antrag von

Prof. Dr. Urs Jenal
PD Dr. Nina Khanna
Prof. Dr. Daniela Finke

Basel, den 24.06.2014

Prof. Dr. Jörg Schibler
Dekan

Part I

Table of Content

Abbreviations

ADEP4	acyldepsipeptide 4
agr	accessory gene regulator
AIPs	autoactivating peptides
AMPs	antimicrobial peptides
C3b	complement component 3b
CA-MRSA	community-associated MRSA
CCMX	Competence Centre for Materials Science and Technology
CHIPS	chemotaxis inhibitory protein of staphylococci
CoNS	coagulase negative staphylococcus
CRISPR	clustered regularly interspaced short palindromic repeats
CV	crystal violet
DNA	deoxyribonucleic acid
DspB	Dispersin B
eDNA	extracellular DNA
ELISA	enzyme-linked immunosorbent assay
EN4	8-hydroxyserrulat-14-en-19-oic aci
EPFL	École polytechnique fédérale de Lausanne
EPS	extracellular polymeric substances
ETH	Eidgenössische Technische Hochschule
GlcNAc	*N*-acetylglucosamine
HA-MRSA	hospital-associated MRSA
IAI	implant-associated infections
IgG	immunoglobulin G
MBC	minimal bactericidal concentration
MIC	minimal inhibitory concentration
MRSA	methicillin-resistant *Staphylococcus aureus*
MSCRAMMs	microbial surface components recognising adhesive matrix molecules
MSSA	methicillin-sensitive *Staphylococcus aureus*
PBPs	penicillin-binding proteins

PEG	poly(ethylene glycol)
PEGMA	poly(poly(ethylene glycol) methacrylate
PHEMA	poly(2-hydroxyethyl methacrylate)
PIA	polysaccharide intercellular adhesin
PMNs	polymorphonuclear cells
PMOXA	poly-2-methyl-2-oxazoline
PNAG	poly-N-acetylglucosamine
PSMs	phenol-soluble modulins
PVL	Panton-Valentine leukocidin
QS	quorum sensing
RGD	arginine-glycine-aspartic acid
rhDNAse I	recombinant human deoxyribonuclease I
RNA	ribonucleic acid
SarA	staphylococcal accessory regulator A
SCIN	staphylococcal complement inhibitor
SCC*mec*	staphylococcal cassette chromosome *mec*
Si	silicone
Vanco	vancomycin
VISA	vancomycin-intermediate *Staphylococcus aureus*
VISE	vancomycin-intermediate *Staphylococcus epidermidis*
VRSA	vancomycin-resistant *Staphylococcus aureus*

Units:

CFU	colony-forming units
cm^2	square centimeter
h	hour
min	minute
ml	milliliter
µg	microgram
ng	nanogram

Summary

The antibiotic tolerance of biofilms and the acquisition of bacterial resistance to virtually all antibiotics highlight the need to develop novel antimicrobials [1,2]. While traditional drug design methods mainly target rapidly growing planktonic bacteria, anti-biofilm antimicrobials have to be selected based on their activity against biofilm-embedded sessile microorganisms [3,4].

This study reports on the activity of EN4 (8-hydroxyserrulat-14-en-19-oic acid), a compound derived from *Eremophila* (Myoporaceae) plant species, for its possible application in implant-associated infections (IAI). IAI are mainly caused by biofilm-forming staphylococci, which hinders treatment using traditional antibiotics [5]. EN4 acts against a variety of Gram-positive bacteria and *Mycobacterium tuberculosis*, but not against Gram-negative microorganisms. Its efficacy is similar against methicillin-susceptible and -resistant *Staphylococcus* (*S.*) *aureus* (MSSA and MRSA, respectively). The minimal inhibitory concentrations (MICs) of EN4 for logarithmic-phase *S. aureus* and *S. epidermidis* are 25 µg/ml and 50 µg/ml and the minimal bactericidal concentrations (MBCs) 50 µg/ml and 100 µg/ml, respectively. EN4 shows rapid and concentration-dependent killing of staphylococci, reducing bacterial counts by > 3 $\log_{10}$ colony-forming units (CFU)/ml within 5 min at concentrations above 50 µg/ml. Additionally, EN4 is bactericidal against stationary-phase and adherent staphylococci independently of polysaccharide intercellular adhesin (PIA)-mediated biofilm. The antimicrobial activity of EN4 comprises a general inhibition of macromolecular biosynthesis and membranolytic properties. Consistently with the membrane-targeted activity, *Pseudomonas aeruginosa* turns susceptible to EN4 upon destabilisation of the outer membrane. Cytotoxicity of EN4 on mouse fibroblasts is time- and concentration-dependent in the range of MBCs suggesting a narrow therapeutic window. In *vivo* in a mouse tissue cage model EN4 showed neither bactericidal nor cytotoxic effect. This *in vivo* inhibition was caused by interaction with albumin. These findings suggest that upon structural changes EN4 might serve as a pharmacophore for the future development of new antimicrobials.

The problems associated with the therapy of IAI have prompted many studies on engineering implant surfaces that could resist microbial colonisation [6]. Within this project the antiadhesive and antibacterial properties of surfaces coated with poly-2-methyl-2-oxazoline (PMOXA), poly(2-hydroxyethyl methacrylate) (PHEMA) and poly(poly(ethylene glycol) methacrylate (PEGMA) were evaluated. These polymer brushes were further covalently functionalised with vancomycin. Vancomycin, a cell wall active antibiotic, was used as it has previously been shown to be effective when covalently coupled [7-9]. Employing various methods, a great nonfouling potential of the coatings against biofilm-forming *S. epidermidis* 1457 was shown. However, the antibacterial effect of covalently coupled vancomycin was not observed, even for *Bacillus subtillis* 6633, which is characterised by a higher susceptibility to vancomycin. The determination of surface concentration of the antibiotic revealed less than 0.02 ng vancomycin per 1 cm^2, which is below the assessed minimal killing concentration range (500 ng to 1 000 ng/1 cm^2). Moreover, assessment of in-solution activity of vancomycin-PMOXA construct pointed toward a decrease in the antimicrobial properties of the antibiotic, especially when the amine group was involved in binding. Altogether, the investigated PMOXA, PHEMA and PEGMA-based surface coatings exhibit great antiadhesive properties. However, covalent functionalisation with vancomycin did not confer antimicrobial properties to the polymers due to decreased activity and too low surface concentration of the antibiotic.

Introduction

Implant-associated infections

Background

Implanted medical devices are characterised by an inherent propensity to microbial colonisation [10]. Despite the progress in understanding the pathogenesis of implant-associated infections (IAI) and applied prophylactic and pre-emptive measures the overall rate of IAI ranges between 0.5% to 40%. These infections result in major morbidity and lead to enormous healthcare costs [11,12].

Inoculation with microorganisms can occur either perioperatively or by haematogenous seeding through blood or lymph [13]. Staphyloccoci, including *Staphylococcus* (*S.*) *aureus* and *S. epidermidis,* account for the leading etiologic agents of IAI (more than 50% of prosthetic joint infections) followed by streptococci (9%) and Gram-negative bacilli (6%) [5]. High prevalence of staphylococci in IAI is caused by their presence on human skin and mucosal surfaces, which predispose to contamination, as well as by the staphylococcal ability to form biofilm [14]. Biofilm determines the persistent character of IAI, inducing tolerance to antibiotics and rendering the host immune response inefficient in coping with infection [5,6,15-18]. Moreover, although the prevalence of methicillin-resistant *S. aureus* (MRSA) in clinical IAI isolates is variable, the presence of MRSA poses an additional challenge to treatment [19]. It has also been suggested that IAI caused by *S. aureus* lead to implant replacement more frequently than in case of *S. epidermidis* infections [14].

Management

Prophylaxis

Since the presence of an indwelling device increases the susceptibility to bacterial infection by at least 10,000-fold [20], prophylactic approaches in implant surgery are well established. To decrease the risk of infection by commensal flora, especially in cases of MRSA carriage, decolonisation of *S. aureus* should be

considered. [21]. The antibiotic regimen used for prophylaxis should be targeted against most common surgical-side isolates and their susceptibility profiles. Moreover, these antibiotics should be reserved for prophylactic application and should not be used as first line treatments for infections. Application of first- or second-generation cephalosporin or, in case of allergy or prevalence of MRSA, vancomycin or teicoplanin are recommended [21].

Treatment

Early diagnosis is the mainstay for a better outcome [13]. The treatment of IAI involves surgical revision to disrupt the biofilm and to reduce the bacterial load together with a three- to six-month antimicrobial therapy [13,21]. Indeed, long-term antibiotic alone ameliorates the symptoms but can result in recurrence of infection upon withdrawal of the drug [21]. Antibiotics for IAI have to be able to eradicate sessile biofilm-embedded bacteria. Furthermore, appropriate antibiotic dosage has to be applied, as subinhibitory concentrations of some antibiotics can in fact promote biofilm formation [22]. The activity of rifampin, an inhibitor of bacterial DNA-dependent RNA polymerase, in the treatment of IAI has been well documented. Nevertheless, owing to rapid resistance development rifampin has to be co-administered with another drug. Thus, in case of infections caused by methicillin-sensitive *S. aureus* (MSSA) rifampin/β-lactam followed by rifampin/fluoroquinolones (inhibitors of bacterial DNA gyrase and topoisomerase IV) is the best choice in case of susceptible microorganisms. Accordingly, the indicated combination for MRSA-mediated IAI is rifampin/vancomycin followed by rifampin/fluoroquinolones and can be further complicated by acquisition of resistance to fluoroquinolones by MRSA [21,23].

Staphylococci

Staphylococcus aureus

S. aureus is a human pathogen which has developed resistance to virtually all currently available antibiotics and which causes life-threatening human infections on a global scale. *S. aureus* colonises transiently 30% to 50% of adult human population and establishes asymptomatic carriage state in 30%

individuals primarily in the nasopharyngeal zone, increasing the risk of subsequent infections [24].

The pathogenic potential of *S. aureus* lies in its diverse arsenal of toxins and other virulence factors and its enhanced ability to acquire foreign DNA encoding them [25]. The sequential expression of these virulence factors reflects adaptation of *S. aureus* to cause infection and thwart host immune response [24]. Thus, expression of bacterial surface adhesins (e.g. collagen-, fibronectin-binding proteins, clumping factor) in the initial step of infection facilitates binding to host matrix molecules and thereby colonisation of the host tissues. Accordingly, synthesis of exoproteins with concomitant downregulation of adhesins allows bacterial tissue invasion and spread of infection. In this phase *S. aureus* expresses a variety of toxins compromising the integrity of eukaryotic cells (e.g. α-toxin, Panton-Valentine leukocidin (PVL), phenol-soluble modulins (PSMs)-α) or activating immune response (e.g. superantigens staphylococcal enterotoxin B and toxic shock syndrome toxin 1), as well as proteases, lipases and hyaluronidases facilitating destruction of the host tissues [24,26]. The mechanism of immune evasion by *S. aureus* does not comprise exclusively toxin-mediated lysis of leukocytes. Staphyloccoccal microcapsule and protein A prevent opsonophagocytosis of bacteria whereas chemotaxis inhibitory protein of staphylococci (CHIPS) and staphylococcal complement inhibitor (SCIN) interfere with the human complement system to inhibit the recruitment of leukocytes and bacterial opsonisation, respectively [24,27].

The remarkable adaptation of *S. aureus* to selective pressure has resulted in acquisition of resistance to almost all antibiotics currently in use. Shortly after its introduction penicillin became ineffective against staphylococci due to enzymatic hydrolysis of β-lactam ring by penicillinase. Nowadays, almost all staphylococcal clinical isolates bear β-lactamase genes [24,28]. Development of methicillin, a β-lactamase-insensitive derivative of penicillin, encountered even greater failure with the emergence of staphylococcal cassette chromosome *mec* (SCC*mec*). The penicillin-binding proteins (PBPs) are membrane-bound transpeptidases catalysing cross-linking reaction in the synthesis of peptidoglycan. Beta-lactams act as substrate analogues and inactivate PBPs by binding to the active site

serine. SCC*mec* contains *mecA* gene encoding an inducible PBP2a, which can functionally substitute for the essential roles of other PBPs. Most importantly, the active site of PBP2a has a low affinity to all β-lactams, providing resistance to entire family of β-lactams (penicillins, cephalosporins and carbapenems) [23,28,29]. MRSA has been increasingly reported in both hospital (hospital-associated MRSA, HA-MRSA) and community (community-associated MRSA, CA-MRSA) settings and the mortality caused by CA-MRSA seems to be higher, which might be due partly to increased number of virulence factors present in CA-MRSA (e.g. PVL, PSMs, α-toxin) [23,26,28].

A glycopeptide antibiotic, vancomycin has been used as a last resort treatment against MRSA. Vancomycin inhibits production of bacterial peptidoglycan by irreversible binding to the terminal D-alanyl–D-alanine of the cell wall precursors and thereby inhibits the transpeptidation by sequestering the substrate of this reaction [30]. Not surprisingly, vancomycin-intermediate and -resistant *S. aureus* (VISA and VRSA, respectively) have emerged from MRSA strains, however until now with a low prevalence [31]. The resistant phenotype of VISA appears to be governed by adaptation of gene expression conferring synthesis of a thicker peptidoglycan layer with an increased number of targets of vancomycin, D-alanyl–D-alanine due to decreased peptidoglycan cross-linking. Overall, increase in exposed D-alanyl–D-alanine residues allows trapping of vancomycin and thereby inhibits its access to the places of cell wall synthesis. In contrast, VRSA acquired vancomycin resistance from vancomycin-resistant enterococci *via* horizontal gene transfer of *vanA* operon, which facilitates the inducible biosynthesis of D-alanyl-D-lactate with a reduced affinity to vancomycin [28,30].

Staphylococcus epidermidis

S. epidermidis, a coagulase negative staphylococcus (CoNS), colonises human skin and mucous membranes and becomes an opportunistic pathogen upon breaching of the epithelial barrier [25,32]. Most diseases caused by *S. epidermidis* are chronic biofilm-mediated infections of indwelling devices [32-34]. *S. epidermidis*

produces a paucity of virulence factors that, in contrast to *S. aureus*, are not primarily targeted against the host but rather facilitate its commensal lifestyle [33]. The major virulence factor of *S. epidermidis* is formation of biofilm and thus production of a variety of adhesins [33,35]. It is well recognised that biofilm protects *S. epidermidis* from the host immunity. The biofilm-induced reduction of killing by polymorphonuclear cells (PMNs) was shown to be due to prevention of C3b and IgG deposition on the bacterial surface [17]. With the exception of several exoenzymes and PSMs, production of toxins by *S. epidermidis* seems to be extremely rare [33]. This is in sharp contrast with the large repertoire of toxins synthesised by *S. aureus* and might be due partly to the limited horizontal gene transfer caused by the presence of clustered regularly interspaced short palindromic repeats (CRISPR) locus in the *S. epidermidis* genome, which interferes with acquisition of foreign DNA [36]. The enriched immune response in the nares in contrast to the skin as well as complex transmission pathway of *S. aureus* in comparison to *S. epidermidis* are additional factors accounting for the differential virulence of both species [25]. Interestingly, despite its lower virulence *S. epidermidis* can outcompete *S. aureus* in colonisation of nasal cavity by the anti-biofilm activity of serine protease Esp [37].

In terms of antibiotic resistance, resistance to methicillin is reported for the majority of clinical isolates of CoNS, including *S. epidermidis*, and the development of intermediate resistance to vancomycin (vancomycin intermediate *S. epidermidis,* VISE) has been emerging [25,30,33].

Biofilm

Biofilm formation

It has been estimated that biofilms account for more than 80% of all human microbial infections [38], highlighting their clinical relevance. Biofilm is a multilayered consortium of microorganisms encased in self-produced extracellular matrix composed of a wide range of adhesive molecules and specialised for surface persistence. This mode of growth is common for a variety of microorganisms [15]. Biofilm governs bacterial recalcitrance to antibiotics and

biocides and allows them to circumvent immune-mediated clearance [14,15,39]. There are conventionally distinguished four stages in biofilm formation: initial bacterial adherence, intercellular aggregation and accumulation, maturation, and dispersal of biofilm [6,15,39]. In the well-orchestrated process of biofilm formation all these phases are characterised by expression of specific factors.

The process of adherence of planktonic bacteria to encountered surface is facilitated by both specific and non-specific interactions. The non-specific interactions originate from the physicochemical properties of medical device and bacterial cell surface and are driven among others by hydrophobic and electrostatic forces [6]. The specific adhesion and subsequent accumulation are caused by the fact that following implantation foreign body undergoes deposition of host matrix proteins such as fibronectin, collagen, fibrinogen and vitronectin. Staphylococci developed a variety of adhesive molecules mediating adherence to these proteins collectively designated 'microbial surface components recognising adhesive matrix molecules' (MSCRAMMs) [39]. Interestingly, bifunctional autolysins AtlE and AtlA of *S. epidermidis* and *S. aureus*, respectively, play an important role not only in turnover of peptidoglycan (as hydrolases) but also in binding to serum proteins, in release of extracellular (e)DNA, as well as in internalisation by host cells [40].

The initial attachment stimulates bacteria to produce extracellular matrix [15], comprising various extracellular polymeric substances (EPS), including proteins, teichoic acids, eDNA and/or exopolysaccharides. The contribution of each of those EPS into the pathogenesis of *S. aureus* and *S. epidermidis* in IAI is very complex and strongly depends not only on bacterial strain but also on the environmental conditions [6,14,39,41].

The most studied mediator of intercellular aggregation and biofilm accumulation is polysaccharide intercellular adhesin (PIA), a partially deacetylated linear homoglycan of β-1, 6-linked *N*-acetylglucosamine (GlcNAc) residues (also known as poly-N-acetylglucosamine, PNAG) [42]. The deacetylation of PIA facilitates acquisition of positive charge that governs electrostatic interactions between negatively charged bacterial surfaces [14,39]. Enzymes encoded by *icaADBC* operon are responsible for the synthesis and deacetylation of PIA and their expression is

controlled either at icaA promoter or by the regulatory protein IcaR [43]. These two regulation mechanisms are additionally controlled by the complex network of bacterial global regulatory proteins [6,14,39,44].

The growing bulk of biofilm acquires its characteristic 3-dimensional architecture during the maturation phase when the fluid-filled channels are formed throughout the biofilm mass. The structuring process allows metabolites and nutrients exchange between the bacteria deeply embedded in biofilm and has been reported to be governed by PSMs, a subclass of staphylococcal leukocidins endowed with surfactant-like properties [14,45].

In the final phase of dispersal bacteria detach from biofilm either as single cells or in aggregates. This process in staphylococci is controlled by the accessory gene regulator (*agr*) quorum sensing (QS) system and, like in the maturation phase, involves PSMs [14]. Thus, the released bacteria can colonise new niches and thereby spread the infection.

The formation of biofilm is synergistically regulated in response to variety of environmental conditions by a complex network of staphylococcal genes. Staphylococcal QS systems encode autoactivating peptides (AIPs) that induce coordinated population-wide response [44]. A role of the staphylococcal QS machinery, *agr* and *luxS* has been demonstrated in biofilm. The *agr* system negatively regulates biofilm formation governing upregulation of exoproteins and downregulation of adhesins [6,39,44]. Thus, a decreased expression of *agr* has been found in staphylococcal biofilms [46]. While *luxS* appears to be inactive in *S. aureus*, it downregulates biofilm by inhibition of PIA production and is involved in interspecies communication in *S. epidermidis* [6,14,44]. Two positive biofilm regulators, alternative sigma factor σ^B and staphylococcal accessory regulator A (SarA) upregulate PIA production by repressing icaR and binding to icaA promoter, respectively [6,14,39].

Antimicrobial tolerance of biofilm

The exact mechanism of dramatically decreased bacterial susceptibility to antibiotics and host defence upon switch to biofilm mode of growth remains still elusive [15]. The antimicrobial tolerance of biofilm is distinguishable from the

genetically driven antibiotic resistance and can be reversed upon biofilm dispersal [16,47,48].

One of the first proposed mechanisms of this tolerance was limited diffusion of antimicrobials at bactericidal concentrations through the biofilm. Indeed, the presence of PIA protects *S. epidermidis* against antimicrobial peptides (AMPs) most likely due to cationic repulsion [49]. Although reduced penetration has been shown for β-lactams and glycopeptides, other antibiotics, e.g. aminoglycosides and fluoroquinolones, could easily penetrate staphylococcal biofilms but eventually did not affect bacterial viability [50,51]. Thus, it has been suggested that metabolic status induced by growth in dense biofilm community (e.g. oxygen limitation) accounts for biofilm antimicrobial tolerance [47,48]. These findings have been further supported by transcriptional and proteomic analysis, which revealed that indeed biofilm-embedded bacteria downregulate biosynthesis of DNA, protein, and cell wall and switch to fermentative processes [46,52]. Thus, as conventional antibiotics have been selected based on their activity against growing bacteria, they will at least partially fail to eradicate their quiescent biofilm counterparts [15]. Moreover, decreased pH within biofilm due to accumulation of metabolites has also been suggested to directly antagonise antibiotic activity [48].

Additional factor in antimicrobial tolerance of biofilms is the presence of persisters, phenotypically heterogeneous subpopulation of specialised survivor cells, which neither grow nor die in the presence of antibiotics [16]. Indeed, it was recently shown that antibiotic-treated biofilm of *S. epidermidis* contains a high number of persisters [53]. Moreover, although persisters are present in both planktonic and biofilm bacterial populations their eradication in biofilm seemed to be additionally hindered by the inefficient host defence [18].

Finally, biofilm can also be formed by microorganisms resistant to antibiotics in a conventional, genetically driven manner. Interestingly, the rate of acquisition of classical resistance genes in biofilm-encased bacteria is substantially increased. This can be due to the exogenous (e.g. antibiotics, host response) and endogenous oxidative stress reactions. Another mechanism is the exposure of

bacteria to the concentration gradient of antibiotics formed throughout biofilm, which selects for resistant microorganisms [54].

Novel strategies to combat staphylococcal biofilms

The heterogeneity of bacterial metabolism and microenvironment in biofilm and thereby the multiple mechanisms of biofilm antimicrobial tolerance and recalcitrance to host defence imply that clinically relevant therapies of biofilm require novel approaches that simultaneously target more than one bacterial processes [15,48].

As the advantage of biofilm lies in its multicellularity attempts have been made to disrupt biofilm structure. The activity of recombinant human DNAse I (rhDNAse I) [55] and Dispersin B (DspB) [56] in conjunction with antimicrobials has been shown *in vivo* against staphylococcal biofilm owing to enzymatic degradation of eDNA and PIA, respectively. Although the risk of resistance development to DNaseI and DspB is very low, as neither directly affects bacterial viability, their clinical application remains to be further evaluated, especially in regard to PIA- and eDNA-independent biofilms. Thus, in order to address a broad range of biofilms, more conserved bacterial systems need to be targeted. Therefore, the effect of *agr* induction was recently investigated, as *agr* is able to impede biofilm formation in staphylococci. Indeed, it has been shown that *agr* activation with exogenous AIPs in established *S. aureus* biofilms caused bacterial detachment in a mechanism dependent on extracellular proteases [57]. Targeting another staphylococcal global regulator, SarA showed initially promising result however the beneficial effect of SarA inhibition might be strain-dependent [58,59].

Another common feature of bacterial biofilms is the presence of subpopulation of dormant persisters responsible for recurrence of biofilm-mediated infections [16]. Interestingly, the acyldepsipeptide antibiotic (ADEP4) activated ClpP protease and caused self-digestion of *S. aureus* persisters. Combination of ADEP4 and rifampin overcame the emergence of resistant bacteria and eradicated biofilm both *in vitro* and *in vivo* [60]. Thus, this study further highlighted the importance of targeting bacteria independent of their metabolic status in designing efficient anti-biofilm drugs.

A recently re-emerging treatment option in infectious diseases is bacteriophage (phage) therapy. The efficacy of phage cocktails in prevention and treatment of biofilm-mediated infection caused by both Gram-positive and -negative pathogens in animal studies and in clinical trials has been proven [61-63]. The anti-biofilm effect of phages has been ascribed not only to their bacteriolytic properties but also to production of enzymes degrading EPS, which can improve phagocytosis and potentiate antibiotic activity [54]. A matter of concern remain among others phage lysogeny (incorporation into bacterial chromosome) and phage-mediated horizontal gene transfer of virulence factors, as well as induction of resistance and adverse immune response to phages [54]. Thus, further standardisation of phage-containing products to meet regulatory criteria is required in order to introduce phage therapy into the clinical routine [63].

The remarkable difficulties in treatment of established biofilms prompted research on engineering implant surfaces that could resist microbial colonisation. This could be achieved by depositing layers of antiadhesive coatings on the surface of medical devices that could counteract bacterial adhesion but retain or even improve its biocompatibility. It is believed that the increase in surface hydrophilicity confers nonfouling properties of biomaterials due to formation of a physical and energetic water-mediated barrier preventing protein and bacterial adsorption [64]. Indeed, these low-fouling properties are well known for poly(ethylene glycol) (PEG). However PEG-based materials are chemically instable due to oxidation [64]. PMOXA, a peptide-like polymer, has been shown to have the same nonfouling properties as PEG while being more stable in oxidative environments [65]. In another study surfaces based on antifouling polymers PHEMA and PEGMA were further functionalised with arginine-glycine-aspartic acid (RGD)-containing peptide ligands. This functionalisation with integrin-recognition sequence promoted *in vitro* colonisation by human cell line and can be a promising step towards designing implants with improved biocompatibility [66].

As the *in vivo* efficacy of "passive" antifouling implant coatings has been limited so far, more advanced "active" approaches, which involve an antimicrobial compound, have been developed. A significant inhibition of biofilm formation by

S. epidermidis on titanium alloy surfaces covalently functionalised with vancomycin has already been reported [7]. Nevertheless, a potential disadvantage of antibiotic-coated surfaces is the covering with bacterial debris, which could lead to loss of their antimicrobial activity. Alternatively, an antibiotic-eluting approach with antimicrobial-treated central venous catheters has shown clinical efficacy in reducing bloodstream infections compared with standard catheters [67].

As application of antibiotics inevitably leads to selection of resistant bacteria, an interest in alternative antimicrobial agents has been renewed. Nanostructured coatings with silver coordination polymer have been shown to impede biofilm of *S. epidermidis* in mouse tissue cage model [68]. Despite substantially improved knowledge of the mechanism of action of silver and lack of resistance among staphylococci reported so far, its clinical use remains controversial due to potential cytotoxic properties and resistance determinants among Gram-negative bacteria [69,70].

Innovative dual-function implant surfaces, which combine both nonfouling and antimicrobial properties, have also been investigated. Indeed, coupling of cationic AMPs to hydrophilic polymer has exhibited excellent biocompatible properties and at the same time a significant potential to reduce biofilm formation and bacterial viability [71].

Serrulatane EN4

One of the compelling approaches in antibacterial drug design is investigation of antimicrobial substances derived from natural sources. The plant genus *Eremophila* (Myoporaceae) that has been traditionally used by Aborigines to treat various infections [72] is native in arid areas of Australia and produces unique secondary metabolites, among others nine classes of diterpenoids including the most commonly occurring serrulatanes [73]. Screening of organic extracts of *Eremophila* species revealed a selective activity against Gram-positive

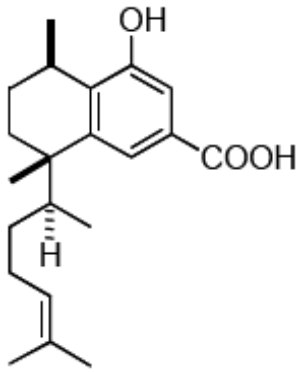

Figure 1 Structure of serrulatane EN4

bacteria [74]. One of the active compounds, EN4 (8-hydroxyserrulat-14-en-19-oic acid) (Fig. 1) was isolated in a bioassay-guided fractionation of the leaves extract of *Eremophila neglecta* and also exhibited activity against Gram-positive pathogens [75,76], which prompted interest in possible use of EN4 in management of IAI.

Aim of the Thesis

The relevance of this project relates to the enormous medical problem and costs caused by IAI.

This study constitutes a part of a project "Serrulatane-based antimicrobial surface platforms" in the framework of the Competence Centre for Materials Science and Technology (CCMX). The project aims at developing novel multifunctional biocompatible surface coatings for the prevention of IAI. These coatings are envisioned to exert both antifouling and antibacterial effects in order to prevent bacterial adhesion, and thereby formation of biofilm, and to kill invading microorganisms. Generation of innovative polymer coatings was performed by the project partners from the Laboratory for Surface Science and Technology (ETH Zürich, Switzerland) and the Polymers Laboratory (EPFL Lausanne, Switzerland). The microbiological evaluation of their antifouling and antimicrobial properties was performed within our project.

Antimicrobial tolerance of bacterial biofilms together with the increasing emergence of multi-drug resistant bacteria pose alarming treats to the public health. Therefore, as a bioactive coating component we decided to investigate a novel plant-derived compound, serrulatane EN4, which was provided by a project partner from the University of Adelaide, Australia. It was known that EN4 exhibits antimicrobial properties against Gram-positive bacteria, including these involved in pathogenesis of IAI [75]. However, the entire spectrum of activity against human pathogens, especially when embedded in biofilm, the mechanism of action, cytotoxicity *in vitro* and efficacy *in vivo* remained to be determined. Establishment of the exact mode of action of EN4 was of a special importance, as the location of its target would determine the chemistry of attachment of EN4 to antiadhesive polymer brushes (Fig. 2a, b). In case of a surface-located target a covalent attachment of EN4 to polymer would be applied (Fig. 2a). However, to ensure the access of EN4 to an intracellular target a hydrolysable linker between the polymer and EN4 would be necessary in order to facilitate the release of EN4 (Fig. 2b).

Thus, the main aim of the presented work was to determine the *in vitro* and *in vivo* activity as well as a detailed mechanism of action of serrulatane EN4 for its possible application in the prevention and/or treatment of IAI.

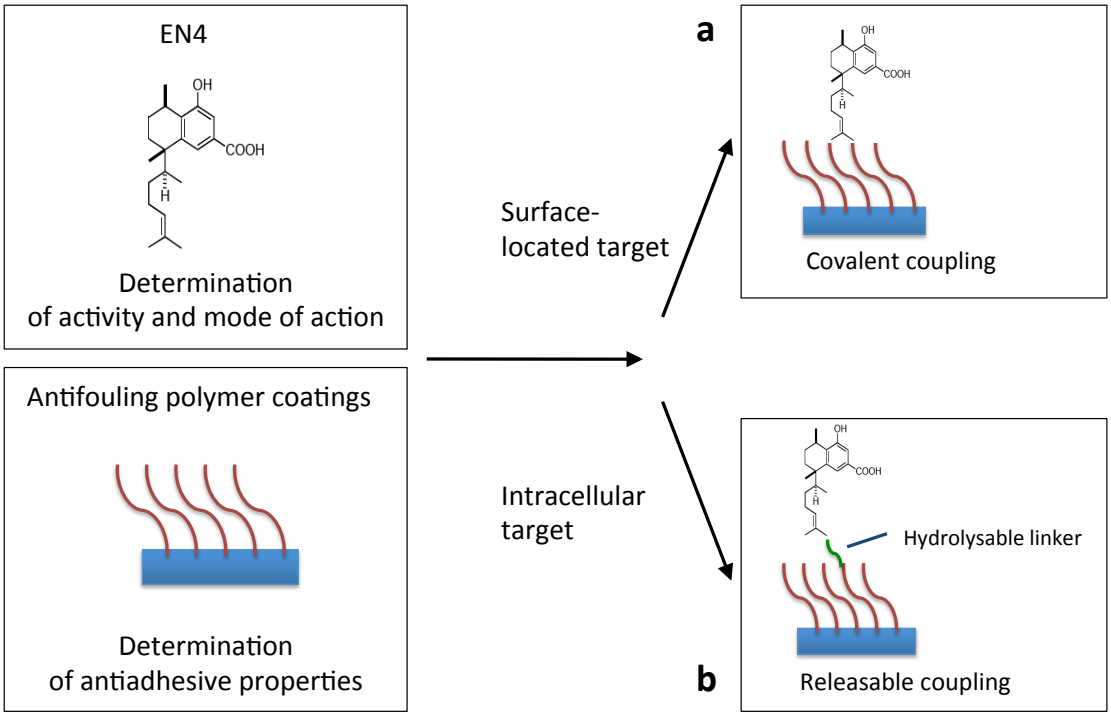

Figure 2 Schematic representation of the aims of the project.

Results

I. Antimicrobial Properties of 8-Hydroxyserrulat-14-en-19-oic Acid for Treatment of Implant-Associated Infections

AAC Journals.ASM.org

Antimicrobial Properties of 8-Hydroxyserrulat-14-en-19-oic Acid for Treatment of Implant-Associated Infections

Justyna Nowakowska,[a] Hans J. Griesser,[b] Marcus Textor,[c] Regine Landmann,[a] Nina Khanna[a]

Laboratory of Infection Biology, Division of Infectious Diseases and Hospital Epidemiology, Department of Biomedicine, University Hospital Basel, Basel, Switzerland[a]; Ian Wark Research Institute, University of South Australia, Mawson Lakes, South Australia, Adelaide, Australia[b]; Department of Materials, ETH Zurich, Zürich, Switzerland[c]

Treatment options are limited for implant-associated infections (IAI) that are mainly caused by biofilm-forming staphylococci. We report here on the activity of the serrulatane compound 8-hydroxyserrulat-14-en-19-oic acid (EN4), a diterpene isolated from the Australian plant *Eremophila neglecta*. EN4 elicited antimicrobial activity toward various Gram-positive bacteria but not to Gram-negative bacteria. It showed a similar bactericidal effect against logarithmic-phase, stationary-phase, and adherent *Staphylococcus epidermidis*, as well as against methicillin-susceptible and methicillin-resistant *S. aureus* with MICs of 25 to 50 μg/ml and MBCs of 50 to 100 μg/ml. The bactericidal activity of EN4 was similar against *S. epidermidis* and its Δ*ica* mutant, which is unable to produce polysaccharide intercellular adhesin-mediated biofilm. In time-kill studies, EN4 exhibited a rapid and concentration-dependent killing of staphylococci, reducing bacterial counts by >3 $\log_{10}$ CFU/ml within 5 min at concentrations of >50 μg/ml. Investigation of the mode of action of EN4 revealed membranolytic properties and a general inhibition of macromolecular biosynthesis, suggesting a multitarget activity. *In vitro*-tested cytotoxicity on eukaryotic cells was time and concentration dependent in the range of the MBCs. EN4 was then tested in a mouse tissue cage model, where it showed neither bactericidal nor cytotoxic effects, indicating an inhibition of its activity. Inhibition assays revealed that this was caused by interactions with albumin. Overall, these findings suggest that, upon structural changes, EN4 might be a promising pharmacophore for the development of new antimicrobials to treat IAI.

Implant-associated infections (IAI) are still a cause of high morbidity and social costs despite the substantial improvement of early diagnosis and treatment. Optimal management of IAI requires surgical intervention and use of antibiotics against adherent bacteria (1). Staphylococci, including *Staphylococcus aureus* (both methicillin-susceptible and methicillin-resistant strains) and *S. epidermidis*, are the bacteria most frequently associated with IAI (2). These bacteria are able to persist on the implant surfaces, forming biofilms. Biofilms are multilayered communities of bacteria embedded in self-produced extracellular matrix characterized by an oxygen and nutrient gradient throughout its structure, inducing sessility in centrally situated cells (3, 4). The biofilm matrix is mainly composed of polysaccharide intercellular adhesin (PIA), proteins and extracellular DNA (4). PIA produced by *ica* operon-encoded enzymes has been implicated in the virulence and immune evasion of *S. epidermidis* and the pathogenesis of IAI (5).

Therefore, to successfully treat IAI, antimicrobials need to penetrate the biofilm and act independently of the bacterial physiological state. Thus far, most of the known antibiotics are dependent on the metabolic status of bacteria hindering the eradication of quiescent pathogens (6, 7). The only antibiotic with a proven activity against staphylococcal biofilm is rifampin (8). However, due to a rapid resistance development, it has to be combined with other antibiotics. This and the recent increasing emergence of drug-resistant bacteria highlight the need for new antimicrobials to combat IAI.

An especially compelling approach is the investigation of antimicrobials from natural sources. The large Australian plant genus *Eremophila* (*Myoporaceae*), of which a few species have been traditionally used by Aborigines to treat various ailments (9), is native to arid areas of Australia and produces unique secondary metabolites, among others nine classes of diterpenoids, including the most commonly occurring serrulatanes (10). Screening of organic extracts of *Eremophila* species revealed a selective effect against Gram-positive bacteria (11).

The aim of the present study was to evaluate the activity *in vitro* and *in vivo* and the mode of action of one of the compounds extracted from leaves of *Eremophila neglecta*, 8-hydroxyserrulat-14-en-19-oic acid (EN4), as a new candidate for the treatment of IAI.

MATERIALS AND METHODS

Antimicrobial agents, media, and chemical reagents. EN4 was extracted from freshly collected *E. neglecta* plant material with a purity of ≥95% (as determined by nuclear magnetic resonance analysis) as described previously (12) and stored at −20°C. EN4 was dissolved in 1% dimethyl sulfoxide (DMSO) (Merck, Darmstadt, Germany) in phosphate-buffered saline (PBS) (Reagens, Basel, Switzerland) (DMSO-PBS) up to a concentration of 400 μg/ml. Nisin (Sigma-Aldrich, Buchs, Switzerland) was solubilized in 0.02 M HCl. Daptomycin (DAP; Cubicin; Novartis, Bern, Switzerland) was dissolved in 0.9% saline (Bichsel, Interlaken, Switzerland) supplemented with 50 μg of calcium ions/ml ($CaCl_2$). Actinomycin D (Sigma-Aldrich), ciprofloxacin (Ciproxin; Bayer, Zürich, Switzerland), vancomycin (Vancocin; Teva Pharma, Aesch, Switzerland), chloramphenicol (Applichem, Darmstadt, Germany), and chlorhexidine dihydrochloride (Sigma-Aldrich) were prepared according to the manufacturer's instructions. Bacterial media were purchased from Becton Dickinson

Received 21 August 2012 Returned for modification 22 September 2012
Accepted 23 October 2012
Published ahead of print 31 October 2012
Address correspondence to Nina Khanna, khannan@uhbs.ch.

doi:10.1128/AAC.01735-12

TABLE 1 Microorganism strains used in this study

Species	Strain[a]	Relevant properties	Source or reference
Staphylococcus aureus	Western Samoan Phage Pattern A (WSPPA)*	MRSA ST30	13
	ME230*	MSSA, isogenic ΔSCC*mec* mutant of WSPPA	M. Ender[b]
	SA113 (ATCC 35556)†	MSSA, production of PIA-mediated biofilm under aerobic conditions	14
Staphylococcus epidermidis	1457‡	Efficient biofilm producer	17
	1457 Δ*ica*‡	Isogenic Δ*ica* mutant, devoid of PIA-mediated biofilm	17
Mycobacterium tuberculosis	ATCC 27294 (H37Rv)§	Rifampin-sensitive strain	15
	ATCC 35838 (H37Rv-RIF-R)‡	Rifampin-resistant strain	
Streptococcus pyogenes	ATCC 19615§	Laboratory strain isolated from human	16
Streptococcus pneumoniae	TIGR4 (JNR.7/87)	Encapsulated, virulent strain	
Enterococcus faecalis	ATCC 19433§	Laboratory strain	
Pseudomonas aeruginosa	PA01¶	Laboratory strain isolated from human	
Escherichia coli	ATCC 25922	Human clinical isolate	
Candida albicans	SC5314‖	Laboratory strain isolated from human	
Candida glabrata	t608919‡	Clinical isolate	This study
Candida krusei	ATCC 6258‡	Reference laboratory strain isolated from human	

[a] Sources: *, B. Berger-Bächi, Zürich, Switzerland; †, F. Götz, Tübingen, Germany; ‡, D. Mack, Swansea, United Kingdom; §, R. Frei, Basel, Switzerland; ¶, U. Jenal, Basel, Switzerland; ‖, S. Leibundgut-Landmann, Zürich, Switzerland.
[b] M. Ender, ETH Zürich, Switzerland (unpublished data).

(BD; Allschwil, Switzerland). ^{3}H-labeled precursors of macromolecules were obtained from Hartmann Analytic (Braunschweig, Germany). Unless otherwise stated, all chemical substances were purchased from Sigma-Aldrich.

Microorganisms and growth conditions. The strains used in experiments are listed in Table 1. Stocks of microorganisms were prepared using a cryovial bead preservation system (Microbank; Pro-Lab Diagnostics, Richmond Hill, Ontario, Canada) and stored at −75°C. Unless otherwise stated, for the preparation of overnight culture, a bead was incubated in 1 ml of tryptic soy broth (TSB) for 7 h at 37°C, diluted 1:100 in fresh TSB, and incubated overnight at 37°C. For experiments with exponential-phase bacteria, the overnight culture was diluted 1:100 and further incubated for 5 to 6 h at 37°C, followed by two washes with 0.9% saline (Bichsel, Interlaken, Switzerland), and adjusted to an appropriate level of CFU/ml. All cultures were prepared without shaking. CFU were determined by plating of aliquots of 10-fold dilutions of bacterial cultures on Mueller-Hinton agar (MHA), followed by 24 h of incubation at 37°C.

Susceptibility *in vitro*. (i) Gram-positive and -negative bacteria. The minimal inhibitory and bactericidal concentrations (MIC and MBC, respectively) of EN4 for logarithmically growing bacteria were determined by using a macrodilutions method according to Clinical and Laboratory Standards Institute guidelines (18).

For staphylococci, the MBC was also assessed in the stationary growth phase (MBC_{stat}), which reflects the metabolic status of biofilm-embedded microorganisms (24). MBC_{stat} was determined using staphylococcal cultures in nutrient-limited medium consisting of 0.1 to 0.25% TSB in PBS. The use of this medium sustains bacterial counts within a range of 5 ± 0.5 $\log_{10}$ CFU/ml for at least 24 h. MBC_{stat} was defined as the lowest concentration of EN4 that reduced the inocula by ≥99.9% in 24 h.

(ii) Mycobacteria. Susceptibility of *Mycobacterium tuberculosis* ATCC 27294 and ATCC 35838 to EN4 was determined by microwell alamarBlue assay as previously described (19). Briefly, 0.5 McFarland inocula of *M. tuberculosis* were diluted 1:25 in 2-fold concentrated medium (5.9 g of Middlebrook 7H9 broth, 1.25 g of Bacto Casitone, 3.1 ml of glycerol, 100 ml of oleic acid-albumin-dextrose-catalase [OADC], 400 ml of distilled water) and mixed with solutions of EN4 (final concentrations of 50, 100, and 200 μg/ml) or 1% DMSO-PBS as untreated controls in a flat-bottom 96-well plate (BD). After 5 days of incubation at 37°C 30 μl of 0.01% (wt/vol) resazurin (Sigma, St. Louis, MO) was added to untreated *M. tuberculosis*, and the plate was reincubated for 24 h at 37°C. If the color turned pink (indicating growth), resazurin was added to the rest of the wells. The MIC was determined as the lowest concentration of EN4 preventing color changes of resazurin (i.e., inhibiting growth of *M. tuberculosis*) after 24 h of incubation at 37°C.

(iii) *Candida*. The susceptibility of *Candida* to EN4 was determined according to CLSI guidelines (48). Five colonies of *Candida* were dissolved in 0.9% saline, and the turbidity adjusted to a 0.5 McFarland standard (1×10^6 to 5×10^6 CFU/ml). The suspension was diluted to 5×10^2 to 2.5×10^3 CFU/ml with RPMI 1640 (Gibco, Paisley, United Kingdom) supplemented with 17.2 g of morpholinepropanesulfonic acid (MOPS) and 10 g of glucose per 500 ml (pH 7.0). Then, 0.9 ml was transferred to glass tubes containing 100 μl of 2-fold EN4 dilutions in 10% DMSO-RPMI 1640. The tubes were incubated for 24 h at 35°C without shaking. The MIC was determined as the lowest concentration of EN4 that inhibited visible fungal growth.

Time-kill studies. Glass tubes containing TSB with EN4 at concentrations representing 0.5× to 4× the MIC were incubated with 10^6 CFU of the test strain/ml at 37°C without shaking. Bacterial survival in the antimicrobial-free culture containing 1% DMSO-PBS in TSB served as a control. At the indicated time points, aliquots were removed and washed with 0.9% saline to avoid potential drug carryover effect. The CFU were determined by plating aliquots of appropriate dilutions on MHA. A bactericidal effect was defined as a ≥3-$\log_{10}$ CFU/ml reduction in the initial inoculum.

Susceptibility of adherent staphylococci *in vitro*. An exponential-phase culture of the test strain was diluted in TSB supplemented with 0.5% glucose (Braun Medical AG, Sempach, Switzerland) to 10^4 CFU/ml. A total of 100 μl was seeded in flat-bottom 96-well plates. After 18 h of incubation at 37°C, the wells were washed and treated with 2-fold dilutions of EN4 for 24 h at 37°C. The activity of EN4 against biofilm was assessed by crystal violet (CV) staining as previously described (20). Briefly, planktonic bacteria were discarded, and adherent bacteria were washed. The plates were then incubated for 60 min at 60°C. Staining was performed with 100 μl of 0.5% CV solution per well for 20 min at room temperature, followed by a thorough washing under running tap water. The bound CV was extracted with 100 μl of 33% acetic acid, and the

extracts were transferred to a fresh 96-well plate to be read. The optical density of the samples was measured at 590 nm using a Molecular Devices reader (Applied Biosystems, Rotkreuz, Switzerland). To determine the effect of EN4 on bacterial viability, adherent bacteria were carefully detached by pipetting up and down and then plated on MHA (21).

Macromolecular biosynthesis assay. Exponential-phase *S. aureus* Western Samoan Phage Pattern A (WSPPA) was prepared in completely defined medium (CDM) for peptidoglycan, RNA, and DNA or in CDM-Leu for protein biosynthesis. CDM contained the following substances per liter: 1.77 g of Na_2HPO_4, 1.36 g of KH_2PO_4, 0.2 g of $MgSO_4 \cdot 7H_2O$, 0.5 g of NH_4Cl, 0.5 g of NaCl, 294.1 g of sodium citrate tribasic dehydrate, 1.5 g of glucose, 160 mg each of various amino acids (i.e., L-alanine, L-valine, L-isoleucine, L-aspartic acid, L-glutamic acid, L-serine, L-threonine, L-cysteine hydrochloride, L-arginine, L-leucine, L-lysine, L-proline, L-phenylalanine, L-tryptophan, and L-histidine monohydrochloride), 1.6 g of glycine, 0.05 mg of cyanocobalamine, 0.04 mg of *p*-aminobenzoate, 0.01 mg of biotin, 0.1 mg of nicotinic acid, 0.1 mg of D-pantotheic acid hemicalcium salt, 0.15 mg of pyridoxine hydrochloride, 0.1 mg of thiamine hydrochloride, 0.1 mg of riboflavin, 69.5 μg of $ZnCl_2$, 0.1 μg of $MnCl_2 \cdot 4H_2O$, 6 μg of BH_3O_3, 0.347 mg of $CoCl_2 \cdot 6H_2O$, 2.6 μg of $CuCl_2 \cdot 2H_2O$, 24 μg of $NiCl_2 \cdot 6H_2O$, 36 μg of $NaMoO_4 \cdot 2H_2O$, 0.15 mg of $FeCl_2 \cdot 4H_2O$, 120 mg of NaOH, 5 mg of uracil, 5 mg of cytosine, 5 mg of adenine, and 5 mg of guanine. The concentration of L-leucine in CDM-Leu was 22.5 mg/liter instead of 160 mg/liter.

The culture (2×10^7 CFU/ml) was aliquoted into prewarmed glass tubes and subsequently treated with 4× the MIC of EN4 (100 μg/ml), vancomycin (8 μg/ml), actinomycin D (25 μg/ml), ciprofloxacin (8 μg/ml), chloramphenicol (32 μg/ml), or chlorhexidine (CHX; 3.12 μg/ml), followed by the immediate addition of 0.1 μCi [^{3}H]*N*-acetylglucosamine/ml, 1 μCi of [^{3}H]uridine/ml, 1 μCi of [^{3}H]thymidine/ml, or 3 μCi of [^{3}H]leucine/ml to investigate the biosynthesis of peptidoglycan, RNA, DNA, and proteins, respectively. Untreated control samples were exposed to 1% DMSO-PBS. After 1 h of incubation at 37°C, 0.5-ml portions of the bacterial suspensions were transferred to ultracentrifuge tubes and precipitated on ice with 1 ml of ice-cold 10% trichloroacetic acid (TCA) for at least 1.5 h. After this time, free fractions of precursors were removed from the precipitates by washing with 5% TCA–1.5 M NaCl and with 5% TCA. Upon solubilization with 0.1% sodium dodecyl sulfate (SDS)–0.1 M NaOH, the precipitates were transferred to scintillation tubes (Perkin-Elmer, Groningen, Netherlands) and thoroughly mixed with 2 ml of scintillation cocktail (Ultima Gold; Perkin-Elmer, Waltham, MA). Radioactivity reflecting the amount of incorporated precursors was measured using a Tri-CARB 1900TR liquid scintillation analyzer (Packard, Meriden, CT). Incorporation was measured in counts per minute (cpm) and expressed as a percentage of the untreated control.

Flow cytometric analysis. Exponential-phase *S. epidermidis* 1457 (5×10^7 CFU) was incubated for 10 min at 37°C with 100 μg of EN4 or CHX/ml. Upon centrifugation, the samples were stained with 0.75 μM propidium iodide and 0.0625 μM SYTO9 from the Live/Dead BacLight bacterial viability kit (Invitrogen, Oregon). After 15 min of incubation at room temperature protected from light, the green and red fluorescence intensities of 10^5 stained bacteria per sample were recorded using a CyAn ADP flow cytometer (Dako Cytomation, Glostrup, Denmark) and analyzed with FlowJo software (TreeStar, Stanford, CA).

ATP leakage assay. Exponential-phase WSPPA (7×10^8 CFU) was exposed for 10 min at 37°C to EN4 (50, 100, and 200 μg/ml), CHX (50 and 100 μg/ml), nisin (32 μg/ml), ciprofloxacin (8 μg/ml), or 1% DMSO-PBS (untreated control). In order to assess ATP release, the bacteria were harvested by centrifugation, and 100 μl of each supernatant was transferred to flat-bottom black-walled 96-well plate (Perkin-Elmer, Groningen, Netherlands). ATP content was determined using the BacTiter-Glo assay (Promega, Madison, WI). Luminescence was measured for 30 min with SpectraMAX GeminiXS (Molecular Devices/Bucher Biotec, Basel, Switzerland). The results are shown as the area under the curve.

Transmission electron microscopy. Exponential-phase WSPPA (5×10^9 CFU) was incubated for 1 h at 37°C with EN4 (100 and 200 μg/ml), CHX (250 μg/ml), or 1% DMSO-PBS (untreated control) and harvested by centrifugation. The pellets were resuspended in 2% glutaraldehyde in PBS, followed by 2 h of fixation at room temperature. Postfixation was carried out with reduced osmium tetroxide (1.5% KFeCN and 1% OsO_4 in PBS) for 40 min, followed by a second postfixation with 1% OsO_4 for 40 min. After a washing step, the bacteria were embedded in 2% agarose and cut in blocks, which were dehydrated using 50, 70, 90, and 100% ethanol (10 min each). The samples were further incubated in acetone (10 min). Infiltration with Epon-acetone (50:50) for 1 h was followed by incubation in pure Epon for 3 to 4 h. The samples were embedded in fresh Epon and polymerized for 48 h at 60°C. Sections (60 nm) were cut at Ultracut E (Leica), stained with 6% uranyl acetate, and analyzed using a Morgagni transmission electron microscope (FEI).

EDTA cotreatment. The effect of EDTA on the susceptibility of Gram-negative bacteria to EN4 and nisin was investigated as previously described (22). Briefly, an overnight culture of *P. aeruginosa* PA01 was prepared in brain heart infusion (BHI) broth, diluted 1:100 in fresh BHI medium, and incubated at 37°C to a population density of 5×10^7 CFU/ml. Bacteria (5×10^5 CFU) were transferred to microcentrifuge tubes containing buffer (50 mM Tris-HCl [pH 7.2]) supplemented with (i) 1 mM EDTA, (ii) 5 mM EDTA, (iii) 100 μg of nisin/ml, (iv) 100 μg of nisin/ml and 1 mM EDTA, (v) 200 μg of EN4/ml, or (vi) 200 μg of EN4/ml and 5 mM EDTA. The samples were incubated for 1 h at 37°C. The numbers of surviving bacteria were determined by plating aliquots on MHA.

Cytotoxicity on eukaryotic cells. The cytotoxicity assay was prepared as previously described (20). Briefly, mouse L929 fibroblasts were cultured in complete RPMI 1640 supplemented with 5% heat-inactivated fetal bovine serum (FBS). To assess the cytotoxicity of EN4 over time, 10^4 cells/well were seeded in a flat-bottom 96-well plate in RPMI 1640 supplemented with 3.75% FBS, followed by incubation for 4 h until the fibroblasts adhered. After this time, EN4 solutions in 3.75% FBS-RPMI were transferred to wells to final concentrations of 25, 50, and 100 μg/ml. Fibroblasts incubated with 1% DMSO-PBS instead of EN4 served as an untreated control. At the indicated time points, the activity of the lactate dehydrogenase (LDH) was assessed in cell supernatants and corresponding lysates (total LDH) using the CytoTox 96 nonradioactive cytotoxicity assay (Promega) according to the manufacturer's instructions. Cytotoxicity was defined as LDH release and was expressed as a percentage of the total LDH.

For determination of the influence of FBS on the cytotoxicity of EN4, fibroblasts were seeded and treated with EN4 at 100 μg/ml in RPMI supplemented with 3.75, 5, or 10% FBS, and then the cytotoxicity was assessed as described above.

Activity *in vivo*. The *in vivo* activity of EN4 against *S. aureus* SA113 was investigated in a mouse model of foreign body infection as described previously (21) with the approval of the Kantonale Veterinaeramt Basel-Stadt (permit 1710). Experiments were conducted according to the regulations of Swiss veterinary law. Female C57BL/6 mice (Harlan Laboratories, Switzerland), 9 to 11 weeks old, kept under specific-pathogen-free conditions in the animal house of the Department of Biomedicine, University Hospital Basel, were anesthetized via intraperitoneal injection of 65 mg of ketamine (Ketalar; Pfizer, Zürich, Switzerland)/kg and 13 mg of xylazinum (Xylasol; Graeub, Bern, Switzerland)/kg, followed by the subcutaneous implantation of sterile Teflon tissue cages (Angst + Pfister AG, Zürich, Switzerland). After surgery, the mice were treated with 0.05 mg of buprenorphine (Temgesic; Essex Chemie, Lucerne, Switzerland)/kg to treat postoperative pain. Upon complete wound healing (2 weeks), the mice were anesthetized with isoflurane (Isofuran; Abbott, Wiesbaden, Germany), and the cages were tested for sterility by plating percutaneously aspirated tissue cage fluid (TCF) on Columbia sheep blood agar plates. To simulate a perioperative infection, the cages were injected with 100 and 250 μg of EN4 (10 mice per group) or 30 μg of DAP (5 mice per

TABLE 2 *In vitro* susceptibility of Gram-positive and Gram-negative bacteria and fungi to EN4 determined as MICs and MBCs

Species	Strain	Concn (μg/ml)	
		MIC	MBC
Streptococcus pyogenes	ATCC 19615	6.25	12.5
Streptococcus pneumoniae	TIGR4 (ATCC BAA-334)	1.6	3.12
Enterococcus faecalis	ATCC 19433	50	50
Pseudomonas aeruginosa	PA01	>200	>200
Escherichia coli	ATCC 25922	>200	>200
Mycobacterium tuberculosis	ATCC 27294	100	–[a]
	ATCC 35838	100	
Candida albicans	SC5314	>200	
Candida glabrata	t608919	200	
Candida krusei	ATCC 6258	200	

[a] Susceptibility was determined only as the MIC.

TABLE 3 *In vitro* susceptibility to EN4 of staphylococci in the logarithmic (MIC_{log} and MBC_{log}) and stationary (MBC_{stat}) growth phases

Species	Strain	Concn (μg/ml)		
		MIC_{log}	MBC_{log}	MBC_{stat}
Staphylococcus aureus	MRSA WSPPA	25	50	100
	MSSA ME230	25	50	100
	MSSA SA113	25	50	50
Staphylococcus epidermidis	1457	25	100	100
	1457 Δ*ica*	50	100	100

group) and then immediately infected with 4×10^3 CFU of SA113. Untreated control cages were injected with 1% DMSO-PBS (8 mice per group). After 24 and 48 h, the TCF was collected into ultracentrifuge tubes containing 10 μl of 1.5% EDTA in 0.45% saline (pH 7.3) to avoid clotting, and the cages were reinjected with the respective substances. TCF was used to determine the numbers of planktonic SA113 by plating appropriate dilutions on blood agar plates and to assess the viability of leukocytes by trypan blue staining. Aspiration of TCF was repeated after 72 h, and the mice were sacrificed. Tissue cages were explanted under aseptic conditions, washed twice with 0.9% saline in order to remove planktonic bacteria, and cultured in TSB. The cages were vortexed at 0, 24, and 48 h to increase the possible regrowth of adherent bacteria. After 48 h of incubation at 37°C, the bacterial presence in the cultures was determined by plating on blood agar plates. Detection of the growth of SA113 was defined as treatment failure. The efficacy of treatment against adherent bacteria was expressed as the cure rate, defined as the percentage of cages without growth in the individual treatment group.

Inhibition of EN4 activity. An overnight culture of SA113 was transferred to glass tubes (2×10^6 CFU/ml) containing TSB supplemented with EN4 (100 μg/ml) in the presence of mouse TCF (2.5, 5, and 75%), pooled normal human serum (NHS; 1.25, 2.5, and 75%), human serum albumin (HSA; Blutspendedienst SRK, Bern, Switzerland) (0.125 and 0.25%), or 300 μg of human fibrinogen (Hyphen BioMed, Allschwil, Switzerland)/ml (representing 10% of the normal blood level). The samples were incubated for 6 h at 37°C. Then, 0.5-ml portions of the suspensions were transferred to microcentrifuge tubes and washed once with 0.9% saline, and the numbers of surviving bacteria were determined by plating. The results were calculated as the $\log_{10}$ CFU/ml reduction from the initial inoculum. None of the supplements influenced the viability of SA113 in the absence of EN4 (data not shown).

Statistical analysis. Data were analyzed by GraphPad Prism 5.0a program (GraphPad Software). The Mann-Whitney U test or one-way analysis of variance (ANOVA) were used to determine the statistical significance (P) of differences in the *in vitro* assays. The statistical tests used for each experiment are specified in the figure legends.

RESULTS

EN4 acts in a rapid and dose-dependent manner against Gram-positive bacteria *in vitro*. The MICs and MBCs of EN4 were determined for different strains of Gram-positive and Gram-negative bacteria, as well as for *M. tuberculosis* and *Candida* species. The results are summarized in Table 2 and Table 3. Both *Streptococcus pyogenes* and *Streptococcus pneumoniae* showed the highest susceptibility to EN4, with MICs of 6.25 and 1.6 μg/ml and MBCs of 12.5 and 3.12 μg/ml, respectively. The MIC and MBC of EN4 for *Enterococcus faecalis* were both 50 μg/ml. As previously reported (12), Gram-negative bacteria were not susceptible to EN4 at concentrations up to 200 μg/ml. Interestingly, EN4 was active against rifampin-susceptible and -resistant *M. tuberculosis* with an MIC of 100 μg/ml. *C. albicans* was not influenced by EN4, whereas *C. glabrata* and *C. krusei* were susceptible with an EN4 MIC of 200 μg/ml, the highest concentration used. EN4 showed a bactericidal effect against various logarithmic-phase staphylococci. The MIC_{log} values for *S. epidermidis* 1457 and its isogenic, biofilm-deficient Δ*ica* mutant were 25 and 50 μg/ml, respectively, and the MBC_{log} was 100 μg/ml. EN4 was similarly active against MRSA strain WSPPA and its isogenic, methicillin-susceptible mutant ME230 with an MIC_{log} of 25 μg/ml and an MBC_{log} of 50 μg/ml. SA113 capable of producing PIA-mediated biofilm under aerobic conditions was susceptible to EN4, with an MIC_{log} and an MBC_{log} of 25 and 50 μg/ml, respectively.

To investigate whether EN4 could be used to treat IAI, further experiments were focused selectively on staphylococci. In time-kill studies EN4 showed a dose-dependent activity against WSPPA with a bactericidal effect (≥3-$\log_{10}$ CFU/ml reduction) within 5 min at MBC_{log} (Fig. 1). Similar kinetics was observed for other staphylococci (data not shown). This is in line with previous findings indicating that *Eremophila duttoni* extract eradicated MRSA within 1 h (23).

Taken together, these results show that EN4 acts specifically against a range of Gram-positive bacteria and *M. tuberculosis* with a rapid and dose-dependent kinetics for staphylococci.

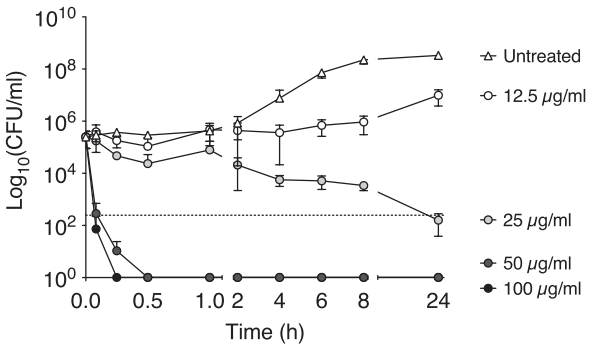

FIG 1 Time-kill studies of WSPPA exposed to titrated concentrations of EN4. Dotted line represents a bactericidal effect, i.e., a 3-$\log_{10}$ CFU/ml reduction from the initial inoculum. The values shown are means of three independent experiments ± the standard deviations (SDs).

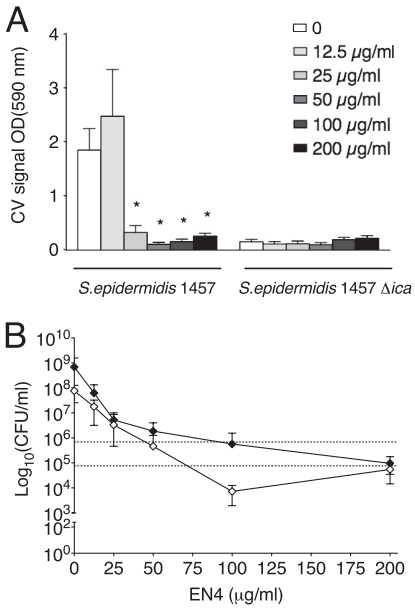

FIG 2 Effect of EN4 on adherent *S. epidermidis* 1457 and its Δ*ica* mutant. Inocula of both strains (10^3 CFU/well in 96-well plates) were incubated for 18 h at 37°C, followed by the addition of EN4 at titrated concentrations. After 24 h of exposure, the influence of EN4 on the biofilm and the viability of staphylococci was determined by CV staining (A) and plating of detached bacteria (B), respectively. The values shown are means of three independent experiments prepared in triplicates ± the SDs. Significant CV signal reduction for *S. epidermidis* 1457 compared to results for the untreated control is indicated (*, $P < 0.05$ [Mann-Whitney U test]). In panel B, dotted lines represent a 3-$\log_{10}$ CFU/ml reduction in *S. epidermidis* 1457 (◆) and Δ*ica* (◇) from untreated samples.

EN4 acts against staphylococci independently of growth phase and PIA-mediated biofilm. IAI are mainly caused by staphylococci growing in biofilms. Therefore, the effect of EN4 on staphylococci in the stationary growth phase, which is believed to reflect the status of biofilm-embedded bacteria (24), was studied. Interestingly, the transition from the logarithmic to the stationary growth phase did not decrease bacterial susceptibility to EN4, as evidenced by comparable MBC values for logarithmically (MBC_{log}) and stationary (MBC_{stat}) growing staphylococci (Table 3). Next, the impact of EN4 on biofilm was investigated using CV staining. EN4 at concentrations of ≥25 μg/ml significantly decreased an abundant biofilm of *S. epidermidis* 1457 (Fig. 2). The *S. epidermidis* 1457 Δ*ica* mutant deficient in PIA used as a control gave an overall low CV signal that was not influenced by EN4 (Fig. 2). Since CV does not distinguish between live and dead bacteria due to its affinity to the negatively charged molecules present both at the bacterial surface and in the biofilm matrix (25), the viability of adherent staphylococci was additionally assessed. Of note, the bactericidal activity of EN4 on *S. epidermidis* 1457 and its Δ*ica* mutant was similar. Treatment with EN4 at ≥100 μg/ml resulted in 3-$\log_{10}$ CFU/ml reduction of adherent bacteria for both strains (Fig. 2B). Similar results were obtained for other staphylococci (WSPPA, ME230, and SA113; data not shown).

These results show that EN4 is similarly active against staphylococci in the logarithmic and stationary growth phases, as well as embedded in PIA-mediated biofilm, making it promising for the treatment of IAI.

EN4 inhibits synthesis of DNA, RNA, protein, and peptidoglycan. To understand the mechanism of action of EN4, macromolecular biosynthesis assays were performed. The incorporation of ^{3}H-labeled precursors of peptidoglycan, RNA, DNA, and proteins by WSPPA was assessed in the presence of EN4, control antibiotics, and the antiseptic CHX at 4× the MIC. The control antibiotics vancomycin, actinomycin D, ciprofloxacin, and chloramphenicol reduced biosynthesis of their specific targets, peptidoglycan, RNA, DNA, and proteins, respectively (Fig. 3). Moreover, actinomycin D consequently reduced also the production of DNA and proteins. In contrast, EN4 inhibited all biosynthetic pathways. This was comparable to the mode of action of CHX and points toward a multitarget antiseptic rather than an antibiotic mechanism of action of EN4.

EN4 affects bacterial membrane integrity causing ATP leakage. To further reveal the mechanism of action of EN4, its effect on bacterial membrane integrity was studied. Flow cytometric analysis with propidium iodide and SYTO9 staining showed that the membrane integrity of *S. epidermidis* 1457 was similarly affected by treatment with bactericidal concentrations of EN4 and CHX (Fig. 4A). This is in agreement with a previous report on membranolytic properties of the extract of *Eremophila duttoni* leaves, which also contain active serrulatanes (26). Exposure to EN4 and CHX also led to ultrastructural changes of WSPPA, as shown by transmission electron microscopy. Membrane invagi-

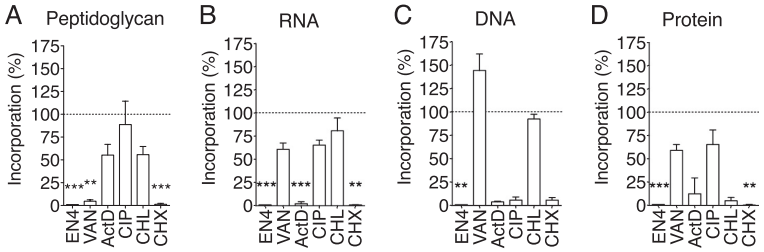

FIG 3 Inhibition of biosynthesis of macromolecules by EN4. The incorporation of [^{3}H]*N*-acetylglucosamine (A), [^{3}H]uridine (B), [^{3}H]thymidine (C), and [^{3}H]leucine (D) by WSPPA treated for 1 h with EN4, vancomycin (VAN), actinomycin D (ActD), ciprofloxacin (CIP), chloramphenicol (CHL), or chlorhexidine (CHX) at 4× the MIC was expressed as the percentage of untreated control (peptidoglycan, 3,444 ± 1,212 cpm; RNA, 115,538 ± 19,533 cpm; DNA, 13,862 ± 762 cpm; protein, 7,065 ± 323 cpm). The values shown are means of at least two independent experiments prepared in duplicates ± the SDs. Dotted lines represent 100% incorporation. Significant reduction of biosynthesis compared to results for the untreated control is indicated (*, $P < 0.05$; **, $P < 0.01$; ***, $P < 0.001$ as determined by one-way ANOVA [Kruskal-Wallis test]) with a Dunn post test).

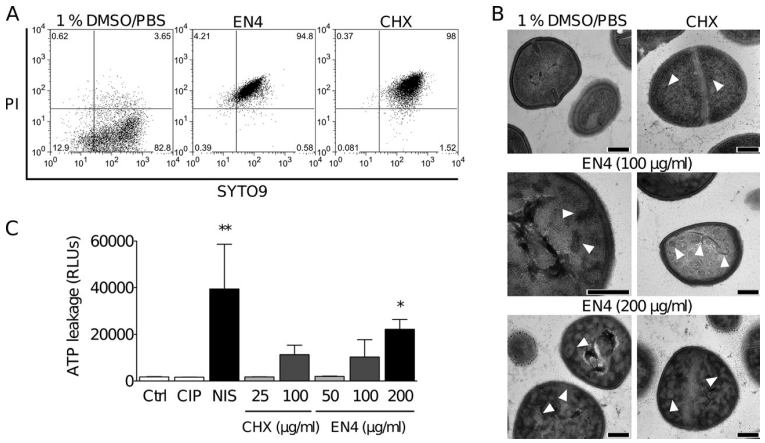

FIG 4 Effect of EN4 on bacterial membrane integrity. (A) *S. epidermidis* 1457 was incubated for 10 min with EN4 or CHX at 100 μg/ml or 1% DMSO-PBS and subsequently double stained with propidium iodide (PI) and SYTO9 and analyzed by flow cytometry. The results of one representative experiment of three performed are shown. (B) Transmission electron microscopy images of ultrathin sections of WSPPA treated for 1 h with 1% DMSO-PBS as a control, EN4 at 100 or 200 μg/ml, or 250 μg of CHX/ml. Arrowheads indicate ultrastructural changes; the bars represent 200 nm. (C) WSPPA was treated for 10 min with EN4 or CHX at 100 μg/ml, followed by centrifugation and investigation of supernatants for the presence of ATP using luciferase reaction. Nisin (NIS) and ciprofloxacin (CIP) were used as a positive and a negative control, respectively, and 1% DMSO-PBS was used as an untreated control (Ctrl). The values shown are means ± the SDs of areas under the concentration-time curve calculated for the first 30 min of luciferase reaction from at least three independent experiments prepared in duplicates. Significant ATP leakage compared to results for the untreated control is indicated (*, $P < 0.05$; **, $P < 0.01$ as determined by one-way ANOVA [Kruskal-Wallis test] with a Dunn post test).

nation and mesosome-like structures were observed after EN4 treatment; such features were previously attributed to membranolytic activity (27) (Fig. 4B). CHX mostly affected the bacterial cytoplasm causing formation of multiple intracellular granules, which possibly mirrored precipitation of cytoplasmic molecules (28).

To elucidate the physiological consequences of membrane disintegration, ATP leakage from WSPPA was measured. The results indicate that the membrane disruption by EN4 is accompanied by a concentration-dependent ATP leakage (Fig. 4C). The release of ATP was also observed for CHX and nisin, known for their membrane activity, but not for ciprofloxacin, in accordance with its intracellular mode of action on DNA gyrase and topoisomerase IV (29). Hence, EN4 was found to affect membrane integrity and to cause ATP leakage.

The tolerance of Gram-negative bacteria to EN4 can be reversed by destabilization of the outer membrane. Since the findings thus far point toward a multitarget mode of action, we wondered why EN4 selectively acts against Gram-positive bacteria. One of the causes of higher antibiotic tolerance of Gram-negative bacteria is the presence of the outer membrane, which poses an efficient permeability barrier. This barrier, however, can be breached by EDTA (30). EDTA chelates Ca^{2+} and Mg^{2+} that are involved in noncovalent binding of lipopolysaccharide molecules, and treatment with EDTA results in an increased permeability of the outer membrane (30). The induced susceptibility of Gram-negative bacteria to antibiotic/EDTA cotreatment has been reported for many antimicrobials, such as nisin (22). Therefore, to assess whether the outer membrane of Gram-negative bacteria is responsible for the lack of susceptibility to EN4, *P. aeruginosa* PA01 was exposed to EN4 and EDTA. Nisin was used as a control (Fig. 5). EDTA induced the activity of EN4 against *P. aeruginosa* PA01 up to a bactericidal level. Similar results were obtained for nisin. This effect was observed to a lesser extent for *E. coli* ATCC 25922 (data not shown), which can be explained by the fact that the impermeability of the *E. coli* membrane is less dependent on divalent cations (31). Thus, the tolerance of Gram-negative bacteria to EN4 is mediated by the outer membrane and can be reversed in the presence of EDTA.

EN4 induces the cytotoxicity of eukaryotic cells *in vitro* in a dose- and time-dependent manner. The cytotoxicity of an antimicrobial compound indicating the adverse potential is important if the compound is to be used to prevent or treat IAI. Therefore, we quantified the cytotoxicity of EN4 on eukaryotic cells by LDH release. EN4 at 25 μg/ml corresponding to MICs of *S. aureus* did not affect the viability of mouse L929 fibroblasts (Fig. 6). Cytotoxicity was observed within the range of MBCs and was time dependent. After 8 h of exposure to EN4 at 50 μg/ml, the cytotoxicity reached 50%, whereas 1 h to 2 h of contact with EN4 at 100 μg/ml had already resulted in a cytotoxicity of ca. 100%. These

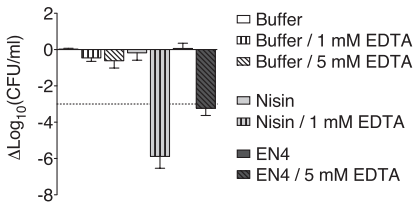

FIG 5 Effect of EN4-EDTA cotreatment on *P. aeruginosa* PA01. *P. aeruginosa* PA01 (10^6 CFU/ml) was incubated for 1 h in the presence of 200 μg of EN4/ml with or without 5 mM EDTA. Bacteria treated with 100 μg of nisin/ml with or without 1 mM EDTA served as control. The results were calculated as the $\log_{10}$ CFU/ml differences between initial and final numbers of bacteria. The dotted line represents a 3-$\log_{10}$ CFU/ml reduction from the initial inoculum. The values shown are means of three independent experiments ± the SDs.

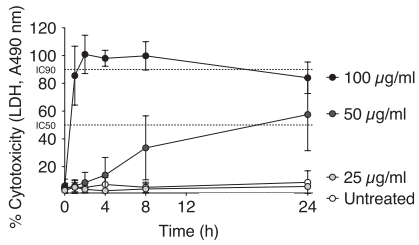

FIG 6 Cytotoxicity of EN4 on mouse L929 fibroblasts. L929 cells were treated with EN4 at antistaphylococcal concentrations, and the cytotoxic effect was assessed over time by measuring the released lactate dehydrogenase (LDH). The results are expressed as the percentage of total LDH obtained from completely lysed cells. The values shown are means of at least three independent experiments prepared in triplicates ± the SDs. The dotted lines represent inhibitory concentrations of EN4 causing the death of 50 or 90% of cells (IC_{50} and IC_{90}, respectively).

results indicate that mouse fibroblasts and staphylococci are similarly susceptible to EN4 and that EN4 therefore has a small therapeutic window *in vitro*.

EN4 exhibits neither antimicrobial nor cytotoxic activity *in vivo*. Since EN4 showed favorable *in vitro* activity against biofilm-forming staphylococci but concomitantly was cytotoxic on eukaryotic cells, we performed *in vivo* studies to test its efficacy in a previously established tissue cage model in mice. Tissue cages were infected with 4×10^3 CFU of SA113, an inoculum mimicking a perioperative infection. Injection of 4× and 10× the MICs of EN4 or 30 μg of DAP per cage was followed by an immediate infection to check whether EN4 is able to prevent bacterial adhesion and consequently clears the infection. EN4 did not decrease the number of planktonic bacteria in the TCF (Fig. 7A), whereas 30 μg of DAP per cage reduced the number of planktonic bacteria by ~2 $\log_{10}$ CFU/ml, as previously reported (32). Reinjection of EN4 at days 1 and 2 did not improve its antimicrobial effect, as opposed to DAP that cleared planktonic bacteria in 80 and 60% cages at days 2 and 3, respectively. The cure rate that corresponds to the regrowth of adherent SA113 from explanted cages was 0% for all cages (data not shown). This indicates a failure of EN4 and also, as previously described (32), of DAP in the eradication of adherent bacteria *in vivo*. In addition, the viability of leukocytes present in TCF was not affected by EN4 (Fig. 7B). In summary, despite its *in vitro* satisfactory activity, EN4 did not exhibit any antibacterial or cytotoxic properties *in vivo*, indicating an inhibition of its activity.

The activity of EN4 is inhibited by interaction with albumin. Pharmacokinetic and pharmacodynamic studies revealed that the *in vivo* efficacy of drugs strongly depends on their interactions with plasma proteins and lipids. These interactions allow a prolonged activity but may also decrease the treatment efficacy (33). Therefore, to elucidate whether interactions with proteins play a role in the inhibition of EN4 observed *in vivo*, the survival of SA113 was determined in the presence of EN4 at 100 μg/ml and various physiological fluids and proteins. TCF and NHS decreased the antibacterial activity of EN4 in a concentration-dependent manner. Similar levels of inhibition were observed for 5% TCF and for 2.5% NHS, in agreement with previous findings that TCF contains around half of the amount of proteins present in serum (34). Both TCF and NHS at 75% resulted in complete inhibition of EN4 (Fig. 8A). Furthermore, a similar effect was observed for

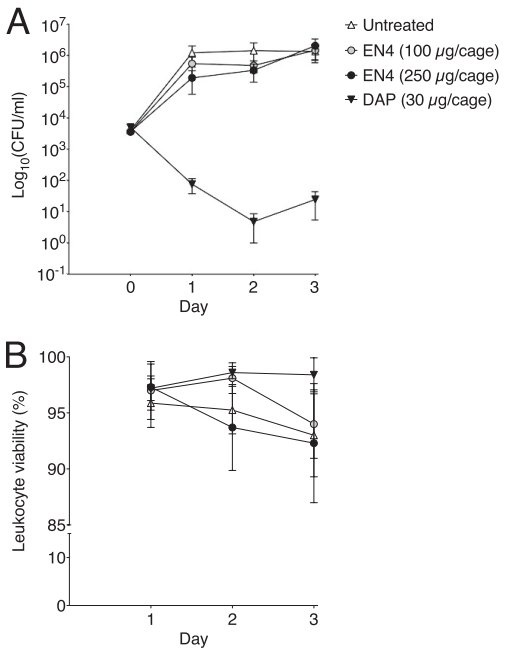

FIG 7 *In vivo* activity of EN4 in a mouse tissue cage model. The numbers of planktonic SA113 (A) and the viability of leukocytes (B) present in tissue cage fluid from cages treated with 100 or 250 μg of EN4 or 30 μg of daptomycin (DAP) and infected with 4×10^3 CFU of SA113 were investigated. Open circles indicate control mice injected with 1% DMSO-PBS. The values shown are means ± the SDs.

HSA at 0.25%, but not for fibrinogen, indicating that binding to albumin is responsible for the inhibition of EN4. Under the same conditions, ciprofloxacin, which is bound by plasma proteins up to 28% (35), was not inhibited, and at a concentration of 4× the MIC reduced the number of SA113 by 3 $\log_{10}$ CFU/ml (data not shown).

Consequently, to assess whether the eukaryotic cytotoxicity of EN4, which is observed *in vitro* but not *in vivo*, is influenced by albumin, mouse L929 fibroblasts were exposed to EN4 at 100 μg/ml in the presence of titrated concentrations of FBS, and the cytotoxic effect was measured. Whereas EN4 at 100 μg/ml in the presence of 3.75% FBS, which was used in the previous cytotoxicity experiment, induced rapid cell death, this effect was completely abolished by 10% FBS (Fig. 8B). These findings indicate that the activity of EN4 is inhibited *in vivo* by interactions with albumin.

DISCUSSION

Over the past several decades, antibiotic pressure has induced selection for resistant bacteria to every clinically used antibiotic. In the search for new antibacterial drugs, natural products derived from traditional medicinal plants are currently used as scaffolds for drug development.

The aim of the present study was to investigate EN4, a new antimicrobial compound extracted from *Eremophila neglecta*. EN4 belongs to a class of derivatives of diterpenes, one of the largest plant-derived families of secondary metabolites with antistaphylococcal activity (36). Due to this activity, the underlying premise of the present study was the potential use of EN4 in the

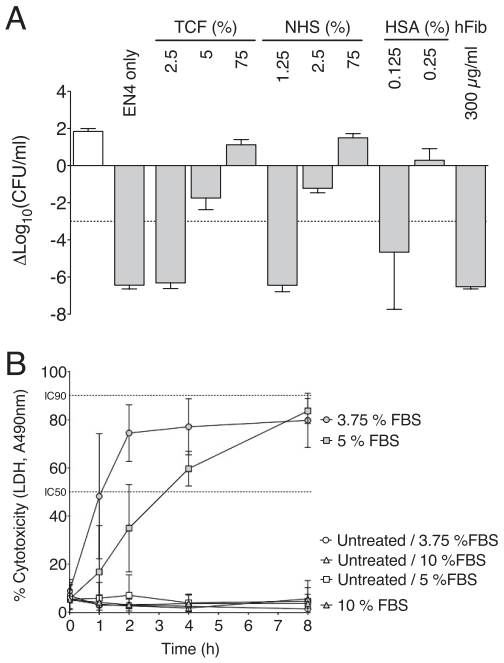

FIG 8 Inhibition of activity of EN4 by interaction with albumin. (A) Survival of SA113 (2×10^6 CFU/ml) incubated for 6 h in the presence (gray bars) and absence (white bar) of EN4 at 100 μg/ml in tryptic soy broth (TSB) supplemented with increasing concentrations of tissue cage fluid (TCF), normal human serum (NHS), human serum albumin (HSA), and human fibrinogen (hFib). The results were calculated as $\log_{10}$ CFU/ml differences between initial and final numbers of SA113. The positive values depict growth; the negative values depict killing. Means ± the SDs of three independent experiments are shown. The dotted line represents a 3-$\log_{10}$ CFU/ml reduction from the initial inoculum. (B) Cytotoxic effect of EN4 at 100 μg/ml on L929 in the presence of 3.75, 5, or 10% FBS investigated over time as described above. The means ± the SDs of three independent experiments prepared in triplicates are shown. The dotted lines represent the inhibitory concentrations of EN4 causing the death of 50 or 90% of cells (IC_{50} and IC_{90}, respectively).

prophylaxis or treatment of IAI. This is, to our knowledge, the first detailed report on an antistaphylococcal activity and the mode of action of an active compound purified from an extract from *Eremophila* plant species.

The activity of EN4 was investigated primarily against staphylococci, since these organisms are the main cause of IAI (2). EN4 showed a rapid, dose-dependent bactericidal effect on logarithmically growing staphylococci regardless of methicillin resistance. Furthermore, its activity was not affected by transition of staphylococci to the stationary phase. This is of great advantage for the treatment of IAI since agents bactericidal for logarithmically growing pathogens may fail to act on slow-growing or nongrowing bacterial populations (37).

Chronic infections with biofilms, such as IAI, pose a challenge for antimicrobials. To date, the only antibiotic with proven *in vivo* activity against staphylococcal biofilm is rifampin, which due to a rapid resistance development has to be used in combination therapy for IAI (8). In this context, EN4 reduced biofilm of *S. epidermidis* 1457 by ≥3 $\log_{10}$ CFU/ml *in vitro*, irrespective of PIA. The mechanism of its antibiofilm activity might be an efficient penetration of the biofilm matrix, which allows accessing and exerting growth-phase-independent properties against sessile bacteria. This is in contrast to DAP. Its activity is decreased against stationary-phase *S. aureus* and biofilm *in vivo* and *in vitro* (21, 32) despite its ability to penetrate the biofilm structure (38). Recent results on antibiotics such as telavancin (39) or oritavancin (40) have demonstrated activity *in vitro* against stationary-phase bacteria or biofilms; however, they still require *in vivo* evaluation. These *in vitro* properties make EN4 a promising compound despite its elevated MIC and MBC values that are often found for plant-derived products. Indeed, it has been suggested, due to the lack of antimicrobials active against nongrowing bacteria, to prioritize such compounds even if the MICs are high (41).

The studies on the mode of action revealed that EN4 affects bacterial membrane integrity, resulting in a rapid leakage of ATP. This finding can in part explain its efficacy against stationary and biofilm bacteria, since the membrane is essential for both metabolically active and inactive microorganisms. Many antibiotics target bacterial molecules that are accessible only in metabolically active bacteria, hindering the eradication of quiescent pathogens (6, 7). Therefore, the importance of membrane-active compounds in the eradication of persistent organisms has recently gained more attention (6). Furthermore, the membranolytic mode of action may prevent the development of resistance (41). This was confirmed for EN4 by several rounds of passages of SA113 in subinhibitory concentrations of EN4, where no decrease in susceptibility was observed (data not shown).

The membranolytic multitarget activity is also one of the attributes of antiseptics. In fact, EN4 exhibits properties similar to CHX, affecting bacterial membrane integrity and macromolecular biosynthesis, and thereby suggesting an antiseptic-like character. Both EN4 and CHX (42) are active against Gram-positive bacteria. EN4 also acts on mycobacteria but, in contrast to CHX, not against Gram-negative bacteria. Gram-negative bacteria are inherently less susceptible to antimicrobials due to the architecture of the cell wall (30). EN4 acts on Gram-negative bacteria only upon destabilization of the outer membrane, which further confirms that the membrane is a target of EN4.

The activity of some antiseptics such as CHX is decreased in the presence of serum (43). EN4 did not influence SA113 in the mouse tissue cage model due to inhibition by albumin. Interestingly, another diterpene compound has also failed *in vivo* (44). However, this finding has not been further investigated. The tendency for protein binding and poor tissue distribution are recognized as an issue of membrane-active agents due to their general lipophilic character (6). This is well exemplified by daptomycin, which undergoes organ-specific inhibition by pulmonary surfactants (45). Furthermore, in contrast to other membrane-active antibiotics such as daptomycin, oritavancin (46), or telavancin (47), the cost of membranolytic activity of EN4 is cytotoxicity on eukaryotic cells, which was also inhibited by serum, suggesting that these properties may be located at similar sites of the chemical structure of EN4. Nevertheless, chemical synthesis and structural modifications will be required to decrease its impairment by albumin and reduce cytotoxicity, while retaining antimicrobial properties.

In summary, the present study is a comprehensive investigation of the activity and mode of action of a plant-derived antimicrobial that impartially evaluates its possible future ap-

plications. Due to the good *in vitro* effect against stationary growing and biofilm-embedded staphylococci and at the same time poor *in vivo* activity, EN4 could serve as a fundamentally new pharmacophore scaffold for the development of a novel class of membrane-active compounds to treat biofilm-mediated infections.

ACKNOWLEDGMENTS

This study was supported by the CCMX Competence Centre for Materials Science and Technology, Lausanne, Switzerland.

We thank R. Frei, B. Berger-Bächi, F. Götz, D. Mack, U. Jenal, and S. Leibundgut-Landmann for providing bacterial and fungal strains and Z. Rajacic, F. Ferracin, A. K. John, and C. Acikgoz for technical assistance. We also thank U. Sauder for transmission electron microscopy analysis, H. Mon for extracting the EN4, and M. Battegay for helpful discussions.

REFERENCES

1. **Trampuz A, Zimmerli W.** 2006. Antimicrobial agents in orthopedic surgery: prophylaxis and treatment. Drugs **66**:1089–1105.
2. **Zimmerli W, Trampuz A, Ochsner PE.** 2004. Prosthetic-joint infections. N. Engl. J. Med. **351**:1645–1654.
3. **Fey PD, Olson ME.** 2010. Current concepts in biofilm formation of *Staphylococcus epidermidis*. Future Microbiol. **5**:917–933.
4. **Otto M.** 2011. Molecular basis of *Staphylococcus epidermidis* infections. Semin. Immunopathol. **34**:201–214.
5. **Vuong C, Voyich JM, Fischer ER, Braughton KR, Whitney AR, DeLeo FR, Otto M.** 2004. Polysaccharide intercellular adhesin (PIA) protects *Staphylococcus epidermidis* against major components of the human innate immune system. Cell Microbiol. **6**:269–275.
6. **Hurdle JG, O'Neill AJ, Chopra I, Lee RE.** 2011. Targeting bacterial membrane function: an underexploited mechanism for treating persistent infections. Nat. Rev. Microbiol. **9**:62–75.
7. **Smith PA, Romesberg FE.** 2007. Combating bacteria and drug resistance by inhibiting mechanisms of persistence and adaptation. Nat. Chem. Biol. **3**:549–556.
8. **Zimmerli W, Widmer AF, Blatter M, Frei R, Ochsner PE.** 1998. Role of rifampin for treatment of orthopedic implant-related staphylococcal infections: a randomized controlled trial. JAMA **279**:1537–1541.
9. **Cribb AB, Cribb JW.** 1981. Wild medicine in Australia. William Collins Pty, Ltd, Sydney, New South Wales, Australia.
10. **Ghisalberti EL, Jefferies PR, Hieu TNV.** 1990. Diterpenes from *Eremophila* species. Phytochemistry **29**:316–318.
11. **Ndi CP, Semple SJ, Griesser HJ, Barton MD.** 2007. Antimicrobial activity of some Australian plant species from the genus *Eremophila*. J. Basic Microbiol. **47**:158–164.
12. **Ndi CP, Semple SJ, Griesser HJ, Pyke SM, Barton MD.** 2007. Antimicrobial compounds from the Australian desert plant *Eremophila neglecta*. J. Nat. Prod. **70**:1439–1443.
13. **Adhikari RP, Cook GM, Lamont I, Lang S, Heffernan H, Smith JM.** 2002. Phenotypic and molecular characterization of community occurring, Western Samoan phage pattern methicillin-resistant *Staphylococcus aureus*. J. Antimicrob. Chemother. **50**:825–831.
14. **Herbert S, Ziebandt AK, Ohlsen K, Schafer T, Hecker M, Albrecht D, Novick R, Gotz F.** 2010. Repair of global regulators in *Staphylococcus aureus* 8325 and comparative analysis with other clinical isolates. Infect. Immun. **78**:2877–2889.
15. **Kubica GP.** 1972. Designation of strain H37Rv as the neotype of *Mycobacterium tuberculosis*. Int. J. Syst. Bacteriol. **22**:99–106.
16. **Owens W, Henley F, Barridge BD.** 1978. Hemolytic mutants of group A *Streptococcus pyogenes*. J. Clin. Microbiol. **7**:153–157.
17. **Rohde H, Frankenberger S, Zahringer U, Mack D.** 2010. Structure, function and contribution of polysaccharide intercellular adhesin (PIA) to *Staphylococcus epidermidis* biofilm formation and pathogenesis of biomaterial-associated infections. Eur. J. Cell Biol. **89**:103–111.
18. **Clinical and Laboratory Standards Institute.** 2006. Methods for dilution antimicrobial susceptibility tests for bacteria that grow aerobically; approved standard, 7th ed. CLSI document M7-A7. CLSI, Wayne, PA.
19. **Franzblau SG, Witzig RS, McLaughlin JC, Torres P, Madico G, Hernandez A, Degnan MT, Cook MB, Quenzer VK, Ferguson RM, Gilman RH.** 1998. Rapid, low-technology MIC determination with clinical *Mycobacterium tuberculosis* isolates by using the microplate Alamar Blue assay. J. Clin. Microbiol. **36**:362–366.
20. **Kuehl R, Al-Bataineh S, Gordon O, Luginbuehl R, Otto M, Textor M, Landmann R.** 2009. Furanone at subinhibitory concentrations enhances staphylococcal biofilm formation by *luxS* repression. Antimicrob. Agents Chemother. **53**:4159–4166.
21. **John AK, Schmaler M, Khanna N, Landmann R.** 2011. Reversible daptomycin tolerance of adherent staphylococci in an implant infection model. Antimicrob. Agents Chemother. **55**:3510–3516.
22. **Delves-Broughton J.** 1993. The use of EDTA to enhance the efficacy of nisin toward gram-negative bacteria. Int. Biodeterior. Biodegrad. **32**: 87–97.
23. **Palombo EA, Semple SJ.** 2002. Antibacterial activity of Australian plant extracts against methicillin-resistant *Staphylococcus aureus* (MRSA) and vancomycin-resistant enterococci (VRE). J. Basic Microbiol. **42**:444–448.
24. **Zimmerli W, Frei R, Widmer AF, Rajacic Z.** 1994. Microbiological tests to predict treatment outcome in experimental device-related infections due to *Staphylococcus aureus*. J. Antimicrob. Chemother. **33**:959–967.
25. **Peeters E, Nelis HJ, Coenye T.** 2008. Comparison of multiple methods for quantification of microbial biofilms grown in microtiter plates. J. Microbiol. Methods **72**:157–165.
26. **Tomlinson S, Palombo EA.** 2005. Characterisation of antibacterial Australian medicinal plant extracts by investigation of the mechanism of action and the effect of interfering substances. J. Basic Microbiol. **45**:363–370.
27. **Shimoda M, Ohki K, Shimamoto Y, Kohashi O.** 1995. Morphology of defensin-treated *Staphylococcus aureus*. Infect. Immun. **63**:2886–2891.
28. **Hugo WB, Longworth AR.** 1966. The effect of chlorhexidine on the electrophoretic mobility, cytoplasmic constituents, dehydrogenase activity, and cell walls of *Escherichia coli* and *Staphylococcus aureus*. J. Pharm. Pharmacol. **18**:569–578.
29. **Hoshino K, Kitamura A, Morrissey I, Sato K, Kato J, Ikeda H.** 1994. Comparison of inhibition of *Escherichia coli* topoisomerase IV by quinolones with DNA gyrase inhibition. Antimicrob. Agents Chemother. **38**: 2623–2627.
30. **Vaara M.** 1992. Agents that increase the permeability of the outer membrane. Microbiol. Rev. **56**:395–411.
31. **Helander IM, Mattila-Sandholm T.** 2000. Fluorometric assessment of gram-negative bacterial permeabilization. J. Appl. Microbiol. **88**:213–219.
32. **John AK, Baldoni D, Haschke M, Rentsch K, Schaerli P, Zimmerli W, Trampuz A.** 2009. Efficacy of daptomycin in implant-associated infection due to methicillin-resistant *Staphylococcus aureus*: importance of combination with rifampin. Antimicrob. Agents Chemother. **53**:2719–2724.
33. **Zeitlinger MA, Derendorf H, Mouton JW, Cars O, Craig WA, Andes D, Theuretzbacher U.** 2011. Protein binding: do we ever learn? Antimicrob. Agents Chemother. **55**:3067–3074.
34. **Zimmerli W, Waldvogel FA, Vaudaux P, Nydegger UE.** 1982. Pathogenesis of foreign body infection: description and characteristics of an animal model. J. Infect. Dis. **146**:487–497.
35. **Chin NX, Neu HC.** 1984. Ciprofloxacin, a quinolone carboxylic acid compound active against aerobic and anaerobic bacteria. Antimicrob. Agents Chemother. **25**:319–326.
36. **Gibbons S.** 2004. Anti-staphylococcal plant natural products. Nat. Prod. Rep. **21**:263–277.
37. **Lewis K.** 2007. Persister cells, dormancy, and infectious disease. Nat. Rev. Microbiol. **5**:48–56.
38. **Stewart PS, Davison WM, Steenbergen JN.** 2009. Daptomycin rapidly penetrates a *Staphylococcus epidermidis* biofilm. Antimicrob. Agents Chemother. **53**:3505–3507.
39. **Gander S, Kinnaird A, Finch R.** 2005. Telavancin: in vitro activity against staphylococci in a biofilm model. J. Antimicrob. Chemother. **56**:337–343.
40. **Belley A, Neesham-Grenon E, McKay G, Arhin FF, Harris R, Beveridge T, Parr TR, Jr, Moeck G.** 2009. Oritavancin kills stationary-phase and biofilm *Staphylococcus aureus* cells *in vitro*. Antimicrob. Agents Chemother. **53**:918–925.
41. **Hu Y, Shamaei-Tousi A, Liu Y, Coates A.** 2010. A new approach for the discovery of antibiotics by targeting non-multiplying bacteria: a novel topical antibiotic for staphylococcal infections. PLoS One **5**:e11818. doi: 10.1371/journal.pone.0011818.
42. **McDonnell G, Russell AD.** 1999. Antiseptics and disinfectants: activity, action, and resistance. Clin. Microbiol. Rev. **12**:147–179.

43. **Russell AD, Day MJ.** 1993. Antibacterial activity of chlorhexidine. J. Hosp. Infect. **25**:229–238.
44. **Woldemichael GM, Wachter G, Singh MP, Maiese WM, Timmermann BN.** 2003. Antibacterial diterpenes from *Calceolaria pinifolia*. J. Nat. Prod. **66**:242–246.
45. **Silverman JA, Mortin LI, Vanpraagh AD, LI T, Alder J.** 2005. Inhibition of daptomycin by pulmonary surfactant: in vitro modeling and clinical impact. J. Infect. Dis. **191**:2149–2152.
46. **Domenech O, Francius G, Tulkens PM, Van Bambeke F, Dufrene Y, Mingeot-Leclercq MP.** 2009. Interactions of oritavancin, a new lipoglycopeptide derived from vancomycin, with phospholipid bilayers: effect on membrane permeability and nanoscale lipid membrane organization. Biochim. Biophys. Acta **1788**:1832–1840.
47. **Higgins DL, Chang R, Debabov DV, Leung J, Wu T, Krause KM, Sandvik E, Hubbard JM, Kaniga K, Schmidt DE, Jr, Gao Q, Cass RT, Karr DE, Benton BM, Humphrey PP.** 2005. Telavancin, a multifunctional lipoglycopeptide, disrupts both cell wall synthesis and cell membrane integrity in methicillin-resistant *Staphylococcus aureus*. Antimicrob. Agents Chemother. **49**:1127–1134.
48. **Clinical and Laboratory Standards Institute.** 2008. Reference method for broth dilution antifungal susceptibility testing of yeasts; approved standard, 3rd ed. CLSI document M27-A3. CLSI, Wayne, PA.

II. Assessment of antiadhesive and antibacterial properties of novel implant coatings based on PMOXA, PHEMA and PEGMA polymer brushes covalently functionalised with vancomycin

As described in the aim of the thesis, we also investigated the properties of innovative antifouling polymers functionalised with an antimicrobial agent. EN4 was chosen to ultimately serve as a novel bioactive component of those coatings and vancomycin-as a control antibiotic, since its antimicrobial activity upon covalent coupling has already been reported [7-9]. These dual-function (antifouling-antimicrobial) polymers could be used for preparation of anti-infective implants and other medical devices.

We analysed surfaces coated with PMOXA [65], which were prepared by the group at the ETH Zürich, as well as with PEGMA and PHEMA [66], provided by collaborators from the EPFL Lausanne. PMOXA, PEGMA and PHEMA with and without covalent functionalisation with vancomycin *via* either its amino ($-NH_2$) or carboxylic (-COOH) group were investigated.

In the first step, anti-adhesive properties against *S. epidermidis* 1457 ($2x10^5$ CFU/cm^2) growing in biofilm for 24 h was assessed using the crystal violet (CV) staining. The results revealed a great anti-fouling potential of all investigated surfaces (Fig. 1). These findings were further confirmed by means of Live/Dead staining in microscopic analysis of surfaces incubated for 6 h with *S. epidermidis* 1457 ($1x10^7$ CFU/cm^2) (Fig. 2a-c). As this staining additionally allows distinguishing between viable and dead bacteria we could demonstrate that the observed reduction in bacterial adhesion was caused by nonfouling, but not antibacterial, properties of investigated surfaces (Fig. 2c). Similarly, detachment of adherent bacteria by sonication followed by determination of CFUs further confirmed the antiadhesive effect of polymer brushes without any activity of coupled vancomycin (Fig. 3). Thus, we next determined MICs and MBCs of vancomycin and a powder form of PMOXA-vancomycin constructs against *S. epidermidis* 1457. We observed a decrease of in-solution activity of vancomycin upon covalent coupling to PMOXA, especially when the amine group of antibiotic

was engaged in the coupling (Table 1). These results indicate that covalent surface coupling of vancomycin, especially *via* the amine groups involved in interactions with its D-alanyl-D-alanine target, may decrease its antimicrobial properties.

However, additional factors could contribute to this effect. These are the surface concentration of vancomycin and the possibility that repulsive forces from the non-fouling polymers prevent not only the bacterial adhesion but also a direct contact of bacteria to vancomycin, which is required for its antibacterial activity.

We therefore first sought to determine the surface-concentration of vancomycin by enzyme-linked immunosorbent assay (ELISA). The ELISA protocol necessary to reliably determine this concentration was established. Using this protocol the amount of vancomycin attached to the PHEMA surfaces was shown to be below 0.02 ng/1cm^2. To ascertain if this amount of bound vancomycin would be sufficient to kill 200 CFU of *S. epidermidis* 1457, a standard inoculum used in our killing experiment, we titrated the concentrations of the antibiotic in solution. The resulted minimal killing concentration ranged between 500 ng and 1 000 ng/1cm^2. This range is well above the concentration of surface-bound vancomycin, which we determined by ELISA. Therefore, the insufficient surface-concentration of vancomycin can additionally explain why we failed to observe antibacterial effect of vancomycin-functionalised surfaces.

Next, to assess whether the antifouling properties of PHEMA brushes can interfere with the access of bacteria to surface-bound vancomycin and thereby prevent its antibacterial properties, PHEMA surfaces with brush density of 1%, 10%, 50% and 100% with and without covalently-coupled vancomycin were investigated. The amount of surface-bound vancomycin was independent of the density of the brushes, as determined by ELISA. There was no decrease in the viability observed with all brush densities for *S. epidermidis* 1457 as determined by LIVE/DEAD staining. Since a previous study has shown an effect of PEG-bound vancomycin surfaces against *Bacillus subtilis* 6633 [9], which is more susceptible to vancomycin, we decided to use this strain in our experiments. Consistently, exposure of *Bacillus subtilis* 6633 to PHEMA-vancomycin did not influence the bacterial viability. Altogether, these results indicate no interference

of the antifoulig forces imposed by PHEMA brushes with the access of bacteria to the surface-bound vancomycin. However, as the surface concentration of vancomycin was below the bactericidal threshold, the possible influence of antifouling forces cannot be entirely ruled out.

Taken together, we could show a great antifouling potential of PMOXA, PEGMA and PHEMA polymer brushes. However, covalent functionalisation with vancomycin did not exhibit antibacterial effect most likely due to a partial decrease in activity of vancomycin upon coupling and insufficient surface-concentration.

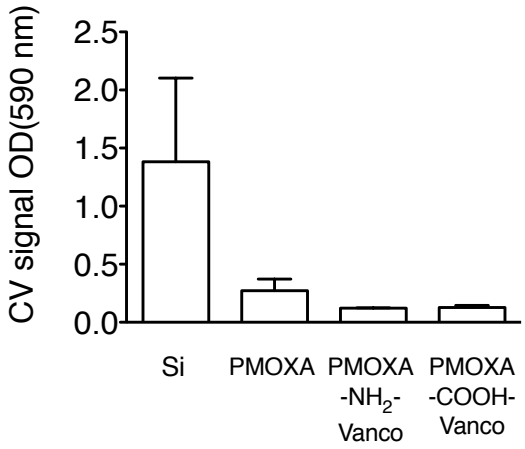

Figure 1 Antiadhesive properties of PMOXA-based surfaces. Indicated surfaces were incubated for 24 h with *S. epidermidis* 1457 ($2x10^5$ CFU/cm^2) followed by determination of biofilm formation using CV staining. Silicone surfaces (Si) served as a fouling control. Experiments performed by C. Acikgöz (ETH Zürich).

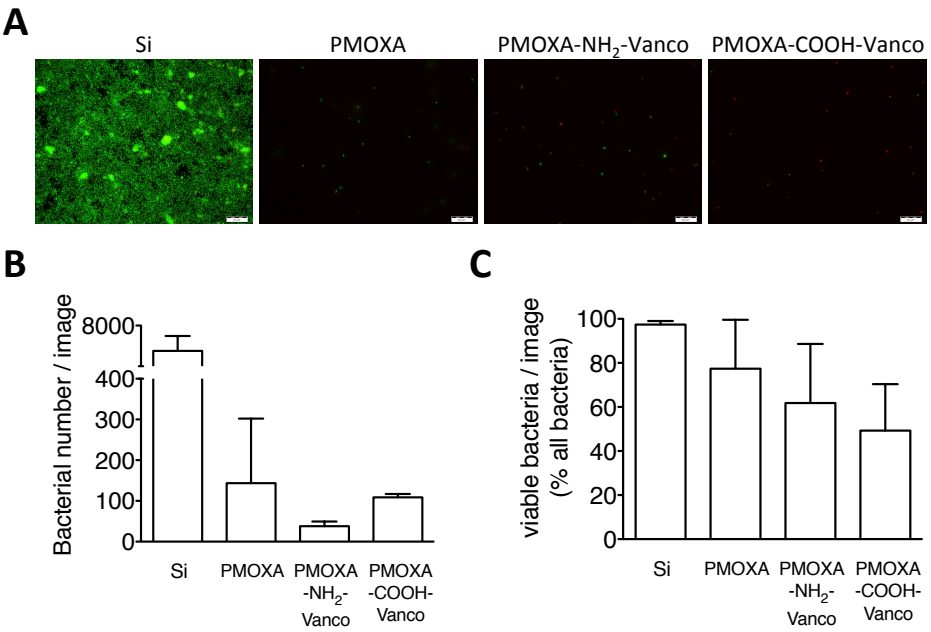

Figure 2 Confirmation of antiadhesive properties of PMOXA-based surfaces using Live/Dead staining. Microscopic analysis of surfaces stained with Live/Dead reagents upon incubation with *S. epidermidis* 1457 ($1x10^7$ CFU/cm^2) for 6 h. Representative pictures of central parts of surfaces are presented (A). The numbers of bacteria per image were assessed by ImageJ software (B), followed by determination of viable bacteria (green), which was then calculated as the percentage of all microorganisms (C).

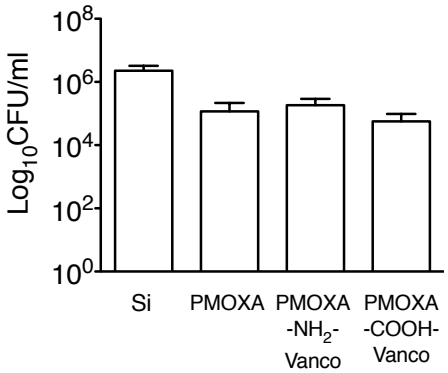

Figure 3 Determination of adherent bacterial numbers. To ascertain the results obtained from the microscopic analysis surfaces were sonicated and the counts of adherent *S. epidermidis* 1457 determined by plating. Similar reduction in adherent bacteria was observed for all PMOXA-based surfaces without an additional effect of functionalisation with vancomycin.

Table 1 Determination of the MIC and MBC of indicated substances for *S. epidermidis* 1457 was performed according to the Clinical and Laboratory Standards Institute. (*Methods for dilution antimicrobial susceptibility tests for bacteria that grow aerobically*; approved standard, 7th ed., 2005 CLSI document M7-A7. CLSI, Wayne, PA.)

	MIC* (µg/ml)	MBC* (µg/ml)
Vancomycin	4	4
PMOXA-NH_2-Vanco	16	64
PMOXA-COOH-Vanco	4	16

*MIC and MBC presented as the amount of vancomycin in the construct

III. Foreign body infection models to study host-pathogen response and antimicrobial tolerance of bacterial biofilm

(Invited review submitted to *Antibiotics* in April 2014)

Antibiotics **2013**, *2*, 1-x manuscripts; doi:10.3390/antibiotics20x000x

OPEN ACCESS

antibiotics

ISSN 2079-6382

www.mdpi.com/journal/antibiotics

Review

Foreign body infection models to study host-pathogen response and antimicrobial tolerance of bacterial biofilm

Justyna Nowakowska [1], Regine Landmann [2] and Nina Khanna [1,*]

[1] Infection Biology, Department of Biomedicine, University and University Hospital Basel, Hebelstrasse 20, 4031 Basel, Switzerland

[2] Vice dean Medical Faculty University Basel, Klingelbergstrasse 61, 4056 Basel

E-Mails: justyna.nowakowska@unibas.ch (J. N.); regine.landmann@unibas.ch (R. L.); nina.khanna@usb.ch (N. K.)

* Author to whom correspondence should be addressed; Tel.: +41 61 328 73 25; Fax: +41 61 265 31 98

Received: / Accepted: / Published:

Abstract: The number of implanted medical devices is steadily increasing and has become an effective intervention improving life quality, but still carries the risk of infection. These infections are mainly caused by biofilm-forming staphylococci that are difficult to treat due to the decreased susceptibility to both antibiotics and host defense mechanisms. To understand the particular pathogenesis and treatment tolerance of implant-associated infection (IAI) animal models that closely resemble human disease are needed. Applications of the tissue cage and catheter abscess foreign body infection models in the mouse will be discussed herein. Both models allow the investigation of biofilm and virulence of various bacterial species and a comprehensive insight into the host response at the same time. They have also been proven to serve as very suitable tools to study the anti-adhesive and anti-infective efficacy of different biomaterial coatings. The tissue cage model can additionally be used to determine pharmacokinetics, efficacy and cytotoxicity of antimicrobial compounds as the tissue cage fluid can be aspirated repeatedly without the need to sacrifice the animal. Moreover, with the advance in innovative imaging systems in rodents, these models may offer new diagnostic measures of infection. In summary, animal foreign body infection models are important tools in the development of new antimicrobials against IAI and can help to elucidate the complex interactions between bacteria, the host immune system and prosthetic materials.

Antibiotics **2013**, *2*

Keywords: foreign body infection; mouse; staphylococcus; catheter abscess model; tissue cage model.

---

1. Introduction

Among the early and late complications of medical implants, implant-associated infection (IAI) is one of the most serious that is associated with a high morbidity [1]. The average rate of IAI ranges between 2% to 40% depending on the type of surgical implant [2]. These infections occur either perioperatively, by direct bacterial contamination during surgery or wound healing, or by the haematogenous route through blood or lymph [3]. More than 50% of IAI is caused by staphylococci (*Staphylococcus* (*S.*) *aureus* and *S. epidermidis*), followed by streptococci (7%) and *Propionibacterium spp.* (6%). Gram-negative bacilli, enterococci and polymicrobial infections are less frequent (less than 5 % each) [3,4]. Over the last four decades methicillin resistant *S. aureus* (MRSA) has created additional therapeutical challenges. Importantly, it has been estimated that in a high endemicity setting more than half of surgical-site infections due to staphylococci can be caused by MRSA [5].

An important feature of IAI is that the presence of a foreign body increases the susceptibility to staphylococcal infection by at least 10,000-fold [6,7]. Hence, these infections can arise from only a few bacteria inoculated locally during surgery or during bacteraemia. They remain local, but if infection becomes chronic, the implant has to be removed or replaced for healing.

The main reason for persistence of IAI is the microbial ability to form biofilm. Staphylococci use biofilm as a dynamic survival strategy, which decreases their susceptibility to both antimicrobials and host response. As the decreased antimicrobial susceptibility is not driven by acquisition of any resistance genes and biofilm-embedded bacteria are isogenic with their planktonic antibiotic-susceptible counterparts this phenomenon is referred to as bacterial tolerance. Indeed, proteomic and RNA profiling studies have shown altered gene expression patterns in staphylococcal biofilms, indicating metabolic adaptation [8]. Although the molecular details of biofilm development have been thoroughly investigated, the exact mechanism of its antimicrobial tolerance remains still elusive. Biofilm allows bacteria to stay in a metabolically quiescent state as a multilayered community embedded in a self-produced extracellular matrix. The matrix can be composed of polysaccharide intercellular adhesin (PIA), the production of which is mediated by the *ica*-locus encoded enzymes, of fibronectin-binding protein and other large proteins, and of extracellular DNA, which is released by bacterial lysis [9]. The expression of these components is governed by four major transcriptional regulators, which are the quorum sensing systems *agr* and *luxS* as well as *sarA* and the stress sigma factor s^B. They interact in a complex network and have variable effects in *S. aureus and S. epidermidis*. Environmental factors like oxygen and glucose levels

contribute as well to the formation, maturation and dispersal of biofilms [9,10]. *Agr*-regulated phenol-soluble modulins (PSM) are of particular importance in structuring and detachment of staphylococcal biofilm and thereby facilitate bacterial dissemination. Thus, PSM have recently been postulated as potential target for the treatment of *S. aureus* infections [11,12].

As a consequence of the biofilm-induced bacterial tolerance antimicrobial treatment of IAI remains challenging. To overcome this tolerance, antimicrobials need to penetrate the biofilm and act on adherent stationary-phase bacteria. Of note, some antibiotics, e.g. vancomycin and daptomycin, are able to penetrate the biofilm but eventually fail to eradicate the adherent bacteria [13,14]. So far, most of the known antibiotics are dependent on the metabolic status of bacteria hindering the eradication of biofilm-embedded quiescent pathogens. The only antibiotic with a proven activity against metabolically inactive staphylococci in IAI is rifampicin [15]. However, due to a rapid emergence of resistance, rifampicin has to be combined with other antibiotics [16,17]. The emergence of resistant bacteria (i.e. MRSA and methicillin resistant *S. epidermidis*) creates additional challenges, as resistance is associated with a poorer response to therapy. Thus, antimicrobial therapy of biofilm-mediated infections is often unsuccessful unless the biofilm is removed by surgical debridement [16]. Therefore, novel anti-biofilm agents, such as the acyldepsipeptide (ADEP4) [18], as well as antifouling and antimicrobial implant coatings[19] are under investigation.

A further important reason for the persistence of staphylococcal biofilm on foreign bodies is its recalcitrance to host immune responses [20]. Contact with implant surface induces impaired granulocyte functions, including reduced bactericidal activity, impaired oxidative metabolism and spontaneous granular enzyme release [21,22]. Interestingly, human PMNs recovered from patients with osteomyelitis exhibited highly activated phenotype with preserved production of superoxide but impaired chemotactic abilities [23,24]. Moreover, biofilm burden seems to be also dependent on macrophage proinflammatory responses highlighting mutual influence between host cells and biofilm [25].

Taken together, IAI belongs to the leading infections in today's medicine. To better understand the biofilm antimicrobial tolerance, host response and molecular pathogenesis as well as to develop effective antimicrobials for these infections adequate animal models are needed. Depending on the question to study, different foreign body infection models can be used.

2. Orthopaedic Implant Infection Models

There are various orthopaedic animal models for investigation of IAI. Many of them involve insertion of implants into bones of the lower limb. They are suitable for studies of materials and their interactions with the bone tissue. The most recent models use bacteria-loaded pins inserted into the mouse tibia [26] or bacteria-loaded holes drilled with screws in the rabbit femur [27]. Other models in rabbits and sheep introduce bacteria in cement into the medullary cavity of tibia [28] or during a tibia osteotomy with a locking

compression plate [29], respectively. All these models were recently comprehensively described [19] and are beyond the scope of this review. The differences between the orthopaedic and the subcutaneous foreign body models described here are summarised in Table 1. Orthopaedic models allow imaging, bacteriological and histological analyses only after sacrifice. They are not suitable for multiple sampling to test antimicrobial activity, pharmacokinetics and to investigate the immune response. Furthermore, these models often require sophisticated surgical techniques and high numbers of large animals in order to determine the time course of infection.

A recent study has overcome these drawbacks by using a genetically engineered mouse strain with fluorescent myeloid cells and infection with bioluminescent staphylococci. The authors inoculated the knee joints after placement of a wire implant into the mouse femur. They determined the quantity and localisation of both bacteria and neutrophils noninvasively and longitudinally by 3D fluorescence and bioluminescence imaging and they assessed the anatomical bone changes using micro-computed tomography registration. However, the advanced equipment required for analysis does not yet allow application of this method in practice to various animal species and bacterial clinical isolates [30].

In summary, IAI models in bone are of a great interest, as they closely mirror the clinical situation of bone-inserted implants. Nevertheless until today they are technically difficult and do not allow an easy assessment of the antibacterial effect and host immune response.

However, subcutaneous foreign body models such as the tissue cage and the catheter model can well simulate extravascular IAI in human settings [22]. They additionally allow accurate analysis of planktonic and adherent bacteria, therapeutic efficacy and host responses. Moreover, these models can easily be applied to study implants of various materials, their interactions with the host immune system and with the bacteria over time without the need to sacrifice an animal. Both models can be used in guinea pigs, rats and mice. Their application, advantages and disadvantages are described below.

3. Tissue Cage Infection Model

3.1. Tissue cage model in different animal species

The tissue cage model was first described by Zimmerli in 1982 [7]. He established the short-term antibiotic therapy of staphylococcal foreign body infection in guinea pigs [31,32] and was the first to observe the granulocyte defects at the site of a foreign body [21]. Since then guinea pigs have been proven as a suitable model for therapeutic studies of IAI [15,33-35]. Guinea pigs present the advantage of a high susceptibility to staphylococcal infection, the infection remains strictly local and pharmaco-dynamics and -kinetics of humans can be simulated [36] (Table 1). A drawback is the intolerance of guinea pigs to prolonged antibiotic treatment as well as to betalactams [36]. Although rats tolerate these antibiotic treatments, they have a 100-fold lower susceptibility to staphylococci. Thus, unless very high inocula are

applied, a high proportion of these animals spontaneously clear staphylococcal implant infection [37]. The availability of genetically engineered mice, their susceptibility to staphylococcal infection and their tolerance to antibiotics, the easy manufacturing of genetically modified bacteria and advanced animal imaging facilities, allowed mice to become an attractive alternative to study pathogenesis and therapy of IAI using tissue cages.

3.2. Tissue cage infection model in the mouse

3.2.1. Technique

Cylindrical tissue cages (8.5 × 1 × 30 mm, volume 1.9 mL) [36] are manufactured from Teflon or from any type of metal or alloy [38]. The wall of each cage is perforated with 130 regularly spaced 1.0-mm holes. A hole of 2 mm in diameter is placed both in the Teflon lid and in the bottom of the cage. To increase the surface area, cages can be filled with beads from sinter glass or from any material. Cages are implanted subcutaneously into the back of anesthetized 12- to 15-week-old C57BL/6 mice (Figure 1 a, b). Bacteria are injected directly into the cage either perioperatively or around 14 days postoperatively. In contrast to guinea pigs, *S. epidermidis* should be injected only peri-operatively as it can be spontaneously cleared if injected postoperatively [38]. *S. aureus* needs to be injected post-operatively after wound healing to avoid the risk of surgical site infections with deep abscesses. Sterility before infection and the establishment of an infection are confirmed by quantitative culture of tissue cage fluid (TCF). The infection with and without subsequent therapy is usually followed for 14 days, however mice tolerate as well a prolonged infection and antimicrobial treatment without systemic signs (unpublished data). The inflammation remains localized and animals in general do not develop bacteraemia.

The load of planktonic bacteria and the local host immune response to infection are assessed by repetitive puncture of TCF (Figure 1. c). TCF resembles the extracellular fluid with about 50% of the serum protein concentration, similarly to noninflammatory interstitial fluid [7]. Antimicrobials can be either injected directly into the cage or applied by all other routes (intraperitoneally (i.p.), subcutaneously, orally, intravenously). The efficacy of antimicrobial treatment is monitored on planktonic bacteria in TCF and on implant-associated microorganisms after explantation. Several applications of the mouse tissue cage model are described below.

3.2.2. Assessment of virulence of bacterial species

The inoculum necessary for induction of a persistent infection in tissue cages of C57BL/6 mice is assessed by identifying the minimal infective dose (MID) of the investigated bacterial species or strains. The MID is an indicator of staphylococcal virulence in this model. For *S. aureus* it ranges between approximately $5x10^2$-$5x10^3$ colony-forming units (CFU)/cage [13,39]. In contrast, the MID of *S. epidermidis*

is much higher, namely above 10^6 CFU/cage, and spontaneous healing occurs, if bacteria are not injected during the perioperative period [38]. In infections with isogenic mutants of staphylococci, which have specific deletions of virulence genes, a higher MID may be required. This was for example shown for the *S. aureus dlt*⁻ mutant, which manifested a 100-fold higher MID than the parental wild type (wt) strain. This mutant expresses non-alanylated lipoteichoic acid, which renders the surface charge of the bacterial cell wall more negative, and thus more susceptible to cationic antimicrobial peptides. Therefore, the *dlt*⁻ mutant is more easily cleared unless the infective dose is increased [40]. On the other hand, the virulence of *S. aureus* mutants lacking the *ica* gene responsible for polysaccharide-mediated biofilm formation, has not been attenuated in the tissue cage model [41]. Even in competitive infection studies with simultaneous inoculation of both wt and *ica*⁻ *S. aureus*, the *ica* mutant did not grow less efficiently than the wt [42]. These observations were surprising, since *ica* expression is considered one of the crucial contributors to staphylococcal biofilm, which is generally considered as the major virulence factor in IAI. Indeed, in contrast to the *S. aureus* counterpart, *ica* mutants of *S. epidermidis*, , showed reduced virulence in the tissue cage model [42] and in catheter-associated infections both in rats [43] and in mice in our own studies [38,44]. Thus, our results illustrate that conclusions on virulence in IAI models can only be applied to the particular bacterial species and the exact model used in the given investigation, i.e. for *S. epidermidis* biofilm plays a more significant role in virulence than for *S. aureus,* which has multiple factors mediating adherence [45,46].

The tissue cage can be considered as a closed *in vivo* system, in which any bacterial species is exposed to host phagocytes. In that context the model has been shown to be suitable to assess the role of a sialidase in *Capnocytophaga canimorsus in vivo*. This commensal bacterium was shown to survive *in vitro* only in the presence of human cells, where it could feed on host glycoproteins using its surface-exposed sialidase. This behaviour could also be demonstrated by infection with wt but not with sialidase-deficient bacteria in normal and leukocyte-depleted tissue cages [47].

Another interesting feature to study biofilm *in vivo* is to combine it with bioluminescence imaging. A chromosomally expressed *lux* operon in *S. aureus* renders bacteria visible in a CCD camera and allows close observation of the bacterial load during infection [48]. A more sophisticated application of this technique is to follow promoter activity of a virulence factor in *S. aureus*. For this aim we transduced a specific promoter-regulated *lux* operon into wt or isogenic mutant of *S. aureus* [49]. We could demonstrate an increasing activity of the *hla* promoter during eight days of a tissue cage infection and its modulation by transcriptional regulators *s*B and *sae* [49] (**Figure 2**). Nevertheless, the targeted bioluminescence is limited by its relatively low sensitivity due to the single copy of the gene in question.

3.2.3. Assessment of host defense in the tissue cage

TCF is an extracellular fluid containing myeloid cells as innate defense system. Strikingly, granulocytes in the neighbourhood of a tissue cage display weakened functions, including bactericidal activity, oxygen burst, phagocytosis and spontaneous loss of granules [21]. To investigate in depth the role of leukocyte subpopulations in the defense against tissue cage infections, experiments in leukocyte- or granulocyte-depleted mice can be performed. Furthermore, the mechanisms of host defense in this infection model can also be unravelled in knockout mouse strains with specific deficiencies of the innate immune system. As an example, we could show that *dlt*⁻ bacteria, which were cleared in *wt* mice, proliferated in TLR2-deficient host, thus identifying a role of TLR2 in murine immune defense against bacteria expressing unalanylated teichoic acids [40].

3.2.4. Assessment of antibiotic resistance in vivo

Little is known about the evolution of antibiotic resistant staphylococci during an infection. The tissue cage model provides the opportunity to investigate an antibiotic-resistant staphylococcal strain during the course of infection over a prolonged period of time (two to four weeks). Stability of genetic and phenotypic changes, which characterize the resistance, can be repeatedly evaluated in the treated or untreated tissue cage. This approach was used to investigate glycopeptide (teicoplanin)-intermediate resistance in *S. aureus* (GISA). This resistance arises from prolonged glycopeptide exposure and is the result of multiple unknown mutations leading to a common phenotype of GISA. Gene expression and phenotype were followed in isogenic GISA and wt strains without antibiotics in the tissue cage. Interestingly, teicoplanin resistance posed a fitness burden on *S. aureus*, which resulted in a negative selection *in vivo* with restoration of fitness incurring the price of resistance loss [50].

3.2.5. Pharmacokinetic (PK) studies

Small, cost-effective pre-development of *in vivo* PK and toxicity studies can be done in the mouse tissue cage model with minimal compound requirement and multiple endpoints. New compounds, which have poor *in vivo* PK profiles, can be injected directly into the cage. Better defined more advanced compound series can be assessed for their potency after intraperitoneal administration.

The goal of antibiotic treatment studies in animals is to mimic the conditions in humans. Therefore, PK of the drugs has to be adapted to those in humans. So far, PKs in our mouse tissue cage model have been determined for daptomycin with 30 mg/kg [13], 40 mg/kg [13] and 50 mg/kg [51] applied i.p. once per day [13], vancomycin 150 mg/kg three times per day and levofloxacin 150 mg/kg three times per day (unpublished results). For every antibiotic, TCF is taken at time points 0, 30 min, 60 min, 2 h, 4 h, 6 h, 8 h, 12 h and 24 h. Mean ± standard deviation (SD) values of the peak (maximum) concentration (C_{max}), the time required

to reach C_{max} (T_{max}), the trough (minimum) concentration at 24 h after dosing (C_{min}), the half-life ($t_{1/2}$), and the area under the curve over a specific time (AUC_{0-24}) can be calculated.

3.2.6. Pharmacodynamic properties and efficacy

While many *in vitro* tests can give hints on antimicrobial properties of new drugs, mouse models have been developed in order to assess their efficacy *in vivo*. This is of great interest, since *in vivo* and *in vitro* results of transcriptional regulator were found to differ [42,52]. Growth curves, minimal inhibitory and bactericidal concentrations (MIC and MBC, respectively) of each antibiotic are determined beforehand for all bacterial strains. For therapeutic studies, infected mice are treated with saline (control group) or the respective antibiotic dosage for three to four days. On day four, TCF is collected to quantify planktonic bacteria and the animals are sacrificed. Tissue cages are removed under aseptic conditions and incubated in broth for 48 h, followed by assessment of bacterial growth. A positive culture is defined as a treatment failure. The efficacy of treatment against adherent bacteria is expressed as the cure rate (in percent), defined as the number of cages without growth divided by the total number of cages in the individual treatment group. Depending on the type of antibiotic used, to avoid the carry-over effect and false negative culture animals can be kept more than four day after drug withdrawal. Using this procedure, it became evident that daptomycin is not efficacious against adherent bacteria. The tolerance of adherent *S. aureus* to daptomycin was not related to biofilm, but was likely due to enhanced membrane stability during adherence and could be reverted by addition of Ca^{2+} ions [13].

In a recent study, we investigated the antimicrobial activity and mode of action of a serrulatane compound, 8-hydroxyserrulat-14-en-19-oic acid (EN4), a diterpene isolated from the Australian plant *Eremophila neglecta*. *In vitro* EN4 elicited antimicrobial activity toward various Gram-positive bacteria in logarithmic, stationary growth phase and embedded in biofilm. Additionally, EN4 was also cytotoxic against eukaryotic cells. *In vivo* however neither bactericidal nor cytotoxic effects were present, indicating an inhibition of its activity. Inhibition assays revealed that this was caused by interaction of EN4 with albumin [39].

3.2.7. Cytotoxicity of new antimicrobial compounds against host cells

In the evaluation of new anti-infective compounds, the therapeutic window is an early predictor of success or failure in drug development. Leukocyte viability in the tissue cage is an indicator of *in vivo* drug cytotoxicity. Mechanistic aspects of eukaryotic cell death can be distinguished *ex vivo* by flow cytometric analysis of apoptosis and necrosis. The evaluation of efficacy and at the same time toxicity from one sample is particularly important for compounds with the same mechanism of action on eukaryotic and prokaryotic cells, such as e.g. silver. Indeed, silver ions, which undergo a revival as

antibacterial compounds, block respiratory enzymes both in human cells and in bacteria. Thus, the therapeutic window is likely very small and the silver concentration the eukaryotic cells are exposed to must be limited e.g. by applying slow-release compounds. We have tested *in vivo* the bactericidal activity of silver coordination polymers coated on titanium cages. Indeed, the bactericidal activity on planktonic *S. epidermidis* was paralleled by a transient decrease in leukocyte viability in the cage [53]. However, histological investigation of the surrounding tissue of silver-coated cages including the capsule and the muscle did not show increased inflammation or necrosis compared to uncoated cages (Fromm K. and Khanna N., unpublished data).

3.2.8. Properties of different tissue cage materials

Tissue cages can be manufactured from Teflon, ceramics or any metal or alloy. We found that the metal titanium or steel played a minor role in propensity to biofilm generation or in persistence of staphylococcal infection [38].

4. Catheter Abscess Model

Another model of IAI is a static subcutaneous catheter abscess model in which, contrary to the tissue cage model, a systemic infection may develop due to an unrestricted blood flow and inflammatory cell recruitment. In that model bacteria are either precultured overnight with the catheter *in vitro* to form biofilm or bacteria are added when the catheter is implanted into subcutaneous tissue in the flank of 10- to 14-week old mice (Figure 3). An abscess formation occurs, which can be quantified by the oedema cross-section dimension. Infection with a high inoculum of virulent *S. aureus* strains leads to bacteremia and sepsis and is not advised with this model. Animals have to be sacrificed at different time points for further analysis. Bacteria that are adherent to the catheter or present in the tissue surrounding the catheter are quantified one to eight weeks after infection. The cytotoxicity of investigated compound can be assessed by analysis of the subcutaneous tissue around the implant.

Various catheter models have been used by other groups to study IAI. In a central venous [43] and a subcutaneous catheter in the rat [44] *S. epidermidis* infections occurred more often with a biofilm-*ica*-positive than with a biofilm-negative strain. In a study on infection with a bioluminescent *S. aureus* the efficacy of a 4-day rifampicin treatment upon an established biofilm was well documented with this noninvasive method [54].

We used the catheter model to study the mechanism, by which biofilm protects *S. epidermidis* from clearance by host defense. The complement component 3 (C3) activation and C3b/IgG deposition on *S. epidermidis* as well as granulocyte-dependent killing of wt and *ica*$^-$ bacteria were compared. We found an enhanced C3 activation by biofilm-positive *S. epidermidis*, yet a decreased complement deposition. These

findings correlated with a stronger survival of wt *S. epidermidis* on catheters [20]. This is the first observation regarding the molecular pathophysiology of host defense against biofilm. Importantly, the host response to catheter infection can differ from the tissue cage, as the recruitment of neutrophils to the catheter can be limited due to the low number of planktonic bacteria [55]. Indeed, macrophages, but not neutrophils, have recently been shown to play an important role in the controlling of staphylococcal biofilm in the catheter infection model [25].

The catheter model is also suitable to study biofilm in other bacteria such as *Pseudomonas aeruginosa*. The role of cyclic di-GMP regulation in small colony variant (SCV) formation, biofilm production and persistence was investigated with mutants overexpressing a diguanylate cyclase YfiN, responsible for the SCV phenotype. Both in single and competitive catheter infections wt bacteria were found to be less persistent after eight weeks despite an initial growth advantage [56].

Altogether, there are numerous applications of the catheter model. In contrast to the tissue cage, inflammation is not localised within the device, but can also induce systemic infection. Toxicity of antibacterial substances can be assessed in the surrounding tissue, which contains, similarly to the tissue cage model, immune and stromal cells.

5. Disadvantages of subcutaneous animal foreign body models

Despite the advantages of these models, they also have some limitations. With the tissue cage and catheter model, only general aspects of host response and biocompatibility can be analyzed. However, specific problems related to bone implants, vascular grafts or neurosurgical devices cannot be studied. In addition, for pharmacokinetic and pharmacodynamic studies, the special situation of metabolic processes in small animals as compared to humans has to be considered.

6. Conclusions

The two described subcutaneous IAI models are well-established long-standing *in vivo* models in which microbiological, pharmacological, immunological, and chemical properties of biomedical implants can be assessed. Both models are easy to perform. Up to 20 animals can be implanted, infected and treated daily by one person. Subcutaneous tissue cages or catheters are well tolerated by mice, even for prolonged periods exceeding one month. The particular advantage of the tissue cage model is the closed system that allows the repeated assessment of the interactions between antimicrobials, host responses and biofilm-forming bacteria *in vivo*. The fact that the cages can be manufactured from any material, which is used in orthopaedic implants, makes the model relevant for pre-clinical application. The cages can be coated with any new compound as local anti-infective or anti-adhesive substance to prevent IAI. The particular advantage of the catheter infection model is its suitability for the molecular *in vivo* studies of biofilm with

various Gram-positive and Gram-negative bacteria. Current and future work focuses on the development of implant surfaces with covalently coated or triggered-release antimicrobials to prevent IAI and on new compounds that inhibit the formation of biofilm.

Acknowledgments

The authors thank Maja Weisser, Anne-Kathrin Woischnig and Werner Zimmerli for critical discussion and review as well as Zarko Rajacic for technical assistance.

Conflicts of Interest

The authors have no conflict of interest.

Antibiotics **2013**, *2* 12

Figure 1. (a) Teflon cage with glass sinter beads. **(b)** Mouse ten days after implantation. **(c)** Aspiration of tissue cage fluid.

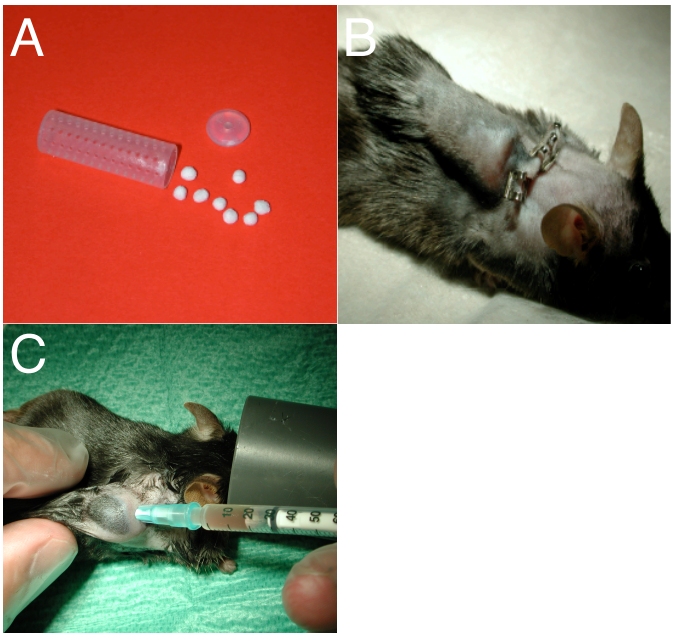

Figure 2. Visualization of *S. aureus hla*- promoter activity using luxABCD integration vector. The p*hla-lux* construct was introduced via a single chromosomal insertion in the *S. aureus* wt strain Newman and its isogenic *sae* and *s*B regulator mutants. *Hla*-expression was followed in real-time at repeated time points of infection (here day eight) of a mouse tissue cage using a photon-sensitive camera. The activation of *hla* in the *s*B-deficient strain and the repression to background levels in a *sae*-deficient strain relative to the *hla*-expression in the wt is shown. Bacterial numbers did not differ among the different strains [49].

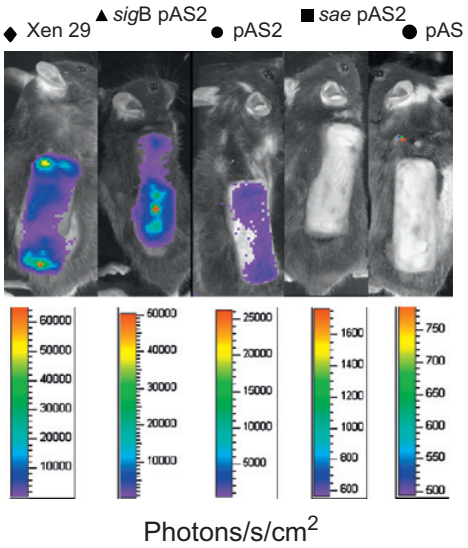

Antibiotics **2013**, *2*

Figure 3. Catheter abscess model. Infection of catheter.

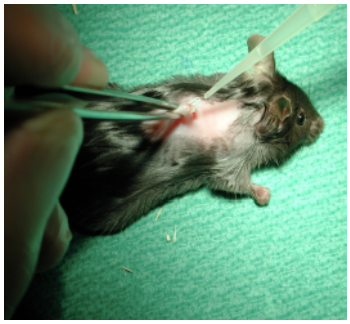

Table 1. Comparisons of orthopaedic and subcutaneous foreign body infection models.

	Orthopaedic models	**Tissue cage model**			**Catheter abscess model**	**Ref.**
Animal species	rabbit/ sheep/ rat/ mouse/ guinea pig/ chicken/ dog/ pig/goat	guinea pig	rat	mouse	mouse	[19,57]
Labour intensity	+++	++	++	++	+	[36,58]
Large scale experiments	no	nd	nd	yes	yes	[59,60]
Localisation	bone	sc	sc	sc	sc	this review, [61]
Susceptibility to staphylococcal infection	species-dependent	yes	no	yes	yes	[19,36,57]
Antibiotic tolerance (long-term treatment)	species-dependent	no	yes	yes	yes	[36]
Use of transgenic animals	nd	nd	nd	yes	yes	[40]
Imaging	yes	nd	yes	yes	yes	[19,28,30,49,61-66]
Bacterial virulence factors	only after sacrifice	yes	no	yes	yes	[19,40-43,56,67-76]
Host immune response	yes	yes	yes	yes	yes	[20,21,25,30,59,62,65,77-80]
Osseointegration	yes	no	no	no	no	[19]
Various implant materials/coatings	yes	nd	nd	yes	yes	[22,38,53,81-83]
Repeated assessment during experiment:						
Cytotoxicity on eukaryotic cells	no	nd	nd	yes	no	[39,53]
Pharmacokinetics (PK) at the infection site	no	yes	yes	yes	no	[7,13,36]
Pharmacodynamics (PD)	no	yes	yes	yes	no	[13,17,19,39,84-88]
Similarity to human disease:						
Localised infection	yes	yes	yes	yes	no	this review, [19,36]

nd: not defined, sc: subcutaneous.

References and Notes

1 Tsaras, G. *et al.* Incidence, secular trends, and outcomes of prosthetic joint infection: a population-based study, olmsted county, Minnesota, 1969-2007. *Infection control and hospital epidemiology : the official journal of the Society of Hospital Epidemiologists of America* **33**, 1207-1212, doi:10.1086/668421 (2012).

2 Darouiche, R. O. Treatment of infections associated with surgical implants. *The New England journal of medicine* **350**, 1422-1429, doi:10.1056/NEJMra035415 (2004).

3 Zimmerli, W., Trampuz, A. & Ochsner, P. E. Prosthetic-joint infections. *The New England journal of medicine* **351**, 1645-1654, doi:10.1056/NEJMra040181 (2004).

4 Zappe, B., Graf, S., Ochsner, P. E., Zimmerli, W. & Sendi, P. Propionibacterium spp. in prosthetic joint infections: a diagnostic challenge. *Archives of orthopaedic and trauma surgery* **128**, 1039-1046, doi:10.1007/s00402-007-0454-0 (2008).

5 Anderson, D. J. *et al.* Variation in the type and frequency of postoperative invasive Staphylococcus aureus infections according to type of surgical procedure. *Infection control and hospital epidemiology : the official journal of the Society of Hospital Epidemiologists of America* **31**, 701-709, doi:10.1086/653205 (2010).

6 Elek, S. D. & Conen, P. E. The virulence of Staphylococcus pyogenes for man; a study of the problems of wound infection. *British journal of experimental pathology* **38**, 573-586 (1957).

7 Zimmerli, W., Waldvogel, F. A., Vaudaux, P. & Nydegger, U. E. Pathogenesis of foreign body infection: description and characteristics of an animal model. *The Journal of infectious diseases* **146**, 487-497 (1982).

8 Resch, A. *et al.* Comparative proteome analysis of Staphylococcus aureus biofilm and planktonic cells and correlation with transcriptome profiling. *Proteomics* **6**, 1867-1877, doi:10.1002/pmic.200500531 (2006).

9 Arciola, C. R., Campoccia, D., Speziale, P., Montanaro, L. & Costerton, J. W. Biofilm formation in Staphylococcus implant infections. A review of molecular mechanisms and implications for biofilm-resistant materials. *Biomaterials* **33**, 5967-5982, doi:10.1016/j.biomaterials.2012.05.031 (2012).

10 Otto, M. Staphylococcal infections: mechanisms of biofilm maturation and detachment as critical determinants of pathogenicity. *Annual review of medicine* **64**, 175-188, doi:10.1146/annurev-med-042711-140023 (2013).

11 Chatterjee, S. S. *et al.* Essential Staphylococcus aureus toxin export system. *Nature medicine* **19**, 364-367, doi:10.1038/nm.3047 (2013).

12 Periasamy, S. *et al.* How Staphylococcus aureus biofilms develop their characteristic structure. *Proceedings of the National Academy of Sciences of the United States of America* **109**, 1281-1286, doi:10.1073/pnas.1115006109 (2012).

13 John, A. K., Schmaler, M., Khanna, N. & Landmann, R. Reversible daptomycin tolerance of adherent staphylococci in an implant infection model. *Antimicrobial agents and chemotherapy* **55**, 3510-3516, doi:10.1128/AAC.00172-11 (2011).

14 Otto, M. Staphylococcal biofilms. *Current topics in microbiology and immunology* **322**, 207-228 (2008).

15 Zimmerli, W., Widmer, A. F., Blatter, M., Frei, R. & Ochsner, P. E. Role of rifampin for treatment of orthopedic implant-related staphylococcal infections: a randomized controlled trial. Foreign-Body Infection (FBI) Study Group. *JAMA : the journal of the American Medical Association* **279**, 1537-1541 (1998).

16 Osmon, D. R. *et al.* Diagnosis and management of prosthetic joint infection: clinical practice guidelines by the Infectious Diseases Society of America. *Clinical infectious diseases : an official publication of the Infectious Diseases Society of America* **56**, e1-e25, doi:10.1093/cid/cis803 (2013).

17 John, A. K. *et al.* Efficacy of daptomycin in implant-associated infection due to methicillin-resistant Staphylococcus aureus: importance of combination with rifampin. *Antimicrobial agents and chemotherapy* **53**, 2719-2724, doi:10.1128/AAC.00047-09 (2009).

18 Conlon, B. P. *et al.* Activated ClpP kills persisters and eradicates a chronic biofilm infection. *Nature* **503**, 365-370, doi:10.1038/nature12790 (2013).

19 Calabro, L. S. E. D., A.F; Richards, R.G.; Moriarty, T.F. in *Biomaterials Associated Infection: Immunological Aspects and Antimicrobial Strategies* (ed Sebastian A.J. Zaat T. Fintan Moriarty, Henk J. Busscher) Ch. 12, 273-304 (Springer Science+Business Media, 2013).

20 Kristian, S. A. *et al.* Biofilm formation induces C3a release and protects Staphylococcus epidermidis from IgG and complement deposition and from neutrophil-dependent killing. *The Journal of infectious diseases* **197**, 1028-1035, doi:10.1086/528992 (2008).

21 Zimmerli, W., Lew, P. D. & Waldvogel, F. A. Pathogenesis of foreign body infection. Evidence for a local granulocyte defect. *The Journal of clinical investigation* **73**, 1191-1200, doi:10.1172/JCI111305 (1984).

22 Zimmerli, W. & Sendi, P. Pathogenesis of implant-associated infection: the role of the host. *Seminars in immunopathology* **33**, 295-306, doi:10.1007/s00281-011-0275-7 (2011).

23 Wagner, C. *et al.* Polymorphonuclear neutrophils in posttraumatic osteomyelitis: cells recovered from the inflamed site lack chemotactic activity but generate superoxides. *Shock* **22**, 108-115 (2004).

24 Wagner, C. *et al.* Post-traumatic osteomyelitis: analysis of inflammatory cells recruited into the site of infection. *Shock* **20**, 503-510, doi:10.1097/01.shk.0000093542.78705.e3 (2003).

25 Hanke, M. L., Heim, C. E., Angle, A., Sanderson, S. D. & Kielian, T. Targeting macrophage activation for the prevention and treatment of Staphylococcus aureus biofilm infections. *J Immunol* **190**, 2159-2168, doi:10.4049/jimmunol.1202348 (2013).

26 Prabhakara, R., Harro, J. M., Leid, J. G., Harris, M. & Shirtliff, M. E. Murine immune response to a chronic Staphylococcus aureus biofilm infection. *Infection and immunity* **79**, 1789-1796, doi:10.1128/IAI.01386-10 (2011).

27 Chai, H. *et al.* Antibacterial effect of 317L stainless steel contained copper in prevention of implant-related infection in vitro and in vivo. *Journal of materials science. Materials in medicine* **22**, 2525-2535, doi:10.1007/s10856-011-4427-z (2011).

28 Lankinen, P., Lehtimaki, K., Hakanen, A. J., Roivainen, A. & Aro, H. T. A comparative 18F-FDG PET/CT imaging of experimental Staphylococcus aureus osteomyelitis and Staphylococcus epidermidis foreign-body-associated infection in the rabbit tibia. *EJNMMI research* **2**, 41, doi:10.1186/2191-219X-2-41 (2012).

29 Stewart, S. *et al.* Vancomycin-modified implant surface inhibits biofilm formation and supports bone-healing in an infected osteotomy model in sheep: a proof-of-concept study. *The Journal of bone and joint surgery. American volume* **94**, 1406-1415, doi:10.2106/JBJS.K.00886 (2012).

30 Niska, J. A. *et al.* Monitoring bacterial burden, inflammation and bone damage longitudinally using optical and muCT imaging in an orthopaedic implant infection in mice. *PloS one* **7**, e47397, doi:10.1371/journal.pone.0047397 (2012).

31 Widmer, A. F., Frei, R., Rajacic, Z. & Zimmerli, W. Correlation between in vivo and in vitro efficacy of antimicrobial agents against foreign body infections. *The Journal of infectious diseases* **162**, 96-102 (1990).

32 Zimmerli, W., Frei, R., Widmer, A. F. & Rajacic, Z. Microbiological tests to predict treatment outcome in experimental device-related infections due to Staphylococcus aureus. *The Journal of antimicrobial chemotherapy* **33**, 959-967 (1994).

33 Drancourt, M. *et al.* Oral rifampin plus ofloxacin for treatment of Staphylococcus-infected orthopedic implants. *Antimicrobial agents and chemotherapy* **37**, 1214-1218 (1993).

34 Furustrand Tafin, U., Corvec, S., Betrisey, B., Zimmerli, W. & Trampuz, A. Role of rifampin against Propionibacterium acnes biofilm in vitro and in an experimental foreign-body infection model. *Antimicrobial agents and chemotherapy* **56**, 1885-1891, doi:10.1128/AAC.05552-11 (2012).

35 Olson, M. E., Slater, S. R., Rupp, M. E. & Fey, P. D. Rifampicin enhances activity of daptomycin and vancomycin against both a polysaccharide intercellular adhesin (PIA)-dependent and -independent Staphylococcus epidermidis biofilm. *The Journal of antimicrobial chemotherapy* **65**, 2164-2171, doi:10.1093/jac/dkq314 (2010).

36 Zimmerli, W. in *Handbook of Animal Models of Infection. Experimental Models in Antimicrobial Chemotherapy.* (ed Oto; Sande Zak, Merle A.) Ch. 47, (Academic Press, 1999).

37 Lucet, J. C. *et al.* Treatment of experimental foreign body infection caused by methicillin-resistant Staphylococcus aureus. *Antimicrobial agents and chemotherapy* **34**, 2312-2317 (1990).

38 Hudetz, D. *et al.* Weak effect of metal type and ica genes on staphylococcal infection of titanium and stainless steel implants. *Clinical microbiology and infection : the official publication of the European Society of Clinical Microbiology and Infectious Diseases* **14**, 1135-1145, doi:10.1111/j.1469-0691.2008.02096.x (2008).

39 Nowakowska, J., Griesser, H. J., Textor, M., Landmann, R. & Khanna, N. Antimicrobial properties of 8-hydroxyserrulat-14-en-19-oic acid for treatment of implant-associated infections. *Antimicrobial agents and chemotherapy* **57**, 333-342, doi:10.1128/AAC.01735-12 (2013).

40 Kristian, S. A. *et al.* Alanylation of teichoic acids protects Staphylococcus aureus against Toll-like receptor 2-dependent host defense in a mouse tissue cage infection model. *The Journal of infectious diseases* **188**, 414-423, doi:10.1086/376533 (2003).

41 Kristian, S. A. *et al.* The ability of biofilm formation does not influence virulence of Staphylococcus aureus and host response in a mouse tissue cage infection model. *Microbial pathogenesis* **36**, 237-245, doi:10.1016/j.micpath.2003.12.004 (2004).

42 Fluckiger, U. *et al.* Biofilm formation, icaADBC transcription, and polysaccharide intercellular adhesin synthesis by staphylococci in a device-related infection model. *Infection and immunity* **73**, 1811-1819, doi:10.1128/IAI.73.3.1811-1819.2005 (2005).

43 Rupp, M. E., Ulphani, J. S., Fey, P. D. & Mack, D. Characterization of Staphylococcus epidermidis polysaccharide intercellular adhesin/hemagglutinin in the pathogenesis of intravascular catheter-associated infection in a rat model. *Infection and immunity* **67**, 2656-2659 (1999).

44 Rupp, M. E., Ulphani, J. S., Fey, P. D., Bartscht, K. & Mack, D. Characterization of the importance of polysaccharide intercellular adhesin/hemagglutinin of Staphylococcus epidermidis in the pathogenesis of biomaterial-based infection in a mouse foreign body infection model. *Infection and immunity* **67**, 2627-2632 (1999).

45 Foster, T. J. Immune evasion by staphylococci. *Nature reviews. Microbiology* **3**, 948-958, doi:10.1038/nrmicro1289 (2005).

46 Wolz, C., Goerke, C., Landmann, R., Zimmerli, W. & Fluckiger, U. Transcription of clumping factor A in attached and unattached Staphylococcus aureus in vitro and during device-related infection. *Infection and immunity* **70**, 2758-2762 (2002).

47 Mally, M., Shin, H., Paroz, C., Landmann, R. & Cornelis, G. R. Capnocytophaga canimorsus: a human pathogen feeding at the surface of epithelial cells and phagocytes. *PLoS pathogens* **4**, e1000164, doi:10.1371/journal.ppat.1000164 (2008).

48 Kadurugamuwa, J. L. *et al.* Direct continuous method for monitoring biofilm infection in a mouse model. *Infection and immunity* **71**, 882-890 (2003).

49 Steinhuber, A., Landmann, R., Goerke, C., Wolz, C. & Fluckiger, U. Bioluminescence imaging to study the promoter activity of hla of Staphylococcus aureus in vitro and in vivo. *International journal of medical microbiology : IJMM* **298**, 599-605, doi:10.1016/j.ijmm.2007.09.008 (2008).

50 McCallum, N. *et al.* In vivo survival of teicoplanin-resistant Staphylococcus aureus and fitness cost of teicoplanin resistance. *Antimicrobial agents and chemotherapy* **50**, 2352-2360, doi:10.1128/AAC.00073-06 (2006).

51 Dominguez-Herrera, J. *et al.* Efficacy of daptomycin versus vancomycin in an experimental model of foreign-body and systemic infection caused by biofilm producers and methicillin-resistant Staphylococcus epidermidis. *Antimicrobial agents and chemotherapy* **56**, 613-617, doi:10.1128/AAC.05606-11 (2012).

52 Pragman, A. A. & Schlievert, P. M. Virulence regulation in Staphylococcus aureus: the need for in vivo analysis of virulence factor regulation. *FEMS immunology and medical microbiology* **42**, 147-154, doi:10.1016/j.femsim.2004.05.005 (2004).

53 Gordon, O. *et al.* Silver coordination polymers for prevention of implant infection: thiol interaction, impact on respiratory chain enzymes, and hydroxyl radical induction. *Antimicrobial agents and chemotherapy* **54**, 4208-4218, doi:10.1128/AAC.01830-09 (2010).

54 Kadurugamuwa, J. L. *et al.* Rapid direct method for monitoring antibiotics in a mouse model of bacterial biofilm infection. *Antimicrobial agents and chemotherapy* **47**, 3130-3137 (2003).

55 Hanke, M. L. & Kielian, T. Deciphering mechanisms of staphylococcal biofilm evasion of host immunity. *Frontiers in cellular and infection microbiology* **2**, 62, doi:10.3389/fcimb.2012.00062 (2012).

56 Malone, J. G. *et al.* YfiBNR mediates cyclic di-GMP dependent small colony variant formation and persistence in Pseudomonas aeruginosa. *PLoS pathogens* **6**, e1000804, doi:10.1371/journal.ppat.1000804 (2010).

57 An, Y. H., Kang, Q. K. & Arciola, C. R. Animal models of osteomyelitis. *The International journal of artificial organs* **29**, 407-420 (2006).

58 Auer, J. A. *et al.* Refining animal models in fracture research: seeking consensus in optimising both animal welfare and scientific validity for appropriate biomedical use. *BMC musculoskeletal disorders* **8**, 72, doi:10.1186/1471-2474-8-72 (2007).

59 Odekerken, J. C., Arts, J. J., Surtel, D. A., Walenkamp, G. H. & Welting, T. J. A rabbit osteomyelitis model for the longitudinal assessment of early post-operative implant infections. *Journal of orthopaedic surgery and research* **8**, 38, doi:10.1186/1749-799X-8-38 (2013).

60 Schimandle, J. H. & Boden, S. D. Spine update. Animal use in spinal research. *Spine* **19**, 2474-2477 (1994).

61 Pearce, A. I., Richards, R. G., Milz, S., Schneider, E. & Pearce, S. G. Animal models for implant biomaterial research in bone: a review. *European cells & materials* **13**, 1-10 (2007).

62 Bernthal, N. M. *et al.* A mouse model of post-arthroplasty Staphylococcus aureus joint infection to evaluate in vivo the efficacy of antimicrobial implant coatings. *PloS one* **5**, e12580, doi:10.1371/journal.pone.0012580 (2010).

63 Broekhuizen, C. A., Sta, M., Vandenbroucke-Grauls, C. M. & Zaat, S. A. Microscopic detection of viable Staphylococcus epidermidis in peri-implant tissue in experimental biomaterial-associated infection, identified by bromodeoxyuridine incorporation. *Infection and immunity* **78**, 954-962, doi:10.1128/IAI.00849-09 (2010).

64 Kuklin, N. A. *et al.* Real-time monitoring of bacterial infection in vivo: development of bioluminescent staphylococcal foreign-body and deep-thigh-wound mouse infection models. *Antimicrobial agents and chemotherapy* **47**, 2740-2748 (2003).

65 Li, D. *et al.* Quantitative mouse model of implant-associated osteomyelitis and the kinetics of microbial growth, osteolysis, and humoral immunity. *Journal of orthopaedic research : official publication of the Orthopaedic Research Society* **26**, 96-105, doi:10.1002/jor.20452 (2008).

66 Stoodley, P. *et al.* Molecular and imaging techniques for bacterial biofilms in joint arthroplasty infections. *Clinical orthopaedics and related research*, 31-40 (2005).

67 Beenken, K. E. *et al.* Global gene expression in Staphylococcus aureus biofilms. *Journal of bacteriology* **186**, 4665-4684, doi:10.1128/JB.186.14.4665-4684.2004 (2004).

68 Christensen, G. D., Simpson, W. A., Bisno, A. L. & Beachey, E. H. Experimental foreign body infections in mice challenged with slime-producing Staphylococcus epidermidis. *Infection and immunity* **40**, 407-410 (1983).

69 Espersen, F., Frimodt-Moller, N., Corneliussen, L., Thamdrup Rosdahl, V. & Skinhoj, P. Experimental foreign body infection in mice. *The Journal of antimicrobial chemotherapy* **31 Suppl D**, 103-111 (1993).

70 Francois, P. *et al.* Lack of biofilm contribution to bacterial colonisation in an experimental model of foreign body infection by Staphylococcus aureus and Staphylococcus epidermidis. *FEMS immunology and medical microbiology* **35**, 135-140 (2003).

71 Laughton, J. M., Devillard, E., Heinrichs, D. E., Reid, G. & McCormick, J. K. Inhibition of expression of a staphylococcal superantigen-like protein by a soluble factor from Lactobacillus reuteri. *Microbiology* **152**, 1155-1167, doi:10.1099/mic.0.28654-0 (2006).

72 Liu, Q. *et al.* The eukaryotic-type serine/threonine protein kinase Stk is required for biofilm formation and virulence in Staphylococcus epidermidis. *PloS one* **6**, e25380, doi:10.1371/journal.pone.0025380 (2011).

73 Luong, T. T., Lei, M. G. & Lee, C. Y. Staphylococcus aureus Rbf activates biofilm formation in vitro and promotes virulence in a murine foreign body infection model. *Infection and immunity* **77**, 335-340, doi:10.1128/IAI.00872-08 (2009).

74 Sander, G. *et al.* Catheter colonization and abscess formation due to Staphylococcus epidermidis with normal and small-colony-variant phenotype is mouse strain dependent. *PloS one* **7**, e36602, doi:10.1371/journal.pone.0036602 (2012).

75 Taj, Y., Abdullah, F. E., Aziz, F. & Kazmi, S. U. Temporal expression of extracellular products of Staphylococcus aureus in vivo mouse cage model. *JPMA. The Journal of the Pakistan Medical Association* **62**, 539-545 (2012).

76 Wang, R. *et al.* Staphylococcus epidermidis surfactant peptides promote biofilm maturation and dissemination of biofilm-associated infection in mice. *The Journal of clinical investigation* **121**, 238-248, doi:10.1172/JCI42520 (2011).

77 Falcieri, E., Vaudaux, P., Huggler, E., Lew, D. & Waldvogel, F. Role of bacterial exopolymers and host factors on adherence and phagocytosis of Staphylococcus aureus in foreign body infection. *The Journal of infectious diseases* **155**, 524-531 (1987).

78 Marriott, I. *et al.* Osteoblasts express the inflammatory cytokine interleukin-6 in a murine model of Staphylococcus aureus osteomyelitis and infected human bone tissue. *The American journal of pathology* **164**, 1399-1406, doi:10.1016/S0002-9440(10)63226-9 (2004).

79 Shahrooei, M. *et al.* Vaccination with SesC decreases Staphylococcus epidermidis biofilm formation. *Infection and immunity* **80**, 3660-3668, doi:10.1128/IAI.00104-12 (2012).

80 Vaudaux, P. *et al.* Contribution of tumor necrosis factor to host defense against staphylococci in a guinea pig model of foreign body infections. *The Journal of infectious diseases* **166**, 58-64 (1992).

81 Cobrado, L., Silva-Dias, A., Azevedo, M. M., Pina-Vaz, C. & Rodrigues, A. G. In vivo antibiofilm effect of cerium, chitosan and hamamelitannin against usual agents of catheter-related bloodstream infections. *The Journal of antimicrobial chemotherapy* **68**, 126-130, doi:10.1093/jac/dks376 (2013).

82 Moriarty, T. F., Schlegel, U., Perren, S. & Richards, R. G. Infection in fracture fixation: can we influence infection rates through implant design? *Journal of materials science. Materials in medicine* **21**, 1031-1035, doi:10.1007/s10856-009-3907-x (2010).

83 Zimmerli, W. Implanted devices: biocompatibility, infection and tissue engineering. *Seminars in immunopathology* **33**, 219-220, doi:10.1007/s00281-011-0277-5 (2011).

84 Chambers, H. F. Ceftobiprole: in-vivo profile of a bactericidal cephalosporin. *Clinical microbiology and infection : the official publication of the European Society of Clinical Microbiology and Infectious Diseases* **12 Suppl 2**, 17-22, doi:10.1111/j.1469-0691.2006.01404.x (2006).

85 Garrigos, C. *et al.* Fosfomycin-daptomycin and other fosfomycin combinations as alternative therapies in experimental foreign-body infection by methicillin-resistant Staphylococcus aureus. *Antimicrobial agents and chemotherapy* **57**, 606-610, doi:10.1128/AAC.01570-12 (2013).

86 Murillo, O. *et al.* Efficacy of high doses of daptomycin versus alternative therapies against experimental foreign-body infection by methicillin-resistant Staphylococcus aureus. *Antimicrobial agents and chemotherapy* **53**, 4252-4257, doi:10.1128/AAC.00208-09 (2009).
87 Van Wijngaerden, E. *et al.* Foreign body infection: a new rat model for prophylaxis and treatment. *The Journal of antimicrobial chemotherapy* **44**, 669-674 (1999).
88 Vaudaux, P. *et al.* Comparison of tigecycline and vancomycin for treatment of experimental foreign-body infection due to methicillin-resistant Staphylococcus aureus. *Antimicrobial agents and chemotherapy* **53**, 3150-3152, doi:10.1128/AAC.01612-08 (2009).

Outlook

Development of novel antimicrobials and treatment approaches for bacterial infections, especially those caused by biofilms, are of highest importance in modern medicine.

Thus, in the first part of this project we aimed at determining the *in vitro* and *in vivo* activity as well as a detailed mechanism of action of serrulatane EN4, a member of a new class of plant-derived antimicrobial compounds [74-76]. We have shown that *in vitro* EN4 exerts a potent time- and dose-dependent activity against Gram-positive bacteria associated with IAI, including CA-MRSA. Moreover, EN4 was equally efficient against staphylococci in stationary phase and in biofilm, which is of great importance in the management of IAI. This growth-independent activity was determined to be due to membranolytic mode of action of EN4. Indeed, it has already been postulated that membrane-active agents are crucial for eradication of infections involving dormant microorganisms, as the classical antibiotics predominantly target only metabolically active bacteria [3]. Furthermore, we could also show that no resistance was induced in staphylococci during several passages at subinhibitory concentrations of EN4 (data not shown). In spite of its promising *in vitro* antibacterial activity EN4 exerted also cytotoxic properties against eukaryotic cells and was inhibited *in vivo* by interaction with albumin. Thus, we postulate that EN4 could be used as a pharmacophore for further development of antimicrobials with optimised pharmacodynamics.

Furthermore, our findings precluded the use of EN4 as a component of dual-function implant coatings because of its interaction with albumin that would ultimately lead to interference with antifouling properties of brushes. Nevertheless, in the second part of our project we evaluated the antiadhesive and antibacterial properties of PMOXA, PEGMA and PHEMA-based coatings that were covalently functionalised with vancomycin. We could show a great nonfouling potential of those polymers. However, coupled vancomycin did not confer any antibacterial properties to the coatings. This effect was shown to be due a decreased activity and too low surface concentration. Thus, future studies

will address alternative approaches to functionalisation of polymer brushes in order to increase the concentration of vancomycin covalently coupled to the surfaces. Moreover, to overcome the effect of covalent binding on antibiotic potential of vancomycin, a triggered-release approach was proposed. Vancomycin could be coupled to polymer brushes *via* a linker that would be specifically cleaved in the presence of bacteria. Two candidate linkers were designed. First, based on β-lactam ring, which could be cleaved by β-lactamases. Second, a peptide linker containing recognition sequences of autolysins, constitutively active bacterial enzymes responsible for peptidoglycan turnover [77].

Moreover, additional types of anti-infective implant surfaces, including those functionalised with heavy metals, are currently under investigation.

References

1 Dr Margaret Chan. 6 April 2011 World Health Day. http://www.who.int/dg/speeches/2011/WHD_20110407/en/.

2 Hughes, J. M. Preserving the lifesaving power of antimicrobial agents. *JAMA : the journal of the American Medical Association* **305**, 1027-1028, doi:10.1001/jama.2011.279 (2011).

3 Hurdle, J. G., O'Neill, A. J., Chopra, I. & Lee, R. E. Targeting bacterial membrane function: an underexploited mechanism for treating persistent infections. *Nat Rev Microbiol* **9**, 62-75, doi:10.1038/nrmicro2474 (2011).

4 Coates, A. R. & Hu, Y. Targeting non-multiplying organisms as a way to develop novel antimicrobials. *Trends in pharmacological sciences* **29**, 143-150, doi:10.1016/j.tips.2007.12.001 (2008).

5 Zimmerli, W. & Sendi, P. Pathogenesis of implant-associated infection: the role of the host. *Semin Immunopathol* **33**, 295-306, doi:10.1007/s00281-011-0275-7 (2011).

6 Arciola, C. R., Campoccia, D., Speziale, P., Montanaro, L. & Costerton, J. W. Biofilm formation in Staphylococcus implant infections. A review of molecular mechanisms and implications for biofilm-resistant materials. *Biomaterials* **33**, 5967-5982, doi:10.1016/j.biomaterials.2012.05.031 (2012).

7 Antoci, V., Jr. *et al.* The inhibition of Staphylococcus epidermidis biofilm formation by vancomycin-modified titanium alloy and implications for the treatment of periprosthetic infection. *Biomaterials* **29**, 4684-4690, doi:10.1016/j.biomaterials.2008.08.016 (2008).

8 Antoci, V., Jr. *et al.* Vancomycin covalently bonded to titanium alloy prevents bacterial colonization. *J Orthop Res* **25**, 858-866, doi:10.1002/jor.20348 (2007).

9 Wach, J. Y., Bonazzi, S. & Gademann, K. Antimicrobial surfaces through natural product hybrids. *Angew Chem Int Ed Engl* **47**, 7123-7126, doi:10.1002/anie.200801570 (2008).

10 Gristina, A. G. Biomaterial-centered infection: microbial adhesion versus tissue integration. *Science* **237**, 1588-1595 (1987).

11 Tsaras, G. *et al.* Incidence, secular trends, and outcomes of prosthetic joint infection: a population-based study, olmsted county, Minnesota, 1969-2007. *Infect Control Hosp Epidemiol* **33**, 1207-1212, doi:10.1086/668421 (2012).

12 Darouiche, R. O. Treatment of infections associated with surgical implants. *N Engl J Med* **350**, 1422-1429, doi:10.1056/NEJMra035415 (2004).

13 Zimmerli, W. & Trampuz, A. in *Biomaterials Associated Infection: Immunological Aspects and Antimicrobial Strategies* (ed T. Fintan Moriarty Sebastian A.J. Zaat, Henk J. Busscher) Ch. 1, 3-24 (Springer Science+Business Media, 2013).

14 Otto, M. Staphylococcal biofilms. *Curr Top Microbiol Immunol* **322**, 207-228 (2008).

15 Costerton, J. W., Stewart, P. S. & Greenberg, E. P. Bacterial biofilms: a common cause of persistent infections. *Science* **284**, 1318-1322 (1999).
16 Keren, I., Kaldalu, N., Spoering, A., Wang, Y. & Lewis, K. Persister cells and tolerance to antimicrobials. *FEMS Microbiol Lett* **230**, 13-18 (2004).
17 Kristian, S. A. *et al.* Biofilm formation induces C3a release and protects Staphylococcus epidermidis from IgG and complement deposition and from neutrophil-dependent killing. *J Infect Dis* **197**, 1028-1035, doi:10.1086/528992 (2008).
18 Lewis, K. Riddle of biofilm resistance. *Antimicrob Agents Chemother* **45**, 999-1007, doi:10.1128/AAC.45.4.999-1007.2001 (2001).
19 Peel, T. N., Cheng, A. C., Buising, K. L. & Choong, P. F. Microbiological aetiology, epidemiology, and clinical profile of prosthetic joint infections: are current antibiotic prophylaxis guidelines effective? *Antimicrob Agents Chemother* **56**, 2386-2391, doi:10.1128/AAC.06246-11 (2012).
20 Elek, S. D. & Conen, P. E. The virulence of Staphylococcus pyogenes for man; a study of the problems of wound infection. *Br J Exp Pathol* **38**, 573-586 (1957).
21 Trampuz, A. & Zimmerli, W. Antimicrobial agents in orthopaedic surgery: Prophylaxis and treatment. *Drugs* **66**, 1089-1105 (2006).
22 Dunne, W. M., Jr. Effects of subinhibitory concentrations of vancomycin or cefamandole on biofilm production by coagulase-negative staphylococci. *Antimicrob Agents Chemother* **34**, 390-393 (1990).
23 Otto, M. MRSA virulence and spread. *Cell Microbiol* **14**, 1513-1521, doi:10.1111/j.1462-5822.2012.01832.x (2012).
24 Lowy, F. D. Staphylococcus aureus infections. *N Engl J Med* **339**, 520-532, doi:10.1056/NEJM199808203390806 (1998).
25 Massey, R. C., Horsburgh, M. J., Lina, G., Hook, M. & Recker, M. The evolution and maintenance of virulence in Staphylococcus aureus: a role for host-to-host transmission? *Nat Rev Microbiol* **4**, 953-958, doi:10.1038/nrmicro1551 (2006).
26 Wang, R. *et al.* Identification of novel cytolytic peptides as key virulence determinants for community-associated MRSA. *Nat Med* **13**, 1510-1514, doi:10.1038/nm1656 (2007).
27 Powers, M. E. & Bubeck Wardenburg, J. Igniting the fire: Staphylococcus aureus virulence factors in the pathogenesis of sepsis. *PLoS pathogens* **10**, e1003871, doi:10.1371/journal.ppat.1003871 (2014).
28 Lowy, F. D. Antimicrobial resistance: the example of Staphylococcus aureus. *J Clin Invest* **111**, 1265-1273, doi:10.1172/JCI18535 (2003).
29 Chambers, H. F., Hartman, B. J. & Tomasz, A. Increased amounts of a novel penicillin-binding protein in a strain of methicillin-resistant Staphylococcus aureus exposed to nafcillin. *J Clin Invest* **76**, 325-331, doi:10.1172/JCI111965 (1985).
30 Srinivasan, A., Dick, J. D. & Perl, T. M. Vancomycin resistance in staphylococci. *Clin Microbiol Rev* **15**, 430-438 (2002).
31 Rossi, F. *et al.* Transferable Vancomycin Resistance in a Community-Associated MRSA Lineage. *New England Journal of Medicine* **370**, 1524-1531, doi:doi:10.1056/NEJMoa1303359 (2014).

32 Rogers, K. L., Fey, P. D. & Rupp, M. E. Coagulase-negative staphylococcal infections. *Infect Dis Clin North Am* **23**, 73-98, doi:10.1016/j.idc.2008.10.001 (2009).
33 Otto, M. Molecular basis of Staphylococcus epidermidis infections. *Semin Immunopathol* **34**, 201-214, doi:10.1007/s00281-011-0296-2 (2012).
34 Otto, M. Staphylococcus epidermidis--the 'accidental' pathogen. *Nat Rev Microbiol* **7**, 555-567, doi:10.1038/nrmicro2182 (2009).
35 Rupp, M. E., Ulphani, J. S., Fey, P. D., Bartscht, K. & Mack, D. Characterization of the importance of polysaccharide intercellular adhesin/hemagglutinin of Staphylococcus epidermidis in the pathogenesis of biomaterial-based infection in a mouse foreign body infection model. *Infect Immun* **67**, 2627-2632 (1999).
36 Marraffini, L. A. & Sontheimer, E. J. CRISPR interference limits horizontal gene transfer in staphylococci by targeting DNA. *Science* **322**, 1843-1845, doi:10.1126/science.1165771 (2008).
37 Iwase, T. *et al.* Staphylococcus epidermidis Esp inhibits Staphylococcus aureus biofilm formation and nasal colonization. *Nature* **465**, 346-349, doi:10.1038/nature09074 (2010).
38 National Institute of Health (NIH) 2007. http://grants.nih.gov/grants/guide/pa-files/PA-07-288.html.
39 Mack, D. *et al.* Microbial interactions in Staphylococcus epidermidis biofilms. *Anal Bioanal Chem* **387**, 399-408, doi:10.1007/s00216-006-0745-2 (2007).
40 Hirschhausen, N. *et al.* A novel staphylococcal internalization mechanism involves the major autolysin Atl and heat shock cognate protein Hsc70 as host cell receptor. *Cell Microbiol* **12**, 1746-1764, doi:10.1111/j.1462-5822.2010.01506.x (2010).
41 Rohde, H. *et al.* Polysaccharide intercellular adhesin or protein factors in biofilm accumulation of Staphylococcus epidermidis and Staphylococcus aureus isolated from prosthetic hip and knee joint infections. *Biomaterials* **28**, 1711-1720, doi:10.1016/j.biomaterials.2006.11.046 (2007).
42 Mack, D. *et al.* The intercellular adhesin involved in biofilm accumulation of Staphylococcus epidermidis is a linear beta-1,6-linked glucosaminoglycan: purification and structural analysis. *J Bacteriol* **178**, 175-183 (1996).
43 Heilmann, C. *et al.* Molecular basis of intercellular adhesion in the biofilm-forming Staphylococcus epidermidis. *Mol Microbiol* **20**, 1083-1091 (1996).
44 Novick, R. P. & Geisinger, E. Quorum sensing in staphylococci. *Annu Rev Genet* **42**, 541-564, doi:10.1146/annurev.genet.42.110807.091640 (2008).
45 Wang, R. *et al.* Staphylococcus epidermidis surfactant peptides promote biofilm maturation and dissemination of biofilm-associated infection in mice. *J Clin Invest* **121**, 238-248, doi:10.1172/JCI42520 (2011).
46 Yao, Y., Sturdevant, D. E. & Otto, M. Genomewide analysis of gene expression in Staphylococcus epidermidis biofilms: insights into the pathophysiology of S. epidermidis biofilms and the role of phenol-soluble

modulins in formation of biofilms. *J Infect Dis* **191**, 289-298, doi:10.1086/426945 (2005).

47 Walters, M. C., 3rd, Roe, F., Bugnicourt, A., Franklin, M. J. & Stewart, P. S. Contributions of antibiotic penetration, oxygen limitation, and low metabolic activity to tolerance of Pseudomonas aeruginosa biofilms to ciprofloxacin and tobramycin. *Antimicrob Agents Chemother* **47**, 317-323 (2003).

48 Stewart, P. S. & Costerton, J. W. Antibiotic resistance of bacteria in biofilms. *Lancet* **358**, 135-138 (2001).

49 Vuong, C. *et al.* Polysaccharide intercellular adhesin (PIA) protects Staphylococcus epidermidis against major components of the human innate immune system. *Cell Microbiol* **6**, 269-275 (2004).

50 Zheng, Z. & Stewart, P. S. Penetration of rifampin through Staphylococcus epidermidis biofilms. *Antimicrob Agents Chemother* **46**, 900-903 (2002).

51 Singh, R., Ray, P., Das, A. & Sharma, M. Penetration of antibiotics through Staphylococcus aureus and Staphylococcus epidermidis biofilms. *J Antimicrob Chemother* **65**, 1955-1958, doi:10.1093/jac/dkq257 (2010).

52 Resch, A., Rosenstein, R., Nerz, C. & Gotz, F. Differential gene expression profiling of Staphylococcus aureus cultivated under biofilm and planktonic conditions. *Appl Environ Microbiol* **71**, 2663-2676, doi:10.1128/AEM.71.5.2663-2676.2005 (2005).

53 Shapiro, J. A., Nguyen, V. L. & Chamberlain, N. R. Evidence for persisters in Staphylococcus epidermidis RP62a planktonic cultures and biofilms. *J Med Microbiol* **60**, 950-960, doi:10.1099/jmm.0.026013-0 (2011).

54 Bjarnsholt, T., Ciofu, O., Molin, S., Givskov, M. & Hoiby, N. Applying insights from biofilm biology to drug development - can a new approach be developed? *Nat Rev Drug Discov* **12**, 791-808, doi:10.1038/nrd4000 (2013).

55 Kaplan, J. B. *et al.* Recombinant human DNase I decreases biofilm and increases antimicrobial susceptibility in staphylococci. *J Antibiot (Tokyo)* **65**, 73-77, doi:10.1038/ja.2011.113 (2012).

56 Darouiche, R. O., Mansouri, M. D., Gawande, P. V. & Madhyastha, S. Antimicrobial and antibiofilm efficacy of triclosan and DispersinB combination. *J Antimicrob Chemother* **64**, 88-93, doi:10.1093/jac/dkp158 (2009).

57 Boles, B. R. & Horswill, A. R. Agr-mediated dispersal of Staphylococcus aureus biofilms. *PLoS pathogens* **4**, e1000052, doi:10.1371/journal.ppat.1000052 (2008).

58 Mrak, L. N. *et al.* saeRS and sarA act synergistically to repress protease production and promote biofilm formation in Staphylococcus aureus. *PLoS One* **7**, e38453, doi:10.1371/journal.pone.0038453 (2012).

59 Abdelhady, W. *et al.* Impact of Vancomycin on sarA-Mediated Biofilm Formation: Role in Persistent Endovascular Infections Due to Methicillin-Resistant Staphylococcus aureus. *J Infect Dis* **209**, 1231-1240, doi:10.1093/infdis/jiu007 (2014).

60 Conlon, B. P. *et al.* Activated ClpP kills persisters and eradicates a chronic biofilm infection. *Nature* **503**, 365-370, doi:10.1038/nature12790 (2013).

61 Wright, A., Hawkins, C. H., Anggard, E. E. & Harper, D. R. A controlled clinical trial of a therapeutic bacteriophage preparation in chronic otitis due to antibiotic-resistant Pseudomonas aeruginosa; a preliminary report of efficacy. *Clin Otolaryngol* **34**, 349-357, doi:10.1111/j.1749-4486.2009.01973.x (2009).

62 Markoishvili, K., Tsitlanadze, G., Katsarava, R., Morris, J. G., Jr. & Sulakvelidze, A. A novel sustained-release matrix based on biodegradable poly(ester amide)s and impregnated with bacteriophages and an antibiotic shows promise in management of infected venous stasis ulcers and other poorly healing wounds. *Int J Dermatol* **41**, 453-458 (2002).

63 Keen, E. C. Phage therapy: concept to cure. *Front Microbiol* **3**, 238, doi:10.3389/fmicb.2012.00238 (2012).

64 Chen, S. F., Li, L. Y., Zhao, C. & Zheng, J. Surface hydration: Principles and applications toward low-fouling/nonfouling biomaterials. *Polymer* **51**, 5283-5293 (2010).

65 Konradi, R., Acikgoz, C. & Textor, M. Polyoxazolines for nonfouling surface coatings--a direct comparison to the gold standard PEG. *Macromol Rapid Commun* **33**, 1663-1676, doi:10.1002/marc.201200422 (2012).

66 Tugulu, S., Silacci, P., Stergiopulos, N. & Klok, H. A. RGD-Functionalized polymer brushes as substrates for the integrin specific adhesion of human umbilical vein endothelial cells. *Biomaterials* **28**, 2536-2546, doi:10.1016/j.biomaterials.2007.02.006 (2007).

67 Hockenhull, J. C. *et al.* The clinical effectiveness of central venous catheters treated with anti-infective agents in preventing catheter-related bloodstream infections: a systematic review. *Crit Care Med* **37**, 702-712, doi:10.1097/CCM.0b013e3181958915 (2009).

68 Gordon, O. *et al.* Silver coordination polymers for prevention of implant infection: thiol interaction, impact on respiratory chain enzymes, and hydroxyl radical induction. *Antimicrob Agents Chemother* **54**, 4208-4218, doi:10.1128/AAC.01830-09 (2010).

69 Mijnendonckx, K., Leys, N., Mahillon, J., Silver, S. & Van Houdt, R. Antimicrobial silver: uses, toxicity and potential for resistance. *Biometals* **26**, 609-621, doi:10.1007/s10534-013-9645-z (2013).

70 Rai, M., Yadav, A. & Gade, A. Silver nanoparticles as a new generation of antimicrobials. *Biotechnol Adv* **27**, 76-83, doi:10.1016/j.biotechadv.2008.09.002 (2009).

71 Gao, G. *et al.* The biocompatibility and biofilm resistance of implant coatings based on hydrophilic polymer brushes conjugated with antimicrobial peptides. *Biomaterials* **32**, 3899-3909, doi:10.1016/j.biomaterials.2011.02.013 (2011).

72 Cribb, A. B., Cribb J. W. *Wild medicine in Australia*. (William Collins Pty Ltd., 1981).

73 Ghisalberti, E. L., Jefferies, P. R. & Hieu, T. N. V. Diterpenes from Eremophila Species. *Phytochemistry* **29**, 316-318 (1990).

74 Ndi, C. P., Semple, S. J., Griesser, H. J. & Barton, M. D. Antimicrobial activity of some Australian plant species from the genus Eremophila. *J Basic Microbiol* **47**, 158-164, doi:10.1002/jobm.200610262 (2007).

75 Ndi, C. P., Semple, S. J., Griesser, H. J., Pyke, S. M. & Barton, M. D. Antimicrobial compounds from the Australian desert plant Eremophila neglecta. *J Nat Prod* **70**, 1439-1443, doi:10.1021/np070180r (2007).

76 Anakok, O. F., Ndi, C. P., Barton, M. D., Griesser, H. J. & Semple, S. J. Antibacterial spectrum and cytotoxic activities of serrulatane compounds from the Australian medicinal plant Eremophila neglecta. *J Appl Microbiol* **112**, 197-204, doi:10.1111/j.1365-2672.2011.05174.x (2012).

77 Zoll, S. *et al.* Structural basis of cell wall cleavage by a staphylococcal autolysin. *PLoS pathogens* **6**, e1000807, doi:10.1371/journal.ppat.1000807 (2010).

Part II

Table of Content

Abbreviations

aa	amino acid
AdV	adenovirus
BCR	B-cell receptor
BFA	brefeldin A
BL	Burkitt's lymphoma
BZLF1	*Bam* HI Z restriction fragment of EBV, beginning with the Leftward OR Frame number 1
CMV	cytomegalovirus
CSA	cyclosporin A
d	day
DCs	dendritic cells
DLI	donor lymphocyte infusion
E:T	effector to target
EBNA	EBV nuclear antigen
EBV	Epstein-Barr virus
ECIL	European Conference on Infection in Leukaemia
ELISpot	Enzyme-linked immunospot
GM-CSF	granulocyte/macrophage colony-stimulating factor
GMP	good manufacturing practice
GvHD	graft-versus-host disease
GvT	graft-versus-tumour
HL	Hodgkin's lymphoma
HLA	human leukocyte antigen
HRS	Hodgkin and Reed–Sternberg
HS	human serum
HSCT	haematopoietic stem cell transplantation
ICC	intracellular cytokine staining
IFN-γ	interferon-γ
IL	interleukin
IM	infectious mononucleosis

U	units
LCLs	lymphoblastoid cell lines
LMP	latent membrane protein
MHC	major histocompatibility complex
MHV-68	mouse γ-herpesvirus 68
NK	natural killer
PD-1	programmed cell death-1
PenStrep	penicillin-streptomycin
PGE2	prostaglandin E2
PMNs	peripheral blood mononuclear cells
PTLDs	post-transplant lymphoproliferative disorders
R:S	responder to stimulator
SDs	standard deviations
SFC	spot-forming cells
SOT	solid organ transplantation
T_{CM}	T-central memory cell
T_H	T-helper cell
T_{SCM}	T memory stem cell
TNF-α	tumour necrosis factor-α

Units

°C	Celsius degree
cpm	counts per minutes
Gy	Gray
mL	milliliter
µCi	microcurie
µg	microgram
µL	microliter
ng	nanogram
rcf	relative centrifugal force

Summary

Epstein-Barr virus (EBV)-associated tumours that include post-transplant lymphoproliferative disorders (PTLDs) belong to the most serious complications of immunosuppression occurring in approximately 5% of all transplant recipients and are still associated with an exuberant morbidity and mortality [3-5]. In these patients, the immunosuppression reduces the number and/or the function of the EBV-specific T-cells leading to uncontrolled proliferation of EBV-infected B-cells and tumour formation [1,2,4,6]. Thus, reconstitution of antigen-specific T-cells of the patients has the potency to provide immediate and also long-term protection against PTLDs [7,8]. Several studies have demonstrated safety and clinical benefit of adoptive transfer of antigen-specific $CD4^+$ and $CD8^+$ T-cells [7,9-18]. Nevertheless, controversial data exist on the necessity of $CD4^+$ and $CD8^+$ T-cell content of T-cell product to control PTLDs [12,14,16]. Moreover, most T-cell generation procedures are very laborious and time-consuming, which precludes its wide application. A more rapid approach has recently been introduced into clinics, by which T-cells are directly isolated based on interferon (IFN)-γ production upon stimulation with virus-derived antigens [9,10,15,17]. Since the T-cell response to EBV is directed against a set of viral proteins and strongly depends on the human leukocyte antigen (HLA) types [19], we aimed at identifying immunogenic antigens to generate a T-cell product consisting of both $CD4^+$ and $CD8^+$ cells covering a broad range of HLA types and at investigating their role in controlling PTLDs.

Thus, we included the commercially available overlapping peptide pools derived from EBV antigens, which are known to be expressed in PTLDs, i.e. EBV nuclear antigen (EBNA)1, EBNA3c, latent membrane protein (LMP)2a and the *Bam* HI Z restriction fragment of EBV, beginning with the Leftward OR Frame number 1 (BZLF1) [19-21]. Moreover, to broaden the antigenic repertoire, we used a pool of 125 $CD8^+$ and $CD4^+$ T-cell epitopes with known HLA restrictions, consisting mainly of 9 and 15 amino acids derived from 15 EBV latent and lytic proteins (EBV_{mix}) [22]. In the initial screening the EBV_{mix} appeared to induce the highest T-cell response among a wide range of donors compared to EBNA1, EBNA3c,

BZLF1 and LMP2a peptide pools. The isolation of specific T-cells from five healthy volunteers using the IFN-γ capture assay allowed to select the highest numbers of T-cells, characterised by the best purity of both $CD4^+IFN\text{-}\gamma^+$ and $CD8^+IFN\text{-}\gamma^+$ for EBV_{mix}.

The expanded T-cell lines were highly specific to their cognate antigens. Moreover, upon encounter of the autologous EBV-infected lymphoblastoid cell lines (LCLs), the T-cells proliferated and produced IFN-γ, which demonstrated their ability to recognise and respond to endogenously processed viral antigens. This effect was especially pronounced for the T-cells specific to the EBV_{mix} and LMP2a. We next proved the safety of these T-cell lines in a mixed lymphocyte reaction, in which they appeared to be devoid of alloreactive potential against third-party dendritic cells (DCs).

With regard to the functionality, all lines exhibited moderate cytotoxic properties of 0%-60% against LCLs, which is in line with previous reports [23-25]. Due to this relatively low cytotoxicity we questioned their *in vivo* efficacy against PTLDs. Therefore, we sought to assess their long-term control over LCLs using an outgrowth assay that revealed the highest efficacy of the EBV_{mix}-specific T-cell lines to inhibit the outgrowth of LCLs. While the T-cells specific to LMP2a, EBNA3c and EBNA1 required higher effector to target ratios to control LCLs, the BZLF1 lines predominantly failed in the outgrowth assay.

The proliferation, the concomitant secretion of IFN-γ in response to autologous LCLs as well as the control of the outgrowth and lack of alloreactivity were promising findings in view of the *in vivo* potential of these T-cells. Moreover, we could show in epitope mapping that the T-cell lines specific to the EBV_{mix} had an oligoclonal epitope signature, which minimises the risk of induction of tumour mutants not susceptible to T-cell therapy [7,26,27].

As the role of EBV-specific $CD4^+$ T-cells in adoptive transfer is controversial, $CD4^+$ cells were purified from the T-cell lines. The generated CD4 lines showed high specificities after re-stimulation with the cognate antigens, but secreted less IFN-γ and exhibited mostly lower cytotoxicity than the original T-cell lines upon encounter of autologous LCLs. Most interestingly and in contrary to some previous reports from clinical studies [12,14,16], the CD4 lines, especially in case of

EBNA3c and EBNA1, exhibited a profoundly decreased controlling capacity of LCL in comparison to the T-cell lines. In contrast, purified CD8 lines, consisting of $CD8^+$ T-cells specific to the peptide pools, inhibited the outgrowth similarly to their T-cell lines counterparts, indicating that EBV-specific $CD8^+$, but not $CD4^+$, T-cell have a crucial function against LCLs *in vitro* and that the $CD4^+$ T-cell helper function might be dispensable in our *in vitro* system.

We could further show that the observed reduced capacity of EBV-specific CD4 lines against LCLs was not caused by their decreased viability, exhaustion, or immune evasion by LCLs. Importantly, when co-cultured with LCLs, $CD4^+$ T-cells produced less cytotoxic effector molecules (perforin, granzyme B and granulysin) over time than the EBV-specific $CD8^+$ T-cells, which at least in part explains their inability to eradicate the LCLs.

Altogether, we could show that the EBV-specific T-cell lines generated using for stimulation the EBV_{mix}, comprised of 125 $CD8^+$ and $CD4^+$ T-cell epitopes derived from 16 EBV latent and lytic proteins, demonstrated the highest efficacy of controlling the autologous LCL. None of the commercially available EBV-derived peptide pools exhibited characteristics similar to the EBV_{mix}. These findings indicated a clear advantage of combining defined T-cell epitopes derived from different EBV proteins over using single viral antigens for the generation of EBV-specific T-cells for adoptive transfer. In support of this notion, during preparation of our study Miltenyi Biotec has introduced a new product optimised for efficient stimulation EBV-specific T-cells. The PepTivator EBV Consensus also contains T-cell epitopes derived from various lytic and latent EBV proteins and 29 (67%) of them are contained within the EBV_{mix}. Our preliminary results however indicated that the EBV Consensus induces lower T-cell responses among healthy individuals.

Introduction

Biology of EBV in Immunocompetent Host

Pathogenesis of EBV infection

Epstein-Barr virus (EBV) is a ubiquitous γ-herpesvirus asymptomatically infecting human hosts *via* oral transmission early in the life followed by a life-long latency phase in more than 90% of the population [2,6,28]. Infection in adolescence occasionally manifests as infectious mononucleosis (IM). The main reservoir of EBV is the resting memory B-cell pool, although EBV can also infect other cell types, such as epithelial cells and T-cells [6]. EBV arrives with saliva to the tonsillar crypts, infects and traverses epithelium layer to reach naïve B-cells present in the nasopharyngeal lymphoid system [6,29] (Fig. 1). The viral entry occurs through interactions between gp350 (BLLF1), the major envelope glycoprotein of EBV, and CD21 on the surface of B-cells with concurrent co-receptor interaction between gp42 and human leukocyte antigen (HLA) class II [2]. Then, EBV exploits the physiological B-cell differentiation process to activate infected B-cell to proliferating lymphoblast. This is followed by driving them into resting memory state, when the number of EBV^+ B-cells stabilises (1-50 cells per million of the B-cell pool) and a low amount of viral particles is constitutively released into saliva [2,6,29,30].

Under physiological conditions in the absence of antigen, B-cell receptor (BCR) provides steady-state survival signal to B-cells in the process of constitutive selection for functional BCRs [31]. However, upon recognition of specific antigen the activated B-cells migrate to lymph nodes, proliferate and differentiate to establish germinal centres, where high-rate mutations in the variable regions of immunoglobulin genes occur in the process of somatic hypermutation, resulting in BCR with changed affinity to the cognate antigen. Next, B-cells differentiate and undergo selection based on the interactions between their BCR with germinal-centre T-cells and follicular dendritic cells (DCs). The B-cells with a low-affinity BCR to the cognate antigen receive signals for apoptosis. However, the improved recognition of the cognate antigen allows receiving survival

signals. These B-cells undergo additional rounds of division, mutation and the selection process to eventually leave germinal centre as memory B-cells or antibody-producing plasma cells. The most crucial receptors in the process of B-cell differentiation are BCR and CD40. The member of tumour-necrosis factor (TNF) receptor superfamily, CD40 requires binding by CD40 ligand (CD154) on T-helper cell (T_H) for induction of survival and proliferative signals in the process of B-cell differentiation [32,33].

EBV latent antigens expression during infection

Thus, the infection with EBV needs to mimic all the stages of physiological B-cell differentiation necessary to achieve the latency state [6,29]. Indeed, during the course of infection, differential sets of EBV antigens are expressed to accomplish this task. At least four programmes of EBV gene usage are distinguished (Table 1) [2,6,7,29,34].

Upon entry, EBV activates naïve B-cells and induces their proliferation (Fig. 1). This process is facilitated by the viral latent genes expressed during the EBV growth programme (III), i.e. all EBV nuclear antigens (EBNAs): EBNA1, 2, 3a, 3b, 3c, LP and the latent membrane protein (LMP) 1 and LMP2a.

EBNA1 is the only EBV antigen detected in all EBV-associated malignancies [2,15,35]. It ensures maintenance and replication of viral genome during B-cell division and through binding to viral promoters acts as transcriptional regulator of EBNAs and LMP1 [2,36]. The central part of EBNA1 molecule contains glycine-alanine repeats that stabilise the mature protein by preventing its proteasomal breakdown [35] and on the mRNA level can prevent its own translation [37]. However, it has been demonstrated that EBNA1, which predominantly induces $CD4^+$ T-cell response to EBV, is delivered for the major histocompatibility complex (MHC) class II presentation through degradation by autophagy [38]. EBNA2 is the master transcription factor of the EBV growth programme (III) and controls not only the expression of viral latent genes but also some activation-associated B-cell genes, allowing proliferation of EBV^+ B-cells [2,6,39]. EBNA3 family of proteins can repress the function of EBNA2 by preventing its association with DNA [2,40]. EBNA3c has been shown to play additional roles in transcriptional

regulation and *in vitro* oncogenesis [2,40-42]. Finally, the LMP1 and LMP2a provide the survival signals to EBV-infected B-cell lymphoblast. Both molecules act as constitutively active receptors with ligand-independent signalling necessary for rescuing EBV-activated B-cell blasts from apoptosis and for differentiating them into the memory phenotype [43,44]. LMP1 is a functional homologue of CD40 inducing both anti-apoptotic and proliferative signals [2,43]. LMP2a mimics the survival signal usually provided by the BCR owing to its ability to sequester tyrosine kinases and thereby inhibit the functions of BCR [2,44].

Following the initial activation by EBV, the proliferating EBV$^+$ B-cells, similarly to their antigen-activated B-cell counterparts, undergo germinal-centre reactions [6]. During this process the switch in the viral transcription profile to the EBV default programme (II) occurs with expression of EBNA1, LMP1, LMP2. This transition requires termination of EBNA2 function, as its expression negatively correlates with B-cell differentiation [6].

Consecutively, the EBV-infected B-cells exit the germinal centre, the expression of all the latent viral genes is suppressed (EBV latency programme, 0) and the generated EBV$^+$ memory B-cells leave the lymph node. The EBV latency programme in circulating peripheral blood B-cells enables the benign life-long persistence of EBV within the host, as in this state EBV is hidden from the immune response [2,6,7,30,34]. The occasional homeostatic division of the EBV$^+$ B-cells induces the EBV EBNA1 programme (I), which entails synthesis of EBNA1 for replication of the viral genome [1,7].

It has been proposed that EBV$^+$ cells parallel other memory B-cells and recirculate through the lymph nodes, where they can also become activated by a cognate antigen. Additionally, some of these B-cells can also undergo differentiation to plasma cells and initiate foci of lytic viral replication in the oropharyngeal mucosa (EBV lytic programme, IV). Thus, low-level shedding of EBV virions allow infection of new naïve B-cells as well as transmission of EBV to a new host [2]. The immediate early protein BZLF1 (the *Bam* HI Z restriction fragment of EBV, beginning with the Leftward OR Frame number 1) acts as a transcriptional activator of viral early lytic genes and facilitates transition from the latent to the lytic viral replication [45,46]. Moreover, EBV$^+$ memory B-cells in the

lymph node activate the EBV default programme to receive survival signals from LMP1 and LMP2a. This process might also take part outside of the germinal centres and replenishes the pool of EBV$^+$ B-cells cells [6].

Altogether, the compartmentalisation allows EBV to ensure its persistence and at the same time to maintain the benign character of infection. The nasopharyngeal lymphoid system is the place of continuously active low-level viral replication, which occurs in lytically infected B-cells within the tonsils [29]. However, in the peripheral blood EBV resides silently in the resting memory B-cells [29,30].

Importantly, EBV infection does not escape the attention of the host immune system. Concomitantly with the initial steps of primary infection a strong T-cell response to EBV-derived antigens is initiated, which eliminates many of the EBV$^+$ B-cells. Hence, the expression of more restricted patterns of viral genes during progression of EBV-life cycle allows avoiding recognition by the EBV-specific T-cells and thereby survival of a subpopulation of latently infected B-cells. Thus, the T-cells play a crucial role in bringing EBV infection under control [2,19].

Most of the data on the T-cells responses to primary EBV infection is known from IM patients. IM is a transient, self-limiting illness where the symptoms coincide with shedding of a high viral titer and overactivation of EBV-specific CD8$^+$ T-cells [2]. Thus, consistently with the lytic viral replication, the mounted CD8$^+$ and, to a lesser extent, CD4$^+$ T-cell response is directed predominantly to EBV lytic cycle antigens and to a lower degree against the latent EBV proteins [19,22].

However, the T-cell response, especially of the CD8$^+$ T-cell, contracts upon primary infection and is stably maintained throughout life in memory CD4$^+$ and CD8$^+$ T-cell pool [2,19,22]. In parallel with the transition from the lytic to the latent EBV cycle, the access to the viral lytic antigens becomes limiting and thereby the magnitude and likely the breadth of EBV-specific T-cell specificities shifts from the lytic to the latent epitopes [19,22,47]. Moreover, the T-cell responses to EBV are spread among a subset of antigens rather than exhibit interindividual immunodominance pattern and are strongly dependent on the HLA types [19]. Thus, the CD8$^+$ memory T-cells respond mainly to the EBV epitopes derived from the latent EBNA3a, 3b, 3c and LMP2 as well as from the lytic BZLF1, BRLF1, BMRF1, BMLF1 proteins [19,22]. The memory CD4$^+$ T-cells are mainly reactive to

EBNA1 followed by EBNA2, EBNA3c, and to BZLF1 and other lytic EBV antigens [19,22,48]. It has been estimated that the memory $CD8^+$ T-cell response specific to a particular EBV-derived epitope from the lytic or the latent antigen can constitute between 0.2% to 2% and 0.05% to 1% of $CD8^+$ T-cell pool, respectively [19,49]. The EBV-specific $CD4^+$ T-cell memory pool among healthy carriers can be, however, much smaller [19,22,50].

Notably, in the absence of immune control the EBV infection of B-cells leads to activation of the EBV growth programme (III) followed by transformation of B-cells into lymphoblastoid cell lines (LCLs), the most comprehensive *in vitro* model of lymphomagenic potential of EBV [2].

Table 1 EBV gene transcription programmes (adapted from [1,6,19]).

Programme	Main genes expressed	B-cell	Function	Disease
III Growth	EBNAs: 1, 2, 3a, 3b, 3c, LP LMP1, LMP2	Naïve B-cells that undergo EBV infection	Activation and proliferation of B-cells	PTLDs
II Default	EBNA1, LMP1, LMP2	Germinal-centre B-cells	Differentiation into memory B-cells	HL
0 latency	none	Peripheral blood resting memory B-cells	Persistence	-
I Ebna1	EBNA1	Dividing peripheral blood memory B-cells	Maintenance of viral DNA within memory B-cells	BL
IV Lytic	all lytic genes	Plasma cells	Viral replication	IM

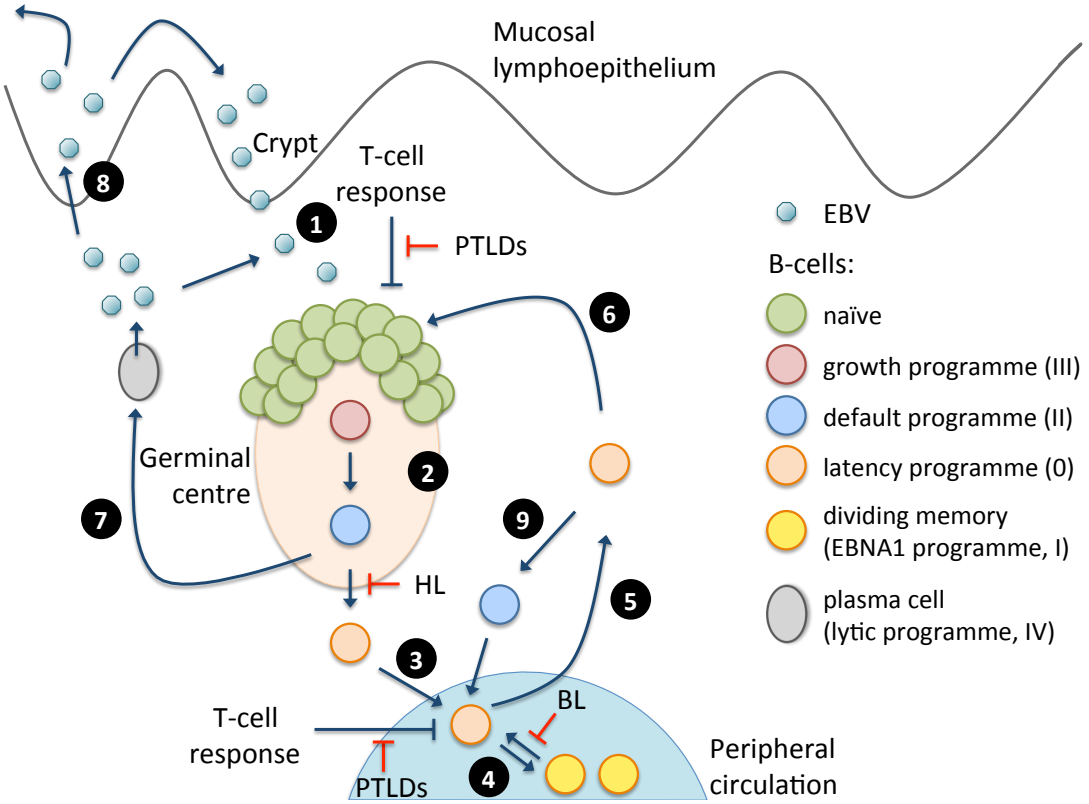

Figure 1 EBV life cycle and infection of B-cells. EBV arrives with saliva to the crypts in the oropharyngeal lymphoid tissue and infects epithelial cells to breach the epithelium and target resting naïve B-cells (1). Expression of the EBV growth programme (III) allows to activate and to induce proliferation of EBV-infected B-cells, which form germinal centres, where the viral gene expression switches to the default programme (II) providing B-cells with survival signals (2). Next, the expression of viral genes is turned off (latency programme, 0) and the generated EBV$^+$ memory B-cells enter the peripheral blood circulation (3). Occasionally, these cells undergo homeostatic division with a concomitant expression of EBNA1 (EBNA1 programme, I) enabling maintenance of viral genome (4). Additionally, the memory B-cells recirculate through the lymph nodes (5), where they can be subject to antigenic selection (6) followed by re-entering peripheral circulation (3) or differentiation to plasma cells (7), in which EBV initiates the lytic replication resulting in shedding of virions to oropharynx for further transmission or re-infection of the host (8). Alternatively, re-circulating EBV$^+$ memory B-cell can enter the default programme (II) and receive survival signal outside of the germinal centres before returning to peripheral blood (9) [1,2]. Putative checkpoints of EBV-associated B-cell lymphomas origin are indicated.

The functions of CD4⁺ T-cell specific to EBV

The adaptive immune response to viral infection is classically associated with the cytotoxic functions of CD8⁺ lymphocytes against virus-infected cells and with B-cells, which produce antibodies targeting viral antigens [47]. According with this view, CD4⁺ T-cells elicit their helper functions to orchestrate the responses of CD8⁺ and B-cells. Indeed, the virus-specific CD4⁺ T-cells can produce T_H1 cytokines, like IFN-γ and TNF-α, to support activation, proliferation and survival of cytotoxic CD8⁺ T-cells together with the immune memory development, as well as to promote anti-viral immunoglobulin G responses [32,47].

Nevertheless, beside the helper role, a direct effector function of virus-specific CD4⁺ T-cells has recently been recognised [32,47]. In studies of mouse γ-herpesvirus 68 (MHV-68), a rodent equivalent of human EBV, the role of virus-specific CD4⁺ T-cells in controlling viral infection has been demonstrated. Whereas B-cells appeared to be dispensable, CD8⁺ and CD4⁺ T-cell were crucial for viral containment and in the absence of CD8⁺ cells, CD4⁺ provided partial protection against lethal infection, which was at least in part mediated by IFN-γ [51,52]. Additionally, EBV-specific CD8⁺ and CD4⁺ T-cell lines exhibited similar granule-mediated cytotoxic properties *in vitro*, and in a mouse model of EBV-associated post-transplant lymphoproliferative disorders (PTLDs), adoptively transferred CD4⁺ T-cells could increase survival of human LCLs-bearing mice when tumour downregulation of MHC class II was inhibited [53]. Consistently with the *in vitro* generated cytotoxic CD4⁺ cells, the presence of perforin⁺ CD4⁺ T-cells specific to EBV has also been shown in human peripheral blood during IM [54].

Multiple mechanisms of the cytotoxic CD4⁺ T-cells response to virus-infected and tumour cells have been proposed [47]. The dominant role in case of EBV-specific CD4⁺ cells appears to play the exocytosis of cytotoxic granules with differential content of perforin, granzyme, and in some reports also granulysin [53,55-57]. Moreover, the expression of perforin and granzyme B requires stimulation of T-cell receptor on CD4⁺ cells, whereas cytotoxic CD8⁺ cells pre-store these molecules in their granules [57]. In addition, the Fas-Fas ligand-dependent mechanism has also been shown for EBNA1-specific CD4⁺ T-cell clones [58].

The cytotoxic function of $CD4^+$ T-cell is dependent on MHC class II-restricted epitope presentation [57]. Thus, the viral antigens need to access this presentation pathway, which was classically viewed to be reserved only for endocytosed molecules. There are two main pathways of virus-derived peptide loading of MHC class II molecule [59]. The exogenous pathway relies upon uptake of virions or infected cell debris [59,60] and can also involve latent viral proteins undergoing intercellular antigen transfer [61]. The endogenous presentation pathway reported for EBV thus far is degradation of EBNA1 by autophagy [38,59].

Finally, the role of EBV-specific $CD4^+$ T-cells has also been shown in the clinical settings. Notably, Haque *et al.* has demonstrated that the clinical response of solid organ transplant (SOT) recipients suffering from PTLDs was better after EBV-specific adoptive T-cell transfer if the T-cell products contained higher percentage of $CD4^+$ T-cells [12]. Interestingly, while beneficial effect of EBV-specific adoptive T-cell transfer was reported for PTLDs patients after hematopoietic stem cell transplantation (HSCT) upon infusion of exclusively $CD4^+$ or $CD8^+$ T-cell lines [14], no correlation was observed between the content of $CD4^+$ cells and the clinical response in a more recent clinical trial [16]. Importantly, in both studies the antigens recognised by the $CD4^+$ T-cell were not clarified. Thus, the specificity, the role and the necessity of $CD4^+$ cells for T-cell therapy remain enigmatic.

EBV-associated B-cell lymphomas

Despite the potential of EBV to drive the activation and proliferation of B-cells, the virus employs various strategies to minimise its pathogenicity and to enter the latency phase establishing asymptomatic life-long infection under the host immune surveillance [1,2,6]. Nevertheless, EBV was first discovered in the cells from biopsies of Burkitt's lymphoma [28] and its tumorigenic potential has since been linked to other human malignancies.

Burkitt's Lymphoma

Although the involvement of EBV in Burkitt's lymphoma (BL) is highlighted by the viral presence in over 95% of cases of the endemic form of BL, which is found predominantly in the areas with holoendemic malaria, the pathogenic role of the

virus in BL remains still elusive [1,2,62]. Notably, the finding that EBV within all tumour cells seems to be clonal, indicates that EBV infection has most likely contributed to malignant transformation [63].

The key factor in pathogenesis of BL is the translocation of the *c-MYC* proto-oncogene under the control of immunoglobulin heavy- or light-chain loci resulting in constitutive high expression of c-myc, which leads to malignant transformation of B-cells [64]. The germinal centre-like phenotype and the pattern of immunoglobulin gene indicating hypermutation of BL cells, led to a conclusion that this translocation most likely occurs during the somatic hypermutation in the germinal centre [1,62,65]. Together with the presence of EBNA1 as the only EBV antigen expressed in BL [66] (Table 1) the tumour has been proposed to originate from EBV$^+$ germinal-centre B-cells during their transition into memory. As these B-cells continuously proliferate due to the activated c-myc and thus cannot enter the latency cycle, they sustain EBNA1 expression to maintain the EBV genome (Fig. 1) [1]. Moreover, the inhibition of EBNA1 in BL cells results in increased level of apoptosis prior to loss of the EBV genome, which further underscores the importance of EBV in BL [67].

Hodgkin's Lymphoma

EBV is associated with about 40% of cases of the classic Hodgkin's lymphoma (HL) [2,68]. The hallmark of HL is the presence of malignant Hodgkin and Reed–Sternberg (HRS) cells, which can co-express markers of several hematopoietic lineages [68]. All HRS cells in EBV-associated HL are positive for clonal virus and express EBNA1, LMP1 and LMP2 (EBV default programme, II) (Table 1) [2,69]. The genotyping of immunoglobulin genes in HRS cells revealed their germinal-centre origin, where most likely the HRS cells acquired mutations. A fraction of these mutations can even preclude the antigenic selection and should cause B-cell death [70]. Interestingly, as IM is a risk factor for EBV$^+$ HL, it seems that the immunological overactivation observed in IM could promote germinal-centre B-cell mutations [1,71]. Thus, the possible pathogenic role of EBV in rescuing malignant progenitors from apoptosis by provision of survival signals by LMP1 and LMP2a has been suggested (Fig. 1) [1,2].

Post-transplant Lymphoproliferative Disorders

HSCT has become a successful treatment option for a range of incurable haematopoietic malignancies and various non-malignant genetic immune disorders [72,73]. If necessary, recipients of HSCT undergo a myelosuppressive conditioning regimen prior transplantation to deplete the host hematopoietic stem cells and thereby reduce disease burden, which allows generating space for donor stem cell engraftment [72]. Allogeneic transplants are associated with a risk of graft-versus-host disease (GvHD), a potentially life-threating condition occurring when donor-derived immune cells attack host tissues, which may require prolonged immunosuppressive treatment [74]. However, the incidence of tumour relapse in allogeneic HSCT is lower due to the concomitant graft-versus-tumour effect (GvT) [73-75]. Therefore, currently investigated strategies aim at preserving the beneficial effect of GvT but at the same time reducing GvHD [74,75].

The period of immune reconstitution - the engraftment of donor-derived hematopoietic stem cells in recipient's bone marrow followed by development of donor-derived haematopoiesis - varies considerably between different immune cell subsets [76,77]. Hence, the recovery of neutrophils has been observed between 2 to 5 weeks after allogeneic HSCT [77]. In contrast, the natural killer (NK) cells recover after 3 months and after 3-6 months first donor-derived T-cells exit the thymus [76,77]. Finally, the reconstitution of B-cell compartment occurs up to 2 years after HSCT [77]. The course of immune reconstitution strongly depends on patient's background, conditioning regimen, type of graft used for HSCT and can be further prolonged in case of GvHD development and application of immunosuppressive agents [76,77].

Importantly, in order to decrease the risk of graft rejection due to host anti-donor effect in the settings of solid organ transplantation (SOT) the immunosuppressive treatment is long-term and more intensive than in allogeneic HSCT, which leads to continued downregulation of immune responses in SOT recipients [3,76].

Altogether, the marked state of cellular immunodeficiency of allogeneic HSCT and SOT recipients results in increased susceptibility to a wide range of infections caused by viruses, fungi and bacteria [3,76,77].

As a consequence of an ablated or decreased T-cell response, the reactivation of EBV occurs, which is asymptomatic in around 60% of HSCT recipients (Khanna N, unpublished data) [19]. However, some transplant recipients were shown to lose the control over replicating EBV, which may ultimately lead to unlimited latently-infected B-cell proliferation and the development of PTLDs [4,7,19,78,79]. PTLDs occur in around 1-5% and 3-10% of HSCT and SOT recipients, respectively, and are associated with an exuberant mortality [3-5].

EBV-positive PTLDs account for more than 90% of all PTLDs and constitute a heterogeneous group of malignancies comprised of four major histological subtypes: early lesions, monomorphic (including Burkitt's lymphoma), polymorphic and classic Hodgkin's lymphoma [80,81]. PTLDs arise predominantly within the first year upon transplantation, during the most intensive immunosuppression phase, and the majority of the early-onset PTLDs are associated with EBV, in contrast to the more aggressive late-onset disease [2-4,7]. EBV-associated PTLDs after HSCT usually originate from donor-derived B-cells, whereas in SOT recipients PTLDs stem mostly from recipient-derived B-cells [82,83]. The characteristics and risk factors of EBV-associated PTLDs after allogeneic HSCT and SOT are summarised in Table 2.

The EBV^+ PTLD cells have been shown to express EBV growth programme (III) with expression of all EBNAs and LMP proteins (Table 1) [21]. The immunoglobulin gene analysis of PTLD cells has revealed presence of naïve, memory, and atypical post-germinal centre EBV-infected B-cells [84]. Therefore, it has been proposed that PTLDs can originate from various stages in the B-cell differentiation, which may also overlap with other EBV-associated malignancies, and can be driven by the EBV-growth programme in the absence of T-cell surveillance (Fig. 1) [2,84]. Finally, the role of oncogenes in PTLDs pathogenesis has only been found for mutations in *BCL-6* gene in 44% SOT recipients, which was linked to poorer prognosis of these patients [85].

Table 2 Characteristics of EBV-associated PTLDs in recipients of allogeneic HSCT and SOT [3-5,7].

HSCT	SOT
Occurrence	
6-12 months after HSCT	Up to 12 months after SOT
Clinical manifestation	
IM-like syndrome Tonsillar enlargement Cervical lymphadenopathy Multiorgan dysfunction (in progressive disease)	IM-like syndrome Abdominal-mass lesions Infiltrative disease of the allograft Hepatocellular or pancreatic dysfunction Central nervous system disease
Major risk factors	
T-cell depleted stem cell product Serological EBV mismatch recipient (+)/donor (-) High HLA-mismatch degree between donor and recipient Intensive immunosuppression with antithymocyte globulin as GvHD prophylaxis or therapy	Serological EBV mismatch recipient (-)/donor (+) High intensity immunosuppression (especially when lymphoid cells present in the graft, e.g. small intestine and lung)

Treatment methods of PTLDs

Prophylactic and treatment approaches of PTLDs aim at eliminating the EBV-infected B-cells or restoring the EBV-specific T-cell immunity.

A considerable proportion of 40-60% of cases with EBV-associated PTLDs responds to the rituximab, a chimeric murine-human monoclonal anti-CD20 antibody. This strategy has indirect antiviral activity by deleting the B-cells with the residing virus but may fail because of down-regulation of the CD20 antigen on malignant B-cells [8,86]. Moreover, the use of rituximab can cause fatal viral reactivation and, as it also extensively depletes EBV-negative B-cells, it may result in decreased response to vaccination and lead to severe infections with encapsulated bacteria (i.e. *Streptococcus pneumoniae*) [87,88]. Notably, the beneficial effect of rituximab appears not to be long-term without reconstitution of viral-specific T-cell, which is of a special concern in SOT recipients, who receive continuous immunosuppression [8,89].

The use of antiviral drugs targeting EBV replication, e.g. acyclovir, as prophylaxis can reduce the risk of PTLDs in seronegative recipients receiving SOT from EBV-positive donor, however it is ineffective against already established PTLDs, where the lytic viral replication seems to play a minor role [8,90]. Application of anti-lymphoma chemotherapy, although effective in some cases, is often associated with high toxicity [3,8].

Altogether, these treatments do not improve EBV-specific T-cell response of the transplant recipients, which is crucial in controlling the virus. Thus, restoration of the balance between outgrowing EBV-infected B-cells and EBV-specific T-cells is of highest importance in the management of PTLDs.

Reduction of immunosuppression, often combined with rituximab treatment, is more effective in SOT than in HSCT recipients, as the latter group, especially in the early phase after transplantation, might not be able to mount a sufficient EBV-specific T-cell response within a short period of time [7,8]. Although reduction of immunosuppression later after transplantation or as a pre-emptive measure can be successful [8], this approach is associated with a risk of GvHD or graft rejection in HSCT and SOT settings, respectively.

Therefore, various strategies to restore EBV-specific immunity by T-cell infusion have been developed (Fig. 2).

Initially, Papadopoulos *et al.* reported in 1994 on the treatment of PTLDs after HSCT with unmanipulated donor lymphocyte infusion (DLI) [91] (Fig. 2A). Although since then DLI has shown an efficacy up to 70% in HSCT recipients, this procedure is associated with an elevated incidence of severe and fatal GvHD caused by high numbers of alloreactive T-cells present in DLI [26,91,92].

Thus, alternative approaches involve selection of EBV-specific T-cells for infusion to reduce the risk of GvHD. To generate the appropriate T-cell product for PTLDs the choice of antigens, to which these cells will be specific, should be based on the EBV growth programme (III), which is found in PTLDs [21]. Thus, LCLs, expressing the same set of viral proteins, appear to be the best antigen presenting cells for a selective *in vitro* stimulation of T-cells specific to EBV-derived antigens presented by PTLDs [2,7,93]. Additional advantages of LCLs are the high expression of HLA class I and II together with co-stimulatory molecules, as well as standardised methods of generation to a large number from healthy individuals [7,19].

The group of Heslop and Rooney has generated donor-derived EBV-specific T-cell lines through donor LCL-stimulation (Fig. 2B) and used them successfully for prevention and treatment of PTLDs in HSCT settings [14,18]. These cell lines comprised $CD4^+$ as well as $CD8^+$ T-cells, both of which appeared to be clinically beneficial for the adoptive T-cell therapy, and substantially expanded *in vivo* without causing *de novo* GvHD [7,14]. None of the prophylactically infused patients developed PTLD and a complete remission was observed in 85% treated patients. Moreover, owing to genetic modification of a part of the T-cell products, the authors could track the presence of infused T-cells after 9 years [14]. This method has been since then used in the management of PTLDs. Nevertheless, it has some limitations. First, it has been reported that PTLDs can be caused by EBV strain different from the laboratory B95.8 EBV used for preparation of LCLs, which resulted in generation of T-cells specific to EBV-derived antigens that were not presented by PTLDs and ultimately led to treatment failure [26,27]. Second, generation of T-cell lines involves the use of live virus, is laborious and

time-consuming (2-4 months), which precludes its emergency application in patients with progressive PTLDs.

Therefore, using the LCL-stimulation method, a cell bank of HLA-characterised EBV-specific T-cells has been generated to make the adoptive T-cell transfer readily available for immediate infusion [12,13,94]. These T-cell lines were used, based on their best HLA-match and *in vitro* cytotoxicity, in SOT recipients suffering from PTLD upon failure of conventional therapy and an overall clinical response of 52% has been reported. The response was dependent on HLA-match, which allows recognition of tumour cells, and the content of $CD4^+$ T-cells [12].

Moreover, to widen the range of targeted pathogens, T-cell lines specific to EBV, cytomegalovirus (CMV), and adenovirus (AdV), the most frequent causes of viral morbidity and mortality after HSCT, have been generated using stimulation with monocytes and LCLs transduced with adenoviral vector expressing antigens of CMV and AdV [95]. In a recent clinical study, these cells were also banked and used as a third-party virus-specific treatment of HSCT recipients suffering from severe refractory viral diseases, including PTLDs, for which the clinical response reached 66.7% [16].

Together, despite the proven clinical efficacy of banked third-party virus-specific T-cells, the procedure of their manufacturing remains still laborious and involves the use of infectious virus and viral vector, which profoundly impede its wide application.

Recently, Gerdemann *et al.* has developed a method to generate trivirus-specific T-cells in a single stimulation step with DCs transfected with plasmids encoding EBV (LMP2, EBNA1, BZLF1), CMV or ADV antigens followed by 1-2-week *in vitro* expansion, which have shown promising clinical results [11]. Although this strategy has significantly reduced the manufacturing time (2-3 weeks) and use of potentially biohazardous viral materials, it still requires generation and transfection of DCs. Hence, the authors have also generated multi-virus-specific T-cell lines by a 10-days expansion protocol using commercially available peptide pools derived from different viruses for *in vitro* reactivation [24]. The T-cell lines obtained this way showed promising characteristics *in vitro*, however the

procedure requires further investigation of its *in vivo* efficacy and the expansion step can only be conducted in highly dedicated GMP clinical laboratories.

Therefore, an alternative antigen-specific T-cell enrichment method has been generated to select T-cells of interest within a short time frame. Cytokine capture assays have initially been developed to study cytokine production at a single-cell level [96,97]. However, IFN-γ capture technology was then used to select tumour-specific T-cells, the anti-tumour efficacy of which has been shown in a mouse model [98]. Soon after, the IFN-γ capture assay (Miltenyi Biotec) has been approved for good manufacturing practice (GMP) and successfully employed for isolation of AdV- and CMV-specific T-cells for adoptive T-cell transfer [9,10,99].

The procedure is based on immunomagnetic isolation of T-cells, which secrete IFN-γ upon stimulation of peripheral blood mononuclear cells (PBMCs) with antigens of interest, and can be directly infused into patients without a need of further *in vitro* expansion (Fig. 2C).

Two recent studies have used the IFN-γ capture assay for EBV-specific adoptive T-cell transfer to treat PTLDs after HSCT. In the first, Moosmann *et al.* isolated T-cells from donor-derived PBMCs stimulated with a pool of 19 HLA class I- and 4 class II-restricted epitopes derived from 11 latent and lytic EBV proteins [17]. The authors reported clinical response in 50% (3 of 6) patients, who were treated for early-stage PTLDs [17]. In the second study by Icheva *et al*. the authors generated donor-derived T-cell products specific to EBNA1 recombinant protein or overlapping peptide pool and reported 70% clinical response rate among 10 patients treated for EBV-related complications after HSCT [15].

Thus, the EBV-specific T-cells generated for adoptive transfer using the IFN-γ capture assay has shown promising clinical results devoid of adverse effects and *de novo* GvHD induction. The procedure is rapid (36-48 hours), very feasible and does not require any use of potentially biohazardous reagents for stimulation, which simplifies the authorisation for manufacturing a clinical-grade T-cell product. Interestingly, IFN-γ capture assay has also been used to select T-cells specific to CMV, EBV and AdV followed overnight stimulation based on transduction of PBMCs with adenoviral vector expressing viral antigens, a procedure that has not yet been evaluated for its *in vivo* efficacy [23].

Nevertheless, application of the IFN-γ capture assay has also raised some important questions [7]. First, which of the EBV antigens should be used for stimulation to enable efficient recognition of PTLDs by generated T-cells and to avoid induction of tumour escape mutant? This issue has recently been addressed in a study, which showed a highest T-cell precursor frequency in healthy individuals to a combination of commercially available, but not fully GMP-approved, EBNA3a, b, c-derived epitopes with EBNA1 and BZLF1 peptide pools. Nevertheless, the T-cell lines generated using the IFN-γ capture assay followed by *in vitro* expansion, although devoid of alloreactive properties, were only moderately cytotoxic against autologous LCLs [25]. Thus, the selection of appropriate antigens of EBV, which is known for its lack of high interindividual immunogenicity [19], requires further investigations. Second, the use of high numbers of peptides for stimulation may increase the risk of antigenic competition for binding to the HLA molecules and thereby not result in broadening the specificity of T-cells. Some peptides can also cause potential cross-reactivity to alloantigens. Additionally, the recovery of circulating virus-specific T-cells with low frequency can be questionable [24]. Moreover, although IFN-γ is well recognised as an important protective mediator of immune response to viruses and to tumours [32,98], the isolation protocol might require inclusion of other cytokines or surface markers to select T-cells with better properties. Thus, these concerns need to be addressed in future studies aiming at optimising the IFN-γ capture-based strategies for generation of EBV-specific T-cell products.

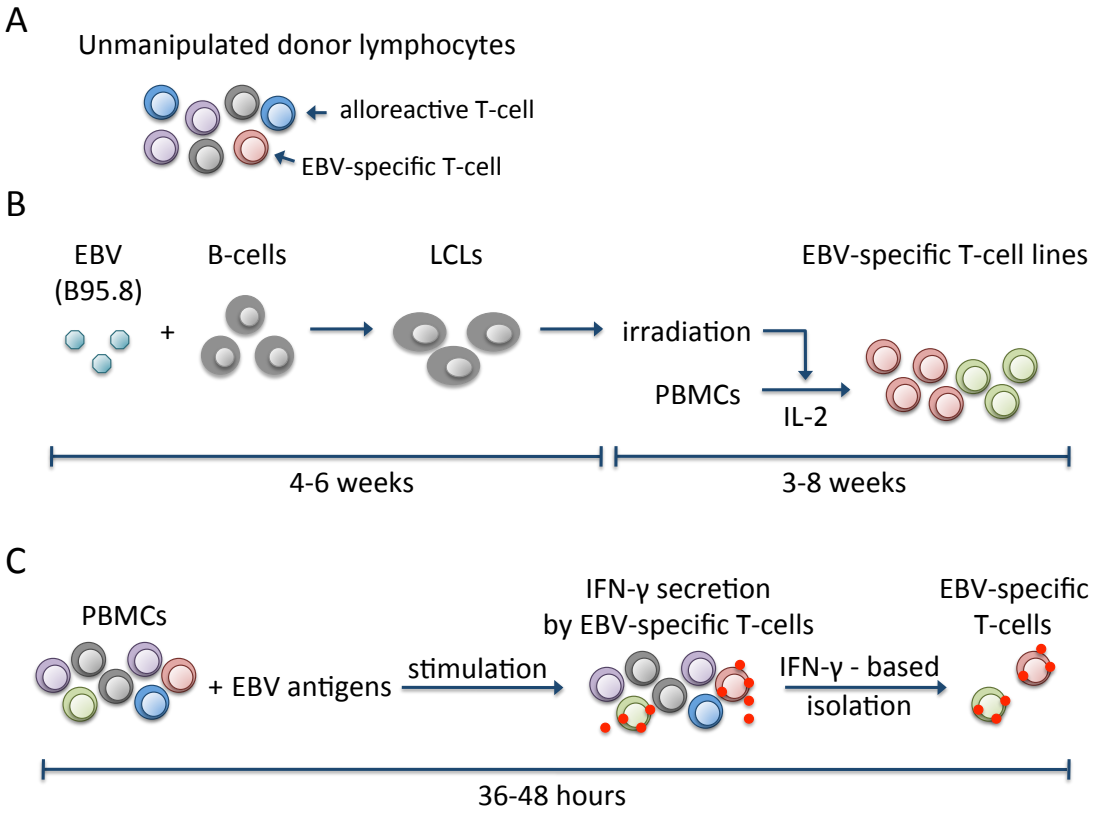

Figure 2 Methods of EBV-specific T-cell generation for adoptive transfer. (A) Infusion of unmanipulated donor-derived lymphocytes (DLI) is associated with a risk of GvHD or graft rejection due to the presence of not only EBV-specific but also alloreactive T-cells. (B) Stimulation of peripheral blood mononuclear cells (PBMCs) with irradiated autologous lymphoblastoid cell lines (LCLs) as antigen presenting cells allows to generate T-cell lines recognising endogenously processed EBV antigens similar to those presented by PTLDs, but the procedure is laborious and time-consuming. (C) Application of IFN-γ capture assay enables immunomagnetic isolation of T-cells responding to stimulation with EBV-derived antigens by IFN-γ production, which can then be directly used for patient infusion.

Aim of the Thesis

EBV infects and establishes asymptomatic life-long latency in more than 90% individuals worldwide [1,2,6]. Despite predominantly benign nature of interactions between the virus and its host, EBV can also exhibit a profound tumorigenic potential, mostly in situations of immunological incompetence of the host, like these observed during the immunosuppressive treatment in HSCT and SOT recipients. There are many approaches to prevent and treat the PTLDs, however adoptive transfer of EBV-specific T-cells is of highest importance, as it has proven its clinical efficacy also in the patients with diseases not responding to other treatments [7]. Thus, adoptive T-cell transfer, especially for these patients, is recommended but currently not available in Switzerland (European Conference on Infection in Leukemia (ECIL) guidelines 2011 [100]). Moreover, most of the methods used nowadays for generation of EBV-specific T-cells rely on long-term, laborious re-stimulation steps, which also require use of potentially biohazardous viral components [7]. The GMP-approved IFN-γ capture assay (Miltenyi Biotec) allows to substantially decrease the manufacturing time, is very feasible and overcomes the need of using viable virus. Indeed, two small studies have already shown its clinical efficacy [15,17]. However, the cellular stimulation step with EBV-derived antigen, which precedes the isolation of responding virus-specific T-cells using the IFN-γ capture assay, has not been fully optimised.

Thus, the major goal of this study is to determine EBV antigens, which induce high numbers of EBV-specific IFN-γ positive $CD4^+$ and $CD8^+$ T-cells that cover a wide range of HLA types and that can ultimately be used in combination with the IFN-γ capture assay to enrich the EBV-specific T-cells for clinically effective adoptive transfer to prevent and treat EBV-associated PTLDs.

Since the T-cell response to EBV in healthy humans strongly depends on HLA types and is spread among a set of immunologically sub-dominant viral proteins [19], and the PTLDs are characterised by the expression of EBV growth programme (III) [21], the antigens used for stimulation have to be carefully chosen to allow the selected T-cells to recognise and ultimately kill the EBV-positive tumour cells *in vivo*. Moreover, although the relevance of cytotoxic $CD8^+$ T-cells is well

recognised [7,19], the EBV-specific $CD4^+$ cells also appear to be important for the efficacy of adoptive T-cell transfer, although their precise function and necessity remain still a matter of debate [12,14,16,32,47,57].

Various antigens can be used for stimulation of EBV-specific T-cells. Indeed, Icheva *et al.* has shown that commercially available overlapping peptide pool of EBNA1 could be of interest [15]. However, concerns regarding the level of EBNA1-derived epitope presentation on PTLDs and their downregulation by tumour point towards further tailoring of the antigen selection for stimulation. Indeed, Moosmann and colleagues have used in their study a mix of 19 HLA class I- and 4 class II-restricted epitopes derived from 11 latent and lytic EBV antigens [17]. Nevertheless, poor HLA coverage and scarcity of HLA class II epitopes might have influenced the clinical outcome. Thus, although an attempt to optimise the EBV antigenic pool by combining EBNA3-derived epitopes with EBNA1 and BZLF1 peptide pools has recently been undertaken [25], this study did not evaluate the efficacy of generated T-cell lines against PTLDs, and especially their long-term controlling potential over the tumour.

Therefore, we decided to generate, using the IFN-γ capture assay, T-cell lines specific to commercially available and partially GMP-certified overlapping peptide pools derived from LMP2a, EBNA1, EBNA3c and BZLF1, some of the most immunogenic EBV antigens expressed in PTLDs [19]. Moreover, we aimed at comparing these pools with a mixture of 125 $CD8^+$ and $CD4^+$ T-cell epitopes with known HLA restrictions, consisting mainly of 9 and 15 amino acids derived from 16 EBV latent and lytic proteins (EBV_{mix}) [22].

Various properties of those generated T-cell lines will be addressed. Their specificity, potential to recognise and respond to autologous LCLs, the best *in vitro* model of PTLDs [2], alloreactivity, and the molecular mechanisms of the control over LCLs, with special focus on the virus-specific $CD4^+$ T-cells will be investigated.

The findings of this translational project will help to introduce EBV-specific adoptive T-cell transfer as a strategy to manage viral-associated complications after transplantation in patients at the University Hospital of Basel.

Results

(Manuscript accepted for publication in Cytotherapy, 08.06.2015)

T cells specific for different latent and lytic viral proteins efficiently control Epstein-Barr virus-transformed B cells

Running title: Efficacious EBV-specific T cells for therapy

Justyna Nowakowska, PhD[1], Claudia Stuehler, PhD[1], Adrian Egli, MD PhD[1,2], Manuel Battegay, MD[3], Georg Rauser, PhD[4], Glenn Robert Bantug, PhD[5], Christian Brander, PhD[6,7], Christoph Hess, MD PhD[5] and Nina Khanna, MD[1,3]

[1]Infection Biology Laboratory, Department of Biomedicine, University and University Hospital of Basel, Switzerland; [2]Clinical Microbiology, University Hospital of Basel, Switzerland; [3]Division of Infectious Diseases and Hospital Epidemiology, Department of Biomedicine and Clinical Research University Hospital of Basel, Switzerland; [4]Research and Development, Miltenyi Biotec, Bergisch-Gladbach, Germany; [5]Immunobiology, Department of Biomedicine, University and University Hospital of Basel, Switzerland; [6]AIDS Research Institute-IrsiCaixa and AIDS Unit, Hospital Germans Trias i Pujol, Autonomous University of Barcelona, 08916 Badalona, Spain; Institució Catalana de Recerca i Estudis Avançats, Barcelona, Spain; and [7]University of Vic and Central Catalonia, Vic. Spain.

Corresponding author:
Nina Khanna, MD
Infection Biology Laboratory and Clinic of Infectious Diseases and Hospital Epidemiology, University Hospital of Basel, Petersgraben 4, 4031 Basel, Switzerland e-mail: nina.khanna@usb.ch
Phone: +41 61 328 7325
Fax: +41 61 265 3198

Abstract

Background aims: Epstein-Barr virus (EBV)-associated post-transplant lymphoproliferative disorders (PTLD) belong to the most dreaded complications of immunosuppression. The efficacy of EBV-specific T-cell transfer for PTLD has been previously shown, yet the optimal choice of EBV-derived antigens inducing polyclonal $CD4^+$ and $CD8^+$ T cells that cover a wide range of human leukocyte antigen types and efficiently control PTLD remain unclear.

Methods: A pool of 125 T-cell epitopes from 7 latent and 9 lytic EBV-derived proteins (EBV_{mix}) and peptide pools of EBNA1, EBNA3c, LMP2a, and BZLF1 were used to determine T-cell frequencies and to isolate T cells using the interferon (IFN)-γ cytokine capture system. We further evaluated the phenotype and functionality of the generated T-cell lines *in vitro*.

Results: EBV_{mix} induced significantly higher T-cell frequencies and allowed selecting more $CD4^+IFN\text{-}\gamma^+$ and $CD8^+IFN\text{-}\gamma^+$ cells than single peptide pools. T cells of all specificities expanded similarly *in vitro*, recognised cognate antigen and, to a lower extend, EBV-infected cells, exerted moderate cytotoxicity and showed reduced alloreactivity. However, EBV_{mix}-specific cells most efficiently controlled EBV-infected lymphoblastoid cell lines (LCL). This control was mainly mediated by EBV-specific $CD8^+$ cells with an oligoclonal epitope signature covering both latent and lytic viral proteins. Notably, EBV-specific $CD4^+$ cells unable to control LCL produced significantly less perforin and granzyme B likely due to limited LCL epitope presentation.

Conclusions: EBV_{mix} induces a broader T-cell response probably due to its coverage of latent and lytic EBV-derived proteins that may be important to control EBV-transformed B cells and might offer an improvement of T-cell therapies.

Key words

Epstein-Barr virus; PTLD; immunotherapy; adoptive T-cell transfer; IFN-γ selection.

Introduction

Epstein-Barr virus (EBV)-associated post-transplant lymphoproliferative diseases (PTLD) cause significant mortality after transplantation.[1-3] Immunosuppression reduces the number and/or function of EBV-specific T cells resulting in uncontrolled proliferation of EBV-infected B cells and tumour formation.[1-5] Treatment strategies include withdrawal of immunosuppression, anti-CD20 antibodies that eliminate B cells –the main reservoir of EBV, or sequential immunochemotherapy with anti-CD20 antibodies and cyclophosphamide, doxorubicin, vincristine, and prednisolone (CHOP) chemotherapy.[6,7] Nevertheless, these treatments fail in up to 60% of cases.[7]

Transfer of functional EBV-specific T cells may control PTLD after transplantation when the recipient's adaptive immunity is not yet restored. It was previously shown that adoptive transfer of donor-derived EBV-specific T cells is safe and can efficiently control PTLD.[8-12] Particularly, recent studies using a rapid expansion protocol or immunomagnetic sorting with the interferon (IFN)-γ cytokine capture system (CCS) for direct infusion are promising.[8,9,11] However, it is not clear yet, which EBV epitopes most efficiently induce polyclonal $CD4^+$ and $CD8^+$ T cells that control PTLD and cover a wide range of human leukocyte antigen (HLA) types.[8,9,13,14] Moreover, the function and necessity of EBV-specific $CD4^+$ cells to control PTLD is debated, especially in relation to their cytotoxic potential.[10,12,15-18]

PTLDs express latent viral proteins, i.e. EBV nuclear antigens (EBNA1, 2, 3, and EBNA-LP) and latent membrane proteins (LMP1 and LMP2), but also several lytic proteins, e.g. BZLF1.[4,19] Since there are no reliable animal models of PTLD,[20] *in vitro* generated EBV-infected B cells (lymphoblastoid cell lines (LCL)) expressing a similar viral gene profile are currently the best model to study PTLDs and PTLD-directed immune responses.[5,21]

Here, we compared a pool of $CD8^+$ and $CD4^+$ T-cell epitopes from 7 latent and 9 lytic EBV-derived proteins (EBV_{mix})[22] to commercially available LMP2a, EBNA1, EBNA3c and BZLF1 peptide pools. We assessed the EBV-specific T-cell frequencies in healthy donors and hematopoietic stem cell transplantation (HSCT) recipients. Using the IFN-γ CCS we isolated EBV-specific cells, evaluated

the $CD4^+$ and $CD8^+$ T-cell specificity and their short- and long-term functionality against LCL.

Materials and Methods

EBV-derived peptide pools

Commercially available peptide pools covering complete sequences of EBNA1, LMP2a, BZLF1 (PepTivator, Miltenyi Biotec, Bergisch Gladbach, Germany), and EBNA3c (JPT Peptide Technologies, Berlin, Germany) consist of 15-mer peptides overlapping by 11 amino acids. The pool of 91 HLA class I and 34 HLA class II T-cell epitopes of 8-20-mers derived from 16 latent and lytic proteins (EBV_{mix}) was provided by C.H. and C.B. (Supplementary Table S1).[22]

Patients and healthy donors, cell isolation and generation of dendritic cells (DC) and lymphoblastoid cell lines (LCL)

Blood was obtained from adult healthy donors and adult HSCT recipients after written, informed consent and approval by the Ethical Committee Nordwest- und Zentralschweiz, Switzerland (number 242/11). Healthy donors were HLA-typed (Donor 3: A1, A11, B08, B35, C04, C07, DR1, DR17, DQ02, DQ05; Donor 4: A11, A24, B07, C07, DRB1 15, DRB5 01, DRB6 02; Donor 6: A02, A203, B13, B44, C05, C06, DR07, DR16, DQ02, DQ05; Donor 9: A02, A203, A23, B44, B55, B22, C03, C04, DR07, DR13, DR14, DQ02, DQ06; Donor 13: A01, A23, B08, B44, DRB1 03, DRB1 07, DQB1 02). HSCT recipients were in median 54 months (range 30-108) after HSCT, under persistent immunosuppression and replicated EBV in the blood 2 to 10 months before blood sampling. EBV-PCR was performed in whole blood as previously published.[23] The study was conducted according to the Declaration of Helsinki. Isolation of peripheral blood mononuclear cells (PBMC) and generation of DCs were performed as previously published.[24] LCL were generated from autologous PBMC infected with B95.8 EBV.[20]

IFN-γ-based CCS and expansion of T cells

After 4-hour stimulation of PBMC ($1x10^8$) with respective peptide pools EBV-specific cells were enriched using the Large Scale IFN-γ Secretion Assay-

Enrichment Kit (Miltenyi Biotec) according to the manufacturer's instruction. Unstimulated PBMC served as control. The positive cell fractions were investigated with anti-IFN-γ-PE (Miltenyi Biotec), anti-CD4-PacificBlue and anti-CD8-APC (all BioLegend, London, UK) staining using CyAn ADP Flow Cytometer (DAKO Cytomation, Glostrup, Denmark) and analysed with FlowJo software (Tree Star, Stanford, CA). The isolated cells were then expanded in order to increase their numbers for further characterisation *in vitro.* Up to $4x10^5$ cells from IFN-γ-positive fraction were expanded with 1:50 γ-irradiated (35 Gy) autologous feeder cells.[25] Cultures were supplemented with 5U/mL IL-2 (Proleukin, Novartis, Nürnberg, Germany) until day 7 and additionally with 10ng/mL IL-7 and IL-15 (PeproTech, Hamburg, Germany) from day 7 to 14.[25] Thereafter specificity was assessed by intracellular cytokine (ICC) staining and cells were cryopreserved. The T-cell lines were expanded for further analysis as previously published.[26] $CD4^+$ and $CD8^+$ T cells were selected from T-cell lines using CD8 or CD4 MicroBeads (Miltenyi Biotec) according to manufacturer's instruction to at least 95% purity and used immediately or expanded by the rapid expansion protocol.

Enzyme-linked immunospot assay (ELISpot) and ICC staining

Frequencies of cytokine-producing cells in PBMC, in T-cell and CD4-lines were assessed by IFN-γ or interleukin (IL)-4 ELISpot after overnight stimulation using 96-well filter plates (Millipore, Darmstadt, Germany) and anti-IFN-γ or anti-IL-4 antibodies (Mabtech, Nacka Strand, Sweden) according to the manufacturers' instructions. For PBMC, $2x10^5$ cells/well were stimulated with LMP2a (0.05-4μg/peptide/mL), BZLF1 (0.5-4μg/peptide/mL), EBNA1 (0.05-2μg/peptide/mL), EBNA3c (0.5-2μg/peptide/mL) or EBV_{mix} (0.1-10μg/peptide/mL).

For expanded cell lines, $5x10^3$ (T-cell lines) and $1x10^4$ (CD4-lines) cells/well were stimulated with peptide-pulsed autologous DC at 10:1 responder-to-stimulator (R:S) ratio or LCL at 1:5 R:S ratio. Spots were counted using ELISpot reader (Cellular Technology Ltd Europe, Bonn, Germany). ICC staining after 6-

hour re-stimulation with antigens (0.5µg/peptide/mL) was performed as earlier described.[25]

Proliferation and mixed lymphocyte reaction by [^{3}H]-thymidine incorporation

For proliferation, T-cell lines (2x10^5 cells/well) were stimulated with 70-Gy-irradiated LCL at 2:1 effector-to-target (E:T) ratio and, where indicated, peptide pools (0.5µg/peptide/mL) were added. For mixed lymphocyte reaction, autologous PBMC and T-cell lines were cultured with 2 different 35-Gy-irradiated third-party DCs (5:1 R:S ratio) for 96 hours. DNA synthesis was assayed by adding 1µCi (0.037MBq [^{3}H]-thymidine (Hartmann Analytic, Braunschweig, Germany) per well for the last 18 hours of culture. The cells were harvested on glass filter paper (Perkin Elmer, Schwerzenbach, Switzerland) and the counts per minute (cpm) determined using TopCount NXT scintillation counter (Packard, Meriden, CT). Background values of samples with effectors and stimulators incubated alone were subtracted.

Short-term cytotoxicity

LCL (0.1x10^6) were incubated for 6 hours with T-cell or CD4-lines at 5:1 and 30:1 E:T ratios. Where indicated, LCL were pulsed with peptide pools (0.5µg/peptide/mL) for 1.5 hour followed by washing. Fc receptors were blocked with Human TruStain FcX followed by anti-CD3-APC staining (BioLegend). Viability was assessed with FITC Annexin V Apoptosis Detection Kit with PI (BioLegend) according to manufacturer's instruction and cytotoxicity calculated using the following formula: % specific lysis = 100−([V_{test}/$V_{control}$]*100). V_{test} and $V_{control}$ represent percentage of viable targets (CD3$^-$FITC$^-$PI$^-$) incubated with and without effectors, respectively. Control experiments confirmed the independency of cytotoxicity from the total cell number up to 3.1x10^6 cells/sample and lack of cytotoxicity against autologous DC (data not shown).

Outgrowth

Two-fold LCLs dilutions were prepared in U-bottom 96-well plate from $2x10^4$ LCL/well (1:2 E:T ratio) to 312 (32:1 E:T ratio) LCL/well and T cells ($1x10^4$ cells/well) were added in triplicates. LCL alone served as control. Half the medium was replenished weekly. After 4 weeks LCL outgrowth was assessed by visual inspection. The readout was defined as the lowest E:T ratio inhibiting LCL outgrowth in at least 2 out of 3 wells with concomitant outgrowth in the corresponding control wells. The results of consecutive experiments were repeatedly confirming. If no outgrowth at 1:2 E:T ratio was observed, the score 0.25 was assigned; outgrowth at 32:1 E:T ratio was scored as 64.

For cytometric analysis, cultures at 1:2 E:T ratio were prepared. To determine the surface markers expression cells were harvested at day 1, 2, and 5, stained with Zombie Aqua together with Fc receptors blocking, followed by anti-CD3-PerCP, anti-CD4-PacBlue, anti-Fas-ligand-PE, anti-PD-1-FITC, anti-CD80-APC, anti-Fas-PECy5, or anti-HLA-DR-APC staining (all BioLegend). For analysis of granule-mediated cytotoxicity brefeldin A (Sigma-Aldrich, Steinheim, Germany) was added to the cultures for 5 hours. After anti-CD3-PerCP, anti-CD4-PacBlue staining ICC staining protocol was followed with anti-perforin-APC, anti-granzyme B-FITC and anti-granulysin-PE antibodies or respective isotype controls (all BioLegend).

Statistical analysis

Statistical analyses were performed using GraphPad Prism (version 6.0). Data are shown with median and inter-quartile ranges unless otherwise indicated. Continuous non-normal distributed data were analysed using a Mann-Whitney U test (MWU) or Kruskal-Wallis test (KW). All tests were two-tailed. *P* values <0.05 were considered statistically significant.

Results

EBV_{mix} is more immunogenic than the commercially available overlapping peptide pools

To determine the memory T-cell frequencies for the different peptide pools in healthy individuals, we measured IFN-γ production in ELISpot assay. Overall, the responses to the different EBV antigens showed a great variability. Moreover, we titrated the concentration of each peptide pool in different healthy individuals and observed that the concentration inducing the highest T-cell response varied between individuals (data not shown). However, overall only EBNA3c and EBV_{mix} induced IFN-γ production in median above 100 SFC/10^6 cells. The response to EBV_{mix} was significantly higher than to LMP2a, BZLF1, and EBNA1 (P<0.001, KW with Dunn's multiple comparisons test; Fig. 1a). EBV_{mix} induced responses in 15 of 16 (94 %) healthy donors, EBNA3c in 9 of 13 (69%), EBNA1 in 5 of 17 (29%), BZLF1 in 4 of 15 (27%) and LMP2a in 2 of 18 (11%) donors. This suggests that the broader range of immunogenic T-cell epitopes in EBV_{mix} stimulates a wider reservoir of memory T cells in the majority of healthy individuals.

As HSCT recipients are at risk to develop PTLD, we investigated the T-cell responses of nine patients after HSCT under persistent immunosuppression with recent low-level EBV replication (300 to 10'000 copies/mL) to the different EBV antigens. Similarly to healthy individuals, HSCT recipients tended to have higher responses to EBV_{mix} than to single peptide pools (P≥0.0557, KW with Dunn's multiple comparisons test; Fig. 1b). However, the frequency of IFN-γ-producing EBV_{mix}-specific T cells was significantly lower in HSCT compared to healthy individuals (P=0.01, MWU).

Thus, EBV_{mix} triggered the highest number of memory T cells in 94% of screened healthy individuals and in 56 % of HSCT recipients after EBV replication.

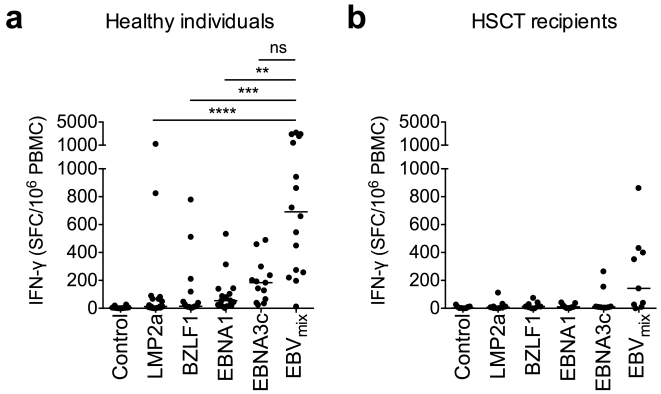

Figure 1. EBV_{mix} is more immunogenic than commercially available peptide pools. EBV-specific memory T-cell frequency in healthy individuals (**a**) and HSCT recipients 30 to 108 months after HSCT (**b**). IFN-γ-response of PBMC was assessed by ELISpot after overnight stimulation with indicated peptide pools and calculated as spot-forming cells (SFC) per 10^6 PBMC. Control represents unstimulated PBMC. Only values higher than 100 SFC/1x10^6 PBMC (upon subtraction of Control) were defined as positive responses. The bars represent medians. Statistical significance (*P*) was determined using KW with Dunn's multiple comparisons test (**, *P*<0.01; ***, *P*<0.001; ****, *P*<0.0001) (n≥13 for healthy individuals and n=9 for HSCT recipients).

EBV_{mix} is superior to single peptide pools in enriching EBV-specific $CD4^+$ and $CD8^+$ T cells

To examine which of these EBV-derived pools is best to generate a T-cell product for adoptive transfer, we isolated IFN-γ-positive cells from 10^8 PBMC of 5 healthy donors using the IFN-γ CCS. PBMC were stimulated with 1µg/peptide/mL of the commercial peptide pools (concentration recommended by the manufacturer) or 2µg/peptide/mL of EBV_{mix} (the concentration inducing highest IFN-γ responses in ELISpot). The number of IFN-γ-secreting cells isolated was significantly higher for EBV_{mix} (median 5.68×10^5 cells) compared to the single antigens (median 0.67-1×10^5 cells; P=0.0317, MWU; Table 1). EBV_{mix} also induced the highest overall median specificity with 8.9% $CD4^+IFN\text{-}\gamma^+$ and 39% $CD8^+IFN\text{-}\gamma^+$ isolated cells, which was at least 5-times higher than for the single peptide pools (Fig. 2 and Table 1). Thus, EBV_{mix} allowed enrichment of the highest number and percentage of specific cells by CCS, making it a promising tool for the generation of an EBV-specific T-cell product.

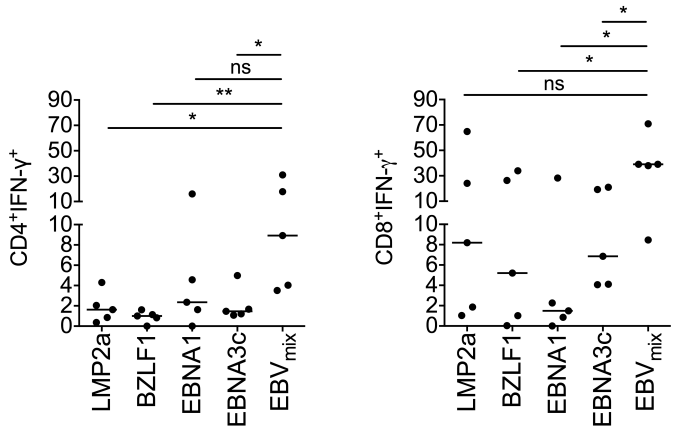

Figure 2. EBV_{mix} is superior to single peptide pools in enrichment of EBV-specific $CD4^+$ and $CD8^+$ T cells. IFN-γ-based enrichment was performed after 4-hour stimulation of PBMC with peptide pools using the CCS (n=5). The fraction of $CD4^+IFN\text{-}\gamma^+$ (left) and $CD8^+IFN\text{-}\gamma^+$ (right) cells of total lymphocytes in the isolated IFN-γ-positive cells is shown. Control values of unstimulated PBMC (ranging from 0% to 1.35%) were subtracted. The bars represent medians. Statistical significance (P) was determined using MWU (*, P<0.05; **, P<0.01).

Table 1. Characteristics of the enriched IFN-γ-positive cell fractions obtained for EBV-derived antigenic pools.

	Donor	Cell No. after isolation ($x10^5$)	% IFN-γ^+ $CD4^+/CD8^+$ cells[a] after selection	after expansion	LCL recognition[b] T-cell line	CD4-line	LCL control[c] T-cell line	CD4-line	CD8-line
LMP2a	D3	0.69	4.3 / 1	38 / 3.7	+++	++	++	+	-
	D4	0.59	0.4 / 1.9	0.3 / 65	++	+	-	-	-
	D6	3.18	2.1 / 24	3.8 / 56	+++	+	+++	+++	+++
	D9	1.03	1.6 / 65	0 / 44	+++	nd	+	nd	nd
	D13	0.23	0.9 / 8.2	0.7 / 59	++	+	+++	+++	nd
BZLF1	D3	0.31	0.8 / 5.2	26 / 19	++	+/-	-	-	-
	D4	0.67	1 / 0	17 / 0	+	+	-	+	nd
	D6	3.10	1.6 / 26	2.8 / 36	++	+	++	++	++
	D9	1.06	0 / 1	1.2 / 7	++	+	-	-	-
	D13	0.28	1.1 /34	0.1 / 6.2	+++	+	++	+++	nd
EBNA1	D3	0.74	16 / 28	3.3 / 43	+++	+/-	++	-	+++
	D4	1.44	2.4 / 0.9	16 / 15	+	+/-	-	-	-
	D6	3.00	1.6 / 1.5	64 / 5.5	+	+/-	+	-	+++
	D9	0.65	4.6 / 2.3	19 / 25	+	+	+	-	+
	D13	0.81	0 / 0	79 / 0.1	+/-	nd	+	-	nd
EBNA3c	D3	0.85	1.7 / 4.1	15 / 11	++	+	+	-	++
	D4	0.10	1.5 / 19	41 / 26	++	+	+	-	++
	D6	3.55	1.1 / 6.9	1.1 / 63	+++	+	+++	-	+++
	D9	1.04	1.2 / 4.1	1.7 / 37	+	+	+	-	++
	D13	1.00	5 / 21	1.5 / 46	+++	+/-	+++	-	nd
EBVmix	D3	1.83	8.9 / 39	0.5 / 48	+++	+	+++	++	++
	D4	1.80	3.5 / 8.5	1.1 / 31	++	+/-	+	-	++
	D6	5.89	31 / 39	0.2 / 82	+++	+	+++	+++	+++
	D9	5.68	4 / 38	0.2 / 45	+	+	+	-	-
	D13	10.0	18 / 71	0.4 / 52	+++	+	+++	+++	+++

[a] Percentage of viable lymphocytes upon subtraction of control values obtained for unstimulated cells. [b] Determined by IFN-γ ELISPOT; +++ >60'000 SFC/$1x10^6$ cells, ++ >30'000 SFC/$1x10^6$ cells, + >15'000 SFC/$1x10^6$ cells, +/- >0-15'000 SFC/$1x10^6$ cells. [c] Determined as the lowest effector-to-target ratio (E:T) inhibiting the outgrowth of LCL in a 4 week co-culture of cell lines with LCL. +++ E:T <0.5, ++ E:T >0.5-8, + E:T >8-32, - E:T >32. nd, not determined.

EBV-specific T-cell lines expand, have high specificity, recognise EBV-infected target cells and are not alloreactive *in vitro*

For further characterisation, the cells isolated by CCS were expanded *in vitro* for 14 days. The cells increased their numbers in median 159-fold to medians of 43.5×10^6 cells for EBV_{mix} and $5.3\text{-}14.5\times10^6$ cells for the single antigens (Supplementary Fig. 1). After expansion the percentage of $CD4^+IFN\text{-}\gamma^+$ cells was very low in all lines (median 0.4-2.8%) except for EBNA1 (19.1%). The percentage of $CD8^+IFN\text{-}\gamma^+$ cells was comparable for LMP2a, EBNA3c and EBV_{mix} (36.8-55.9%) and lower for BZLF1 and EBNA1 (7.0 and 14.7%, respectively; Fig. 3a and Table 1). These results show that after expansion LMP2a-, EBNA3c- and EBV_{mix}-lines contain highly specific $CD8^+$ T cells and a small fraction of specific $CD4^+$ cells. By contrast, both $CD4^+$ and $CD8^+$ T cells of moderate specificity were found in EBNA1-lines. All T-cell lines contained predominantly $CD45RO^+CD62L^-$ effector memory T cells (Supplementary Fig. 2). $CD3^+CD45RA^+CD95^+$ T memory stem cells[41,42] were not detected (data not shown).

To assess whether the EBV_{mix}-specific T-cell lines recognise both latent and lytic antigens, we determined the HLA-class I epitope specificity of those cells. As shown in Table 2, individuals recognised 3 to 7 HLA-class I epitopes, derived from the latent antigens EBNA3b (3/5 donors), EBNA3a (2/5), EBNA3c (2/5), LMP2 (2/5) and EBNA1 (1/5) and the lytic antigens BMLF1 (4/5), BRLF1 (3/5) and BZLF1 (2/5).

Next, to elucidate whether the peptide-specific T-cell lines also respond to EBV-infected target cells, we co-cultured them with autologous LCL. Most T-cell lines showed high IFN-γ responses (37'700-79'200 SFC/10^6 cells) except for the EBNA1-specific lines (13'650 SFC/10^6 cells; Fig. 3b and Table 1). All T-cell lines also proliferated upon encounter of LCL further demonstrating their ability to recognise naturally processed EBV-derived antigens. However, proliferation substantially increased after peptide-loading (P=0.0286 for LMP2a and P>0.05 for all other pools, MWU) of LCL suggesting that the level of antigen presentation by LCL is limiting (Supplementary Fig. 3).

Finally, as adoptive T-cell transfer may induce graft-versus-host disease or organ rejection, we assessed alloreactivity in a mixed-lymphocyte reaction using third-party HLA-mismatched DCs. All EBV-reactive T-cell lines showed significantly reduced alloreactivity compared to PBMC ($P\leq$0.0357, MWU; Fig. 3c), which also

further confirmed their strict EBV-directed specificity. Thus, all generated T-cell lines were highly peptide-specific, recognised EBV-infected target cells and had reduced alloreactivity.

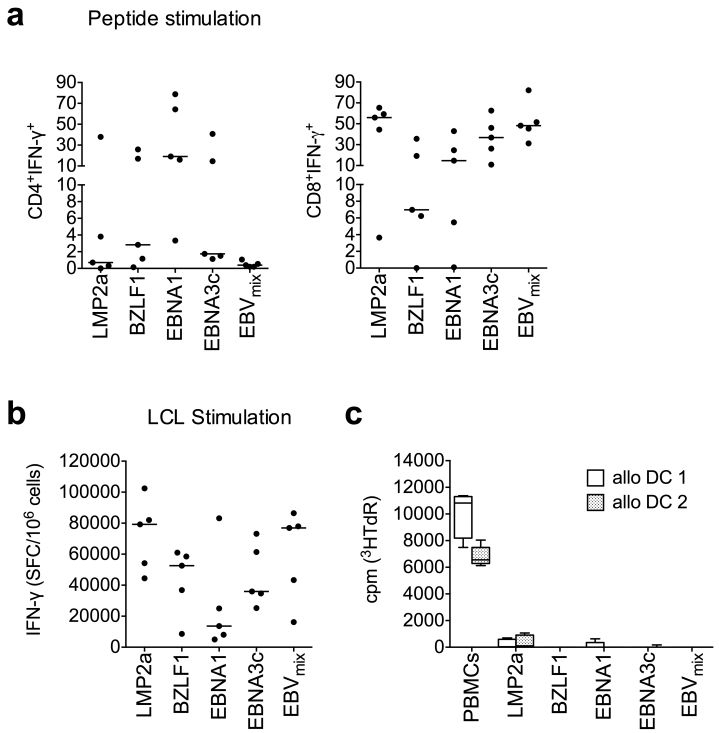

Figure 3. Peptide-specific T-cell lines recognise EBV-infected cells and are not alloreactive. (**a**) Specificity of the T-cell lines after two-week expansion *in vitro*. Intracellular IFN-γ production of the expanded EBV-specific T cells upon 6-hour restimulation with peptide pools (0.5μg/peptide/mL) was analysed by flow cytometry and are shown for $CD4^+$ and $CD8^+$ cells (left and right, respectively); background values of unstimulated controls (median 0.2, range 0.01-1.51) were subtracted. (**b**) IFN-γ response of T-cell lines to LCL. T cells were incubated overnight with autologous LCL (1:5 E:T ratio) and IFN-γ production measured by ELISpot; background values of unstimulated T cells (median 33.3, range 0-9200) and of control LCL (median 1834, range 50-9800) were subtracted; mean values from at least two independent experiments performed in duplicates are shown for each donor. All bars indicate medians. *P* values for all comparisons > 0.05 (MWU). (**c**) Alloreactivity of T-cell lines. Mixed lymphocyte reaction was

performed with 2 donors and 2 different third-party DCs. [^{3}H]-thymidine incorporation was measured after 96-hour co-culture. Medians and range of at least 2 independent experiments performed in triplicates are shown. Differences between PBMC and each cell line for both allo DC are statistically significant ($P \leq 0.0357$, MWU).

Table 2. Epitope signature of EBV_{mix}-specific T-cell lines. HLA class I epitope mapping was performed using IFN-γ ELISpot. Initially, the response to EBV_{mix} divided into 10 sub-pools was assessed, followed by analysis of single peptides from reactive sub-pools and all peptides that matched donor's HLA class I; all recognized epitopes match the HLA class I of the donor as previously reported,[22] except for ([a]). Only values higher than 1000 SFC/1x10^6 T cells were defined as positive responses.

Donor	Restricting HLA class I allele	Sequence	EBV protein
D3	A2[a]	GLCTLVAML	BMLF1
	B35	YPLHEQHGM	EBNA3a
	A11	IVTDFSVIK	EBNA3b
D4	A24	TYGPVFMCL	LMP2
	A24	TYPVLEEMF	BRLF1
	B7	RPPIFIRRL	EBNA3a
	A24	DYNFVKQLF	BMLF1
	B7	IPQCRLTPL	EBNA1
D6	A2	YVLDHLIVV	BRLF1
	A2	FLYALALLL	LMP2
	A2	GLCTLVAML	BMLF1
	B44	VEITPYKPTW	EBNA3b
	A2	CLGGLLTMV	LMP2
	B44	EENLLDFVRF	EBNA3c
	Cw6	RKCCRAKFKQLLQH	BZLF1
D9	A2	YVLDHLIVV	BRLF1
	B44	VEITPYKPTW	EBNA3b
	A2	GLCTLVAML	BMLF1
D13	B8	RAKFKQLL	BZLF1
	B44	EENLLDFVRF	EBNA3c
	B44	EGGVGWRHW	EBNA3c

EBV_{mix}-specific T-cell lines most efficiently control EBV-infected B cells

We next evaluated the cytotoxicity of T-cell lines against LCL. The median cytotoxicity after 6 hours was 5% to 30% at an effector-to-target ratio of 30:1 for all EBV-specific lines. EBV_{mix} exerted significantly higher cytotoxicity only compared to EBNA1 (P<0.05, MWU; Fig. 4a). Similar to the proliferation assay, the cytotoxicity was increased by peptide-loading (P<0.05 for LMP2a and EBNA1, P<0.01 for EBV_{mix}, MWU; Fig. 4a). These findings were further confirmed in Cr^{51} and calcein release assay (data not shown).

Since the T-cell lines were moderately cytotoxic, we further determined the capacity of each line to control EBV-infected B cells in a 4-week co-culture outgrowth assay. This assay is probably a more suitable *in vitro* correlate of therapeutic potential against PTLDs than the 6-hour cytotoxicity assay.[17,27] EBV_{mix}-specific lines showed the highest efficacy to control LCL (5/5 donors, 0.25 median E:T ratio), whereas the inhibitory potential of lines specific to LMP2a (4/5, 6.0 median E:T), EBNA3c (4/5, 13.7 median E:T) and EBNA1 (4/5, 24.0 median E:T) was considerably lower. The BZLF1-lines failed to control LCL in 3 of 5 individuals (48 median E:T; Fig. 4b and Table 1).

Altogether, despite similar 6-hour cytotoxicity, the EBV-specific T-cell lines showed substantial differences in long-term control of LCL with EBV_{mix}-specific lines showing the highest efficacy.

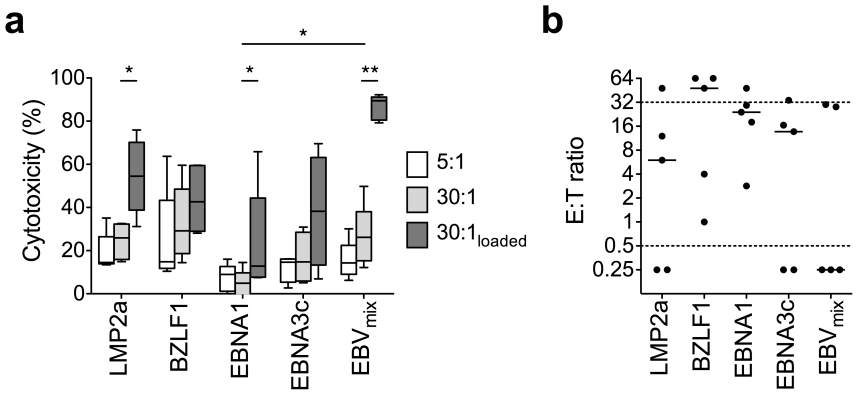

Figure 4. EBV_{mix}-specific T-cell lines are superior in controlling EBV-infected B cells over 4 weeks. (**a**) Short-term cytotoxicity of T-cell lines. T-cell

lines were incubated for 6 hours with autologous LCL at 5:1 and 30:1 E:T ratio and cytotoxicity was determined by flow cytometry using Annexin V and PI staining. Where indicated, LCLs were pre-loaded for 1.5 hours with a cognate antigen (0.5µg/peptide/mL). Statistical significance (*P*) was determined using MWU (*, $P<0.05$; **, $P<0.01$). (**b**) Long-term capacity of EBV-specific T cells to control autologous LCL. T cells were co-cultured with LCL at E:T ratios from 1:2 to 32:1. After 4 weeks the outgrowth of LCL was assessed. The readout was defined as the lowest E:T ratio inhibiting the outgrowth of LCL. The score equal 0.25 and 64 indicates inhibition below and above the investigated range of E:T ratios (indicated by dotted lines), respectively; mean values from at least two independent experiments performed in triplicates are shown for each donor, the bars represent medians.

LMP2a, BZLF1 and EBV_{mix} induce $CD4^+$ T cells that are able to control LCL

Clinical experience strongly suggests an important role of adoptively transferred $CD4^+$ T cells either by maintaining $CD8^+$ EBV-specific T-cell responses by providing 'cognate help' and/or their cytotoxic properties.[12,17,18] To elucidate the functionality of EBV-specific $CD4^+$ cells, we selected the $CD4^+$ cell fractions from the *in vitro* generated T-cell lines to a purity of at least 95% (CD4-lines). Except for LMP2a, the CD4-lines were highly peptide-specific (median 28-56% $CD4^+$IFN-γ^+ cells; Fig. 5a). All CD4-lines, except for BZLF1, showed significantly lower IFN-γ responses to LCL than the bulk T-cell lines ($P=0.0159$, $P=0.0317$, $P=0.0079$ and $P=0.0159$ for LMP2a, EBNA1, EBNA3c and EBV_{mix}, respectively, MWU; Fig. 5b *vs*. 3b and Table 1). Moreover, their ability to control LCL outgrowth differed markedly between the antigens. For LMP2a, BZLF1 and EBV_{mix} nearly all bulk T-cell lines that were able to control LCL also contained $CD4^+$ T cells that could control LCL growth. On the other hand, of the 9 EBNA1- or EBNA3c-specific cell lines that could inhibit LCL growth, none contained $CD4^+$ cells with this ability. Remarkably, in most cases the CD8-lines inhibited LCL outgrowth similarly or even better than the bulk T-cell lines (Fig. 5c and Table 1), indicating that *in vitro* inhibition of LCL is primarily mediated by $CD8^+$ cells.

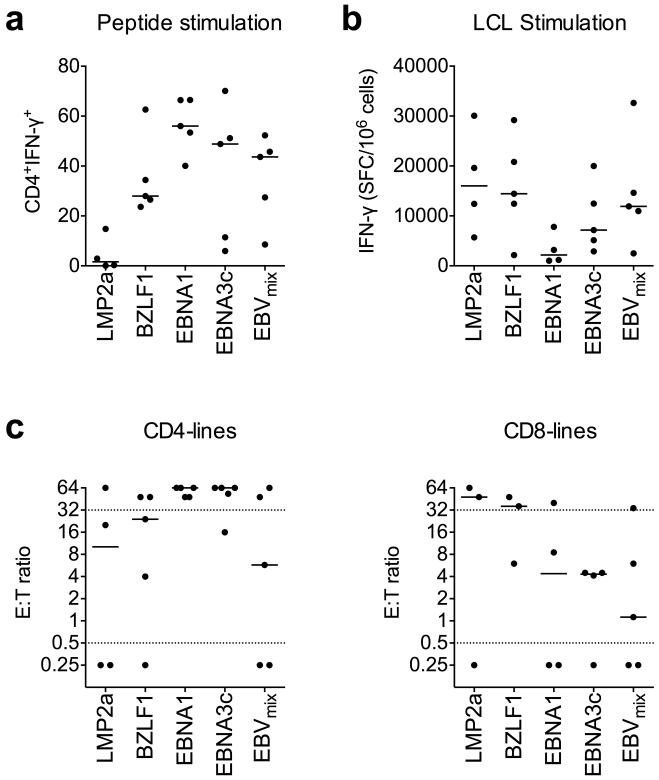

Figure 5. The CD4-lines have high specificity to cognate antigens but show lower IFN-γ production and controlling capacity in response to LCL than the T-cell lines. (**a**) Recognition of cognate peptide pools by CD4-lines. Intracellular production of IFN-γ after 6-hour re-stimulation with indicated pools (0.5μg/peptide/mL) was analysed by flow cytometry; background values of unstimulated controls (median 0.2, range 0.05-3.44) were subtracted, mean values from at least 2 independent experiments for each donor are shown. (**b**) Recognition of naturally processed antigens by CD4-lines. T cells were incubated overnight with autologous LCLs (E:T ratio 1:5) and IFN-γ response measured by ELISpot; background values of unstimulated T cells (median 16.7, range 0-2100) and of control LCL (median 1213, range 25-4050) were subtracted; mean values from at least two independent experiments performed in duplicates are shown for each donor. All the bars represent medians. (**c**) Long-term capacity of CD4- and CD8-lines to control autologous LCL. T cells were co-cultured with LCL at E:T ratios from 1:2 to 32:1. After 4 weeks the outgrowth of LCL was assessed. The readout was defined as described in Fig. 3b; mean values from at least two independent experiments performed in triplicates are shown for each donor, the bars represent medians.

EBV-specific CD4$^+$ T cells inefficiently controlling LCL produce less cytotoxic mediators due to insufficient recognition of LCL

We then determined why some of the EBV-specific CD4-lines failed to control the growth of LCL. Inability to control LCL could be caused by reduced viability of the CD4-cell lines, T-cell exhaustion, or their reduced expression of cytotoxic mediators such as Fas-ligand, perforin or granzyme B. Alternatively, EBV-infected cells could have several mechanisms of immune evasion such as down-regulation of CD80, Fas[28], HLA class II[20] or induction of the anti-inflammatory cytokines, e.g. IL-10 or TGF-β.

We did not find any indications of LCL immune evasion as their surface expression of CD80, Fas[28] and HLA-DR[20] remained unaffected over 5-day *in vitro* co-culture with CD4-lines. Also secretion of IL-10 and TGF-β was very low and comparable between co-cultures with controlling or non-controlling CD4-lines (data not shown). Moreover, the T-cell viability and T-cell exhaustion were not affected, as determined by surface expression of PD-1, or decreased expression of Fas-ligand in non-controlling CD4-lines (Fig. 6a and data not shown). By contrast, we found that controller CD4-lines produced significantly higher levels of perforin and granzyme B and also higher levels of granulysin, after 2-day co-culture with LCL compared to non-controllers (Fig. 6b) suggesting that granule-mediated cytotoxicity is the major effector mechanisms of controlling LCL *in vitro*.

As mentioned previously, we observed a general decrease in the IFN-γ response of CD4-lines to LCL despite their high peptide-specificity, suggesting that the CD4-lines inefficiently recognise LCL. We therefore compared the response to peptide and to LCL between controlling and non-controlling CD4-lines. Interestingly, non-controller CD4-lines produced significantly lower levels of IFN-γ when stimulated with LCL than the controllers (P=0.0006, MWU), whereas no such difference was seen for peptide-stimulation (Fig. 6c). These findings indicate that the inefficacy to produce cytotoxic mediators is rather due to limited antigen presentation by LCL than an intrinsic dysfunction of the non-controller CD4$^+$ cells.

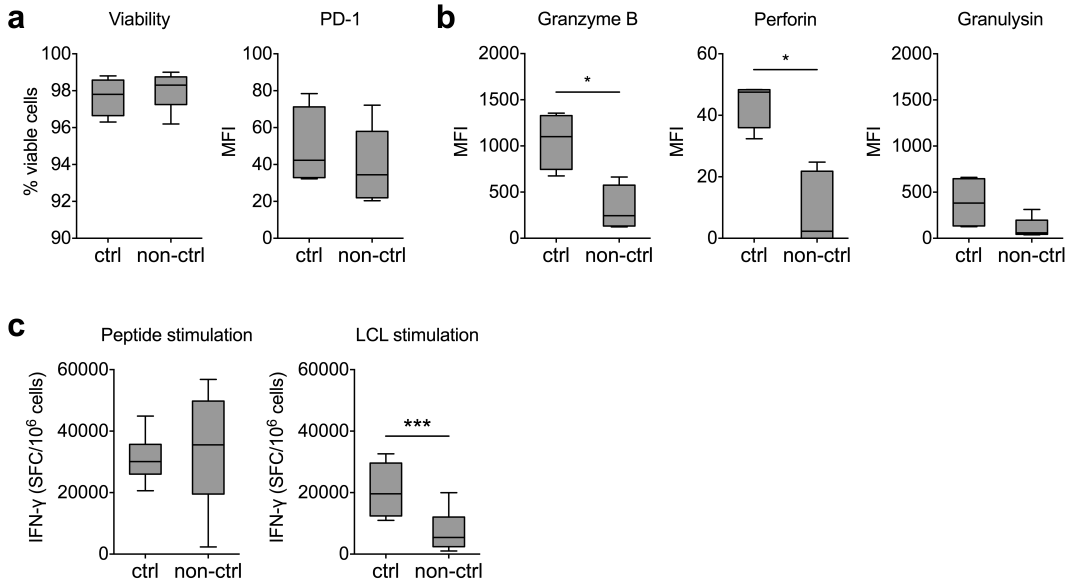

Figure 6. The CD4-lines unable to control LCL produce significantly less cytotoxic effector mediators due to their lower LCL recognition. Viability and PD-1 expression (**a**) and production of perforin, granzyme B and granulysin (**b**) of CD4-lines was assessed by flow cytometry at day 2 of co-culture with LCL at 1:2 E:T ratio. Combined data from lines specific to EBV_{mix}, LMP2a, and EBNA1 of 3 donors are shown and stratified into LCL-controllers (ctrl) (n=2 for LMP2a and EBV_{mix}) and LCL-non-controllers (non-ctrl) (n=1 for LMP2a and EBV_{mix}, n=3 for EBNA1); viability was determined with Zombie Aqua Fixable Viability Kit; mean fluorescence intensity (MFI) values for respective isotype controls were subtracted; bars represent medians. (**c**) IFN- γ response of ctrl or non-ctrl CD4-lines to stimulation with peptide or LCL (1:5 E:T ratio) were determined by IFN-γ ELISpot; background values of unstimulated T cells (median 16.7, range 0-2100) and of control LCL (median 1213, range 25-4050) were subtracted. Statistical significance (*P*) was determined using MWU (*, $P<0.05$).

Discussion and Conclusions

In this study, we demonstrate that EBV_{mix}, a pool of 91 HLA class I- and 34 HLA class II-restricted T-cell epitopes derived from 7 latent and 9 lytic EBV proteins[22], induces highly specific and effective $CD4^+$ and $CD8^+$ cells that control LCL *in vitro* more efficiently than T cells specific for individual EBV proteins.

The therapeutic potential of EBV-specific adoptive T-cell transfer strongly depends on the antigens used for generation of EBV-specific cells. The use of LCL to stimulate EBV-specific T cells probably covers best the different EBV antigens as well as most HLA types and was already successfully used in clinical studies.[7,10,14,15] However, generation of T-cell lines by stimulation with LCL under good manufacturing practice conditions is time-consuming, laborious and expensive. Therefore the Miltenyi CliniMACS system offers an alternative allowing isolation of antigen-specific cells within 24 hours after *in vitro* stimulation with synthetic antigen. Successful treatment of patients was reported using peptide pools for single EBV antigens[9] as well as a combination of 23 peptides derived from 11 EBV proteins.[8] In this study we compared *in vitro* the specificity and efficacy of T-cell lines generated by stimulation with EBV_{mix} to cell lines specific to the single EBV proteins EBNA1, EBNA3c, LMP2a and BZLF1. These proteins were chosen based on their immunogenicity[21], expression in PTLDs[4,19] as well as their reported relevance in T-cell therapy.[9,11,13,29]

We saw that stimulation of PBMC with EBV_{mix} induced significantly higher responses in healthy individuals compared to stimulation with LMP2a, BZLF1 and EBNA1. In line with previous reports, EBNA3c elicited the highest response of the single EBV antigens.[13] The same pattern was observed in HSCT recipients controlling recent low-level EBV replication, although the response to EBV_{mix} was significantly lower compared to healthy individuals and only about 50% of patients responded. The missing T-cell surveillance can explain the increased risk for EBV replication, which might be associated with PTLD development, in those patients.

Consistent with the high frequency of EBV_{mix}-specific T cells in peripheral blood we obtained a significantly higher number of cells after CCS that also showed a higher specificity compared to the single antigens. Therefore, only EBV_{mix}

achieved a purity of above 10% in all investigated donors fulfilling regulatory requirements for direct transfer of the isolated cells in the clinical setting.[30] As for the individual peptide pools, only in case of one or two of five donors the purity was high enough for clinical application.

We expect that EBV_{mix} would be superior to the single antigens in the generation of EBV-specific T cells not only because of the higher frequency of antigen-specific cells, but also because of the broad coverage of different EBV antigens and different HLA types. For instance a previous study showed, that patients who recovered from PTLD recognised a higher number of different epitopes than those with poor outcome, highlighting the importance of broader T-cell specificity for the treatment of PTLD.[8] Indeed, investigation of EBV_{mix}-specific T cells revealed an oligoclonal HLA class I epitope signature with specificities for latent and lytic proteins. Unfortunately, as single peptides from the overlapping pools as well as the HLA class II-restricted epitopes from the EBV_{mix} were not available, we were unable to elucidate further epitope specificities.

Initially, generation of EBV-specific T cells mainly focused on latent antigens, because of the viral gene expression pattern observed in PTLD and other EBV-associated malignancies.[4,9] However, we saw that in 2 of 5 tested individuals BZLF1-specific cell lines and respective CD4-lines efficiently controlled LCL in a long-term co-culture, suggesting that also T cells specific for lytic EBV antigens could contribute to PTLD control *in vivo* as also previously reported.[11,13] Interestingly, the EBV_{mix}-specific lines of all donors contained T cells specific for at least one lytic protein. However, as we did not analyse the functionality of the different antigen-specific T-cell clones in the EBV_{mix}-lines individually, we cannot dissect the actual contribution of the different specificities to LCL control.

During preparation of this study, Miltenyi Biotec has introduced PepTivator EBV Consensus, a peptide pool containing 43 epitopes of 8-20-mers derived from 13 lytic and latent EBV proteins with 29-peptide (67%) overlap with EBV_{mix}. Although our preliminary results indicate that the EBV Consensus showed significantly lower median memory T-cell frequencies than EBV_{mix} but also significantly higher frequencies than the single peptide pools (data not shown),

further investigations are required to fully correlate the functional efficacy of both pools.

The high number of epitopes in EBV_{mix} raises concerns about antigenic competition.[31-33] This might indeed be the case, as not all donor's HLA-matched epitopes in EBV_{mix}-specific T-cell lines were detected. Despite this potential risk of qualitative loss of specificities in EBV_{mix}-specific T cells, they were highly functional. Additionally, the broader epitope specificities may increase the T-cell efficacy and reduce the risk of inducing tumour escape mutants.[8,34]

Although many conflicting clinical and mouse model data exist about the role and necessity of EBV-specific $CD4^+$ cells in immune control of PTLD[10,12,15,20], the clinical experience strongly argues for an important helper and/or cytotoxic role of adoptively transferred $CD4^+$ cells.[12,17,18] In accordance with previous publications, most EBV antigens predominately induced $CD8^+$ T cells, with the exception of EBNA1 that often induced more antigen-specific $CD4^+$ than $CD8^+$ T cells.[21] Depending on the antigen, only the $CD4^+$ or $CD8^+$ T cells or both were able to control LCL in a 4-week outgrowth assay. This long-term control of LCL is probably the best *in vitro* correlate of the therapeutic potential of T cells against PTLD.[17,27,35] LMP2a and EBV_{mix}, and in some donors also BZLF1, induced antigen-specific and cytotoxic $CD4^+$ and $CD8^+$ T cells. In contrast, EBNA1 and EBNA3c-specific CD4-lines did not control LCL. We further found that the CD4-lines able to control LCL produced significant more perforin and granzyme B than their non-controller counterparts. This is in accordance with the view that exocytosis of cytotoxic granules is probably the most relevant cytotoxicity mechanism of EBV-specific $CD4^+$ T cells.[17,36] Interestingly, although both the controller and non-controller CD4-lines were mostly highly peptide-specific, they recognised LCL in general only poorly in comparison to the bulk T-cell lines, and the non-controllers produced significantly less IFN-γ then controllers. Thus, the inability to control LCL is probably due to the limited level of epitope presentation on LCL.[27,37,38]

Nevertheless, CD4 cells do not necessarily have to be cytotoxic to contribute to viral control *in vivo* and the non-controlling EBNA1- and EBNA3c-specific $CD4^+$ T cells might be beneficial and even essential in the control of PTLD.

Finally, the finding that the limiting epitope presentation is the main reason for failure to control LCL further strengthens the rationale to use a broad antigenic pool, such as EBV_{mix}, to ensure isolation of diverse EBV-specific cells for generation of an efficient T-cell product. Despite these findings, due to the low number of donors these data should be interpreted with caution and the actual superiority of the EBV_{mix} lines in controlling PTLD can only be proven in clinical application.

Altogether, EBV_{mix} presents a novel approach for EBV-specific T cell stimulation that could be more advantageous compared to the commercial single peptide pools. First, EBV_{mix}-specific T cells showed superior functionality compared to the cells specific for the single pools. This is potentially due to broad coverage of both HLA types and EBV-derived epitopes, which additionally reduces the risk of induction of tumour escape mutants that could more likely occur with single pools. Second, EBV_{mix} could also potentially reduce the costs of combining various single peptide pools for cellular stimulation. The clear disadvantage of EBV_{mix} is that, in contrast to some of the single peptide pools and to the LCL-based method, it is not yet good manufacturing practice-compliant. However, T cells generated by stimulation with LCL, transformed using a laboratory EBV strain, can fail due to the lack of recognition of patient's EBV mutant strain.[34,39] This effect could potentially be reduced using EBV_{mix}. Additionally, EBV_{mix} in combination with the IFN-γ CCS offers a faster, cheaper and clinically more feasible T-cell generation method compared to the LCL-based stimulation.

In conclusion, we could show that EBV_{mix} containing epitopes from 16 EBV proteins induces highly EBV-specific and effective $CD4^+$ and $CD8^+$ T cells with properties for long-term control of LCL superior to T cells of individual EBV proteins. Our findings indicate that application of EBV_{mix} may help to generate efficacious EBV-specific T cells by the CCS or other methods involving peptide stimulation[11,29] for prophylactic and curative treatment of PTLD.

Disclosure of Interest

The authors declare no competing financial interests. This work was supported by the Stiftung Forschung Infektionskrankheiten. N.K. and J.N. received a Swiss National Foundation (SNF) grant (PZ00P3_142403). A.E. received an SNF grant (PZ00P3_154709) from the Swiss National Foundation. The funding institutions had no role in study design, data collection, analysis and interpretation, decision to publish, or preparation of the manuscript. Authorship Contribution: J.N. performed experiments, analysed results and made the figures; J.N., C.S., and N.K. designed the research and wrote the paper; M.B., C.H., C.B., A.E., and G.R. provided reagents and edited the paper.

References

1 Gottschalk, S., Rooney, C. M. & Heslop, H. E. Post-transplant lymphoproliferative disorders. *Annual review of medicine* **56**, 29-44, doi:10.1146/annurev.med.56.082103.104727 (2005).

2 Fishman, J. A. Infection in solid-organ transplant recipients. *The New England journal of medicine* **357**, 2601-2614, doi:10.1056/NEJMra064928 (2007).

3 Uhlin, M. *et al.* Risk factors for Epstein-Barr virus-related post-transplant lymphoproliferative disease after allogeneic hematopoietic stem cell transplantation. *Haematologica* **99**, 346-352, doi:10.3324/haematol.2013.087338 (2014).

4 Thorley-Lawson, D. A. & Gross, A. Persistence of the Epstein-Barr virus and the origins of associated lymphomas. *The New England journal of medicine* **350**, 1328-1337, doi:10.1056/NEJMra032015 (2004).

5 Young, L. S. & Rickinson, A. B. Epstein-Barr virus: 40 years on. *Nature reviews. Cancer* **4**, 757-768, doi:10.1038/nrc1452 (2004).

6 Trappe, R. *et al.* Sequential treatment with rituximab followed by CHOP chemotherapy in adult B-cell post-transplant lymphoproliferative disorder (PTLD): the prospective international multicentre phase 2 PTLD-1 trial. *The Lancet. Oncology* **13**, 196-206, doi:10.1016/S1470-2045(11)70300-X (2012).

7 Heslop, H. E. How I treat EBV lymphoproliferation. *Blood* **114**, 4002-4008, doi:10.1182/blood-2009-07-143545 (2009).

8 Moosmann, A. *et al.* Effective and long-term control of EBV PTLD after transfer of peptide-selected T cells. *Blood* **115**, 2960-2970, doi:10.1182/blood-2009-08-236356 (2010).

9 Icheva, V. *et al.* Adoptive transfer of epstein-barr virus (EBV) nuclear antigen 1-specific t cells as treatment for EBV reactivation and lymphoproliferative disorders after allogeneic stem-cell transplantation. *J Clin Oncol* **31**, 39-48, doi:10.1200/JCO.2011.39.8495 (2013).

10 Heslop, H. E. *et al.* Long-term outcome of EBV-specific T-cell infusions to prevent or treat EBV-related lymphoproliferative disease in transplant recipients. *Blood* **115**, 925-935, doi:10.1182/blood-2009-08-239186 (2010).

11 Papadopoulou, A. *et al.* Activity of Broad-Spectrum T Cells as Treatment for AdV, EBV, CMV, BKV, and HHV6 Infections after HSCT. *Science translational medicine* **6**, 242ra283, doi:10.1126/scitranslmed.3008825 (2014).

12 Haque, T. *et al.* Allogeneic cytotoxic T-cell therapy for EBV-positive posttransplantation lymphoproliferative disease: results of a phase 2 multicenter clinical trial. *Blood* **110**, 1123-1131, doi:10.1182/blood-2006-12-063008 (2007).

13 Wang, Y. *et al.* Combination of Epstein-Barr virus nuclear antigen 1, 3 and lytic antigen BZLF1 peptide pools allows fast and efficient stimulation of Epstein-Barr virus-specific T cells for adoptive immunotherapy. *Cytotherapy* **16**, 122-134, doi:10.1016/j.jcyt.2013.07.008 (2014).

14 Bollard, C. M., Rooney, C. M. & Heslop, H. E. T-cell therapy in the treatment of post-transplant lymphoproliferative disease. *Nature reviews. Clinical oncology* **9**, 510-519, doi:10.1038/nrclinonc.2012.111 (2012).

15 Leen, A. M. *et al.* Multicenter study of banked third-party virus-specific T cells to treat severe viral infections after hematopoietic stem cell transplantation. *Blood* **121**, 5113-5123, doi:10.1182/blood-2013-02-486324 (2013).

16 Marshall, N. B. & Swain, S. L. Cytotoxic CD4 T cells in antiviral immunity. *Journal of biomedicine & biotechnology* **2011**, 954602, doi:10.1155/2011/954602 (2011).

17 Martorelli, D. *et al.* Role of CD4+ cytotoxic T lymphocytes in the control of viral diseases and cancer. *International reviews of immunology* **29**, 371-402, doi:10.3109/08830185.2010.489658 (2010).

18 Swain, S. L., McKinstry, K. K. & Strutt, T. M. Expanding roles for CD4(+) T cells in immunity to viruses. *Nature reviews. Immunology* **12**, 136-148, doi:10.1038/nri3152 (2012).

19 Montone, K. T. *et al.* Identification of Epstein-Barr virus lytic activity in post-transplantation lymphoproliferative disease. *Modern pathology : an official journal of the United States and Canadian Academy of Pathology, Inc* **9**, 621-630 (1996).

20 Merlo, A. *et al.* Virus-specific cytotoxic CD4+ T cells for the treatment of EBV-related tumors. *J Immunol* **184**, 5895-5902, doi:10.4049/jimmunol.0902850 (2010).

21 Hislop, A. D., Taylor, G. S., Sauce, D. & Rickinson, A. B. Cellular responses to viral infection in humans: lessons from Epstein-Barr virus. *Annual review of immunology* **25**, 587-617, doi:10.1146/annurev.immunol.25.022106.141553 (2007).

22 Woodberry, T. *et al.* Differential targeting and shifts in the immunodominance of Epstein-Barr virus--specific CD8 and CD4 T cell responses during acute and persistent infection. *The Journal of infectious diseases* **192**, 1513-1524, doi:10.1086/491741 (2005).

23 Durovic, B. *et al.* Epstein-Barr virus negativity among individuals older than 60 years is associated with HLA-C and HLA-Bw4 variants and tonsillectomy. *Journal of virology* **87**, 6526-6529, doi:10.1128/JVI.00169-13 (2013).

24 Stuehler, C. *et al.* Cross-protective TH1 immunity against Aspergillus fumigatus and Candida albicans. *Blood* **117**, 5881-5891, doi:10.1182/blood-2010-12-325084 (2011).

25 Khanna, N. *et al.* Generation of a multipathogen-specific T-cell product for adoptive immunotherapy based on activation-dependent expression of CD154. *Blood* **118**, 1121-1131, doi:10.1182/blood-2010-12-322610 (2011).

26 Beck, O. *et al.* Generation of highly purified and functionally active human TH1 cells against Aspergillus fumigatus. *Blood* **107**, 2562-2569, doi:10.1182/blood-2005-04-1660 (2006).

27 Haigh, T. A. *et al.* EBV latent membrane proteins (LMPs) 1 and 2 as immunotherapeutic targets: LMP-specific CD4+ cytotoxic T cell

recognition of EBV-transformed B cell lines. *J Immunol* **180**, 1643-1654 (2008).

28 Park, G. B. *et al.* CD80 (B7.1) and CD86 (B7.2) induce EBV-transformed B cell apoptosis through the Fas/FasL pathway. *International journal of oncology* **43**, 1531-1540, doi:10.3892/ijo.2013.2091 (2013).

29 Gerdemann, U. *et al.* Rapidly generated multivirus-specific cytotoxic T lymphocytes for the prophylaxis and treatment of viral infections. *Molecular therapy : the journal of the American Society of Gene Therapy* **20**, 1622-1632, doi:10.1038/mt.2012.130 (2012).

30 Feuchtinger, T. *et al.* Adoptive transfer of pp65-specific T cells for the treatment of chemorefractory cytomegalovirus disease or reactivation after haploidentical and matched unrelated stem cell transplantation. *Blood* **116**, 4360-4367, doi:10.1182/blood-2010-01-262089 (2010).

31 Kedl, R. M. *et al.* T cells compete for access to antigen-bearing antigen-presenting cells. *The Journal of experimental medicine* **192**, 1105-1113 (2000).

32 Kedl, R. M., Schaefer, B. C., Kappler, J. W. & Marrack, P. T cells down-modulate peptide-MHC complexes on APCs in vivo. *Nature immunology* **3**, 27-32, doi:10.1038/ni742 (2002).

33 Fujita, Y. *et al.* Exploiting cytokine secretion to rapidly produce multivirus-specific T cells for adoptive immunotherapy. *J Immunother* **31**, 665-674, doi:10.1097/CJI.0b013e318181b4bd (2008).

34 Gottschalk, S. *et al.* An Epstein-Barr virus deletion mutant associated with fatal lymphoproliferative disease unresponsive to therapy with virus-specific CTLs. *Blood* **97**, 835-843 (2001).

35 Herr, W. *et al.* Identification of naturally processed and HLA-presented Epstein-Barr virus peptides recognized by CD4(+) or CD8(+) T lymphocytes from human blood. *Proceedings of the National Academy of Sciences of the United States of America* **96**, 12033-12038 (1999).

36 Walton, S., Mandaric, S. & Oxenius, A. CD4 T cell responses in latent and chronic viral infections. *Frontiers in immunology* **4**, 105, doi:10.3389/fimmu.2013.00105 (2013).

37 Long, H. M. *et al.* CD4+ T-cell responses to Epstein-Barr virus (EBV) latent-cycle antigens and the recognition of EBV-transformed lymphoblastoid cell lines. *Journal of virology* **79**, 4896-4907, doi:10.1128/JVI.79.8.4896-4907.2005 (2005).

38 Taylor, G. S. *et al.* A role for intercellular antigen transfer in the recognition of EBV-transformed B cell lines by EBV nuclear antigen-specific CD4+ T cells. *J Immunol* **177**, 3746-3756 (2006).

39 Doubrovina, E. *et al.* Adoptive immunotherapy with unselected or EBV-specific T cells for biopsy-proven EBV+ lymphomas after allogeneic hematopoietic cell transplantation. *Blood* **119**, 2644-2656, doi:10.1182/blood-2011-08-371971 (2012).

Supplementary data

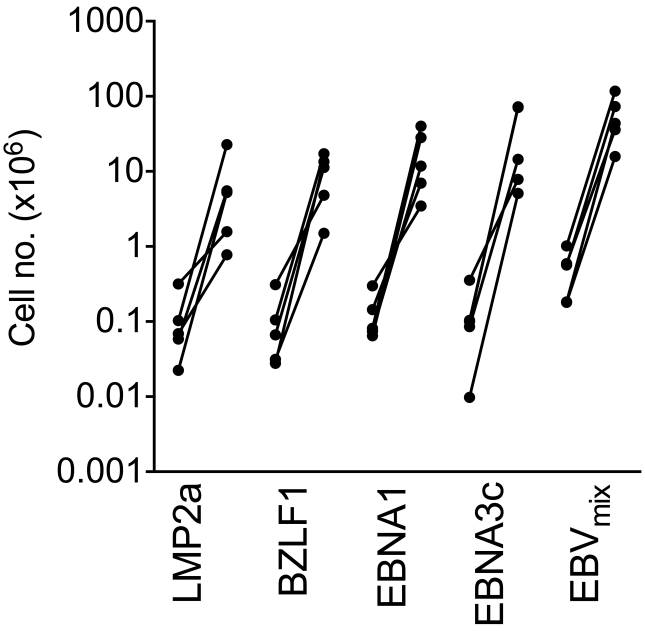

Supplementary Figure 1. EBV-specific T-cell lines expand in median 159-fold within 2 weeks. Expansion of the EBV-specific IFN-γ-positive T-cell fractions. After two-week expansion *in vitro* the total number of cells in EBV-specific lines was determined and is shown along with the isolated cell numbers before expansion.

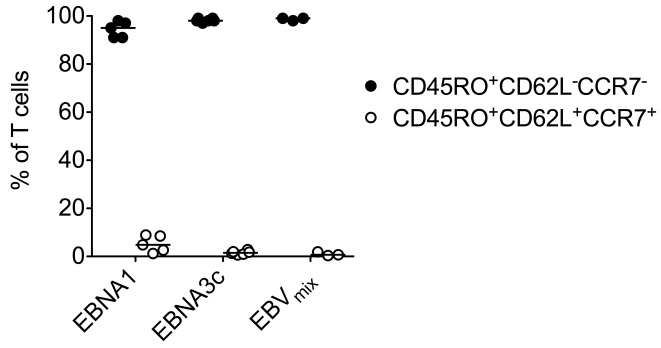

Supplementary Figure 2. Expanded EBV-specific T-cell lines show mainly the effector memory phenotype. After two-week expansion *in vitro* the phenotype of T-cell lines was analysed by flow cytometry to distinguish the

central (CD45RO$^+$CD62L$^+$CCR$^+$) and the effector (CD45RO$^+$CD62L$^-$CCR$^-$) memory cells.

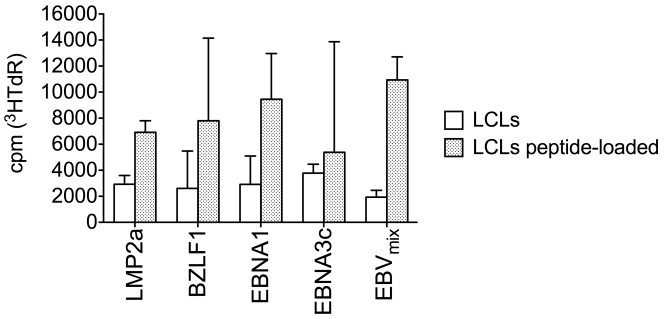

Supplementary Figure 3. Peptide-loading increases the recognition of LCL by EBV-specific T-cell lines. Proliferation of T cells after 96-hour co-culture with autologous LCL or peptide-loaded autologous LCL was measured by [^{3}H]-thymidine incorporation; background values of T cells alone (median 458, range 0-4050) and LCL alone (median 632, range 535-803) were subtracted. Median with range for 2 donors from at least 2 independent experiments performed in triplicates are shown. *P* values for all comparisons between the peptide pools > 0.05 (MWU).

Supplementary Table S1. The sequences of EBV-derived T-cell epitopes contained in EBV_{mix} and their known HLA restrictions.[22]

EBV protein	HLA Restriction	Sequence
HLA class I-restricted epitopes		
BMLF1	A2	GLCTLVAML
	A24	DYNFVKQLF
	B18	DEVEFLGHY
BMRF1	Cw3	FRNLAYGRTCVLGK
	Cw6	YRSGIIAVV
		KDTWLDARM
BRLF1	A2	RALIKTLPRASYSSH
	A2	YVLDHLIVV
	A3	RVRAYTYSK
	A11	ATIGTAMYKL
	A24	DYCNVLNKEF
	A24	TYPVLEEMF
	B18	LVSDYCNVLNKEFT
	B40	QKEEAAICGQMDLSH
	Cw4	ERPIFPHPSKPTFLP
BZLF1	B7	LPCVLWPVL
	B8	RAKFKQLL
	Cw6	RKCCRAKFKQLLQH
gp350	A2	VLQWASLAV
	A2	VLTLLLLLV
	A2	LIPETVPYI
	A2	QLTPHTKAV
gp110	A2	ILIYNGWYA
	B35	VPGSETMCY
	B35	APGWLIWTY
gp85	A2	TLFIGSHVV
	A2	LMIIPLINV
	A2	SLVIVTTFV
EBNA1	B7	RPQKRPSCI
	B7	IPQCRLTPL
	B53	HPVGEADYF
	A2	FMVFLQTHI
EBNA2	A2/B51	DTPLIPLTIF
EBNA3a	A2	SVRDRLARL
	A3	RLRAEAQVK
	A24	RYSIFFDY
	A29	VFSDGRVAC

	A30	AYSSWMYSY
	B7	RPPIFIRRL
	B7	VPAPAGPIV
	B8	FLRGRAYGL
	B8	QAKWRLQTL
	B35	YPLHEQHGM
	B46	VQPPQLTLQV
	B62	LEKARGSTY
		HLAAQGMAY
EBNA3b	A11	NPTQAPVIQLVHAVY
	A11	AVFDRKSDAK
	A11	LPGPQVTAVLLHEES
	A11	DEPASTEPVHDQLL
	A11	IVTDFSVIK
	A24	TYSAGIVQI
	B27	RRARSLSAERY
	B27	HRCQAIRK
	B35	AVLLHEESM
	B44	VEITPYKPTW
	B58	VSFIEFVGW
	B62	GQGGSPTAM
EBNA3c	B37	LDFVRFMGV
	B7	QPRAPIRPI
	B27	RRIYDLIEL
	B27	FRKAQIQGL
	B27	RKIYDLIEL
	B27	RRIFDLIEL
	B27	LRGKWQRRYR
	B39	HHIWQNLL
	B44	KEHVIQNAF
	B44	EENLLDFVRF
	B44	EGGVGWRHW
	B62	QNGALAINTF
LMP1	A2	YLQQNWWTL
	A2	YLLEMLWRL
	A2	LLVDLLWLL
	A2	TLLVDLLWL
	A2	LLLIALWNL
	B51	DPHGPVQLSYYD
LMP2	A2	LLSAWILTA
	A2	SLREWLLRI
	A2	FLYALALLL
	A2	LLWTLVVLL
	A2	CLGGLLTMV
	A2	LTAGFLIFL

	A11	SSCSSCPLSKI
	A23	PYLFWLAAI
	A24	IYVLVMLVL
	A24	TYGPVFMCL
	A25	VMSNTLLSAW
	B27	RRRWRRLTV
	B40	IEDPPFNSL
	B63	WTLVVLLI
BARF0	A2	LLWAARPRL
HLA class II-restricted epitopes		
BHRF1		AGLTLSLLVICSYLFISRG
		TVVLRYHLLEEI
EBNA1		NPKFENIAEGLRALL
		LRALLARSHVERTTD
	DR1	TSLYNLRRGTALAI
	DR14	PQCRLTPLSRLPFGM
		KTSLYNLRRGIALAIPQCRL
		PTCNIKATVCSFDDGVDLPP
		RRPQKRPSCIGCKGT
		RPFFHPVGEADYFEY
		VPPGAIEQGPADDPGEGPST
		DGGRRKKGGWFGRHR
	DR11	VYGGSKTSLYNLRRGTALAI
		NLRRGTALAIPQCRL
		APGPGPQPGPLRESIVCYFM
		LRESIVCYFMVFLQTHIFAE
	DR15	MVFLQTHIFAEVLKD
		VLKDAIKDLVMTKPAPTCNI
		RVTVCSFDDGVDLPPWFPPM
		DGEPDMPPGAIEQGPADDPG
EBNA2	DQ2 DQ7	TVFYNIPPMPL
EBNA3c	DR13	ILCFVMAARQRLQDI
		QQRPVMFVSRVPAKK
		QKRAAPPTVSPSDTG
		PPAAGPPAAGPRILA
		PQCFWEMRAGREITQ
	DQ5	SDDELPYIDPNMEPV
		PSMPFASDYSQGAFT
		AQEILSDNSEISVFPK
		PAPGAPTGGTGGPPAPGAPT
LMP1		LWRLGATIWQLLAFF
		TDGGGGHSHDSGHGG
		SGHESDSNSNEGRHH
LMP2		STEFIPNLFCMLLL

Outlook

In the study presented here we have demonstrated that the EBV_{mix}, a pool of 89 $CD8^+$ and 36 $CD4^+$ T-cell epitopes with known HLA restrictions, consisting mainly of 9 and 15 amino acids derived from 16 EBV latent and lytic proteins [22], induces EBV-specific T-cells endowed with superior efficiency in controlling the outgrowth of autologous LCLs, when compared to the commercially available single-antigen peptide pools. Moreover, our preliminary experiments have revealed that the PepTivator EBV Consensus peptide pool, which has been introduced by Miltenyi Biotec for improved stimulation of EBV-specific T-cells, produces significantly lower median responses in healthy individuals than the EBV_{mix}. These data however need to be further investigated in additional donors to prepare a thorough comparison between the EBV_{mix} and the EBV Consensus. Interestingly, 67% of the peptides included in the EBV Consensus overlaps with the EBV_{mix}. It is thus likely that the comparative single-epitope analysis of both pools could lead to establishment of a peptide combination best suited for clinical application. Moreover, as the composition of the EBV_{mix} was predominantly based on the previously reported EBV-derived T-cell epitopes [22], further peptides mediating better T-cell recognition of PTLDs could possibly be included. To achieve that a detailed analysis of epitopes presented by EBV-infected cells within PTLDs is needed. This type of analysis, although already performed for LCLs, is very complex and novel epitope identification strategies should be investigated [101].

Together, these approaches would allow tailoring the EBV_{mix} to reduce the content of unnecessary epitopes with a concomitant preservation of its functionality and thereby to decrease the costs of its manufacturing.

Moreover, epitopes derived from other viruses causing infections among immunocompromised patients, e.g. CMV and AdV, could be incorporated into the EBV_{mix} to increase the specificities within one T-cell product. Indeed, generation of multi-pathogen specific T-cells based on peptide stimulation of PBMCs and selection of specific cells using the IFN-γ capture system without further *in vitro* expansion has not been investigated so far [7].

The well-established but very labour-intensive method of generating EBV-specific T-cells for adoptive transfer is based on repeated stimulations with LCLs [7]. As LCLs present endogenously processed EBV antigens this method ensures that the reactivated T-cells can recognise with high avidity epitopes displayed on PTLDs [7]. Thus, comparison of the T-cells generated by the EBV_{mix}- or LCLs-based stimulation with regard to the breadth and magnitude of response as well as the capacity of controlling LCLs could provide valuable information about possible differences between both methods. A similar analysis was performed by Gerdemann *et al*. [24] for CMV- and AdV-specific T-cells generated with peptide pool *vs*. nucleofected DCs stimulation. The authors revealed that both methods reactivate T-cells with similar phenotype, expansion potential, functional avidity, as well as qualitative and quantitative response to the cognate antigens. Nevertheless data regarding the EBV-specific cells are largely missing.

Additionally, since a subset of epitopes derived from the EBV lytic cycle antigens is included within the EBV_{mix} [22], and we could map the response of our T-cell lines to the immediate early (BZLF1 and BRLF1) as well as to early (BMLF1) proteins a combination of the EBV_{mix}-specific T-cells together with induction of the lytic viral replication and anti-viral agents (e.g. gancyclovir) might potentially result in an improved clinical effectiveness [48]. Indeed, co-application of arginine butyrate, an agent inducing the lytic EBV replication, and gancyclovir has shown promising results against refractory EBV^+ malignancies in clinical trials and novel lytic cycle inducers are currently under investigation [102,103].

Multiple clinical and *in vivo studies* have revealed that T memory stem cells (T_{SCM}) and central memory T-cells (T_{CM}) are endowed with preferable capacity to engraft, proliferate, and to mediate anti-tumour effect upon adoptive transfer [104]. In order to specifically enrich our T-cell product for the T_{SCM} and T_{CM} populations the fact of their CD62L expression [104,105] could be employed. Thus, the IFN-γ capture-based isolation could be preceded by immunomagnetic selection of the CD62L-positive cells using the monoclonal anti-human CD62L antibody, which has recently been generated in clinical grade [106]. Alternatively, the anti-CD62L could directly replace the anti-CD45 antibody in the IFN-γ capture system.

Finally, the ultimate perspective of this study is the establishment of the adoptive T-cell therapy for viral complications after transplantation in the University Hospital of Basel. This goal includes not only the monitoring of clinical efficacy but also long-term analysis T-cell faith upon infusion. Therefore, to target also the EBV-associated diseases the EBV_{mix} should be produced with GMP approval.

References

1 Thorley-Lawson, D. A. & Gross, A. Persistence of the Epstein-Barr virus and the origins of associated lymphomas. *N Engl J Med* **350**, 1328-1337, doi:10.1056/NEJMra032015 (2004).

2 Young, L. S. & Rickinson, A. B. Epstein-Barr virus: 40 years on. *Nat Rev Cancer* **4**, 757-768, doi:10.1038/nrc1452 (2004).

3 Fishman, J. A. Infection in solid-organ transplant recipients. *N Engl J Med* **357**, 2601-2614, doi:10.1056/NEJMra064928 (2007).

4 Gottschalk, S., Rooney, C. M. & Heslop, H. E. Post-transplant lymphoproliferative disorders. *Annu Rev Med* **56**, 29-44, doi:10.1146/annurev.med.56.082103.104727 (2005).

5 Uhlin, M. *et al.* Risk factors for Epstein-Barr virus-related post-transplant lymphoproliferative disease after allogeneic hematopoietic stem cell transplantation. *Haematologica* **99**, 346-352, doi:10.3324/haematol.2013.087338 (2014).

6 Thorley-Lawson, D. A. Epstein-Barr virus: exploiting the immune system. *Nat Rev Immunol* **1**, 75-82, doi:10.1038/35095584 (2001).

7 Bollard, C. M., Rooney, C. M. & Heslop, H. E. T-cell therapy in the treatment of post-transplant lymphoproliferative disease. *Nat Rev Clin Oncol* **9**, 510-519, doi:10.1038/nrclinonc.2012.111 (2012).

8 Heslop, H. E. How I treat EBV lymphoproliferation. *Blood* **114**, 4002-4008, doi:10.1182/blood-2009-07-143545 (2009).

9 Feuchtinger, T. *et al.* Safe adoptive transfer of virus-specific T-cell immunity for the treatment of systemic adenovirus infection after allogeneic stem cell transplantation. *Br J Haematol* **134**, 64-76, doi:10.1111/j.1365-2141.2006.06108.x (2006).

10 Feuchtinger, T. *et al.* Adoptive transfer of pp65-specific T cells for the treatment of chemorefractory cytomegalovirus disease or reactivation after haploidentical and matched unrelated stem cell transplantation. *Blood* **116**, 4360-4367, doi:10.1182/blood-2010-01-262089 (2010).

11 Gerdemann, U. *et al.* Safety and clinical efficacy of rapidly-generated trivirus-directed T cells as treatment for adenovirus, EBV, and CMV infections after allogeneic hematopoietic stem cell transplant. *Mol Ther* **21**, 2113-2121, doi:10.1038/mt.2013.151 (2013).

12 Haque, T. *et al.* Allogeneic cytotoxic T-cell therapy for EBV-positive posttransplantation lymphoproliferative disease: results of a phase 2 multicenter clinical trial. *Blood* **110**, 1123-1131, doi:10.1182/blood-2006-12-063008 (2007).

13 Haque, T. *et al.* Treatment of Epstein-Barr-virus-positive post-transplantation lymphoproliferative disease with partly HLA-matched allogeneic cytotoxic T cells. *Lancet* **360**, 436-442, doi:10.1016/S0140-6736(02)09672-1 (2002).

14 Heslop, H. E. *et al.* Long-term outcome of EBV-specific T-cell infusions to prevent or treat EBV-related lymphoproliferative disease in transplant recipients. *Blood* **115**, 925-935, doi:10.1182/blood-2009-08-239186 (2010).

15 Icheva, V. *et al.* Adoptive transfer of epstein-barr virus (EBV) nuclear antigen 1-specific t cells as treatment for EBV reactivation and lymphoproliferative disorders after allogeneic stem-cell transplantation. *J Clin Oncol* **31**, 39-48, doi:10.1200/JCO.2011.39.8495 (2013).

16 Leen, A. M. *et al.* Multicenter study of banked third-party virus-specific T cells to treat severe viral infections after hematopoietic stem cell transplantation. *Blood* **121**, 5113-5123, doi:10.1182/blood-2013-02-486324 (2013).

17 Moosmann, A. *et al.* Effective and long-term control of EBV PTLD after transfer of peptide-selected T cells. *Blood* **115**, 2960-2970, doi:10.1182/blood-2009-08-236356 (2010).

18 Rooney, C. M. *et al.* Use of gene-modified virus-specific T lymphocytes to control Epstein-Barr-virus-related lymphoproliferation. *Lancet* **345**, 9-13 (1995).

19 Hislop, A. D., Taylor, G. S., Sauce, D. & Rickinson, A. B. Cellular responses to viral infection in humans: lessons from Epstein-Barr virus. *Annu Rev Immunol* **25**, 587-617, doi:10.1146/annurev.immunol.25.022106.141553 (2007).

20 Porcu, P. *et al.* Successful treatment of posttransplantation lymphoproliferative disorder (PTLD) following renal allografting is associated with sustained CD8(+) T-cell restoration. *Blood* **100**, 2341-2348, doi:10.1182/blood-2002-01-0210 (2002).

21 Young, L. *et al.* Expression of Epstein-Barr virus transformation-associated genes in tissues of patients with EBV lymphoproliferative disease. *N Engl J Med* **321**, 1080-1085, doi:10.1056/NEJM198910193211604 (1989).

22 Woodberry, T. *et al.* Differential targeting and shifts in the immunodominance of Epstein-Barr virus--specific CD8 and CD4 T cell responses during acute and persistent infection. *J Infect Dis* **192**, 1513-1524, doi:10.1086/491741 (2005).

23 Fujita, Y. *et al.* Exploiting cytokine secretion to rapidly produce multivirus-specific T cells for adoptive immunotherapy. *J Immunother* **31**, 665-674, doi:10.1097/CJI.0b013e318181b4bd (2008).

24 Gerdemann, U. *et al.* Rapidly generated multivirus-specific cytotoxic T lymphocytes for the prophylaxis and treatment of viral infections. *Mol Ther* **20**, 1622-1632, doi:10.1038/mt.2012.130 (2012).

25 Wang, Y. *et al.* Combination of Epstein-Barr virus nuclear antigen 1, 3 and lytic antigen BZLF1 peptide pools allows fast and efficient stimulation of Epstein-Barr virus-specific T cells for adoptive immunotherapy. *Cytotherapy* **16**, 122-134, doi:10.1016/j.jcyt.2013.07.008 (2014).

26 Doubrovina, E. *et al.* Adoptive immunotherapy with unselected or EBV-specific T cells for biopsy-proven EBV+ lymphomas after allogeneic hematopoietic cell transplantation. *Blood* **119**, 2644-2656, doi:10.1182/blood-2011-08-371971 (2012).

27 Gottschalk, S. *et al.* An Epstein-Barr virus deletion mutant associated with fatal lymphoproliferative disease unresponsive to therapy with virus-specific CTLs. *Blood* **97**, 835-843 (2001).

28 Epstein, M. A., Achong, B. G. & Barr, Y. M. Virus Particles in Cultured Lymphoblasts from Burkitt's Lymphoma. *Lancet* **1**, 702-703 (1964).
29 Babcock, G. J., Hochberg, D. & Thorley-Lawson, A. D. The expression pattern of Epstein-Barr virus latent genes in vivo is dependent upon the differentiation stage of the infected B cell. *Immunity* **13**, 497-506 (2000).
30 Babcock, G. J., Decker, L. L., Volk, M. & Thorley-Lawson, D. A. EBV persistence in memory B cells in vivo. *Immunity* **9**, 395-404 (1998).
31 Lam, K. P., Kuhn, R. & Rajewsky, K. In vivo ablation of surface immunoglobulin on mature B cells by inducible gene targeting results in rapid cell death. *Cell* **90**, 1073-1083 (1997).
32 Swain, S. L., McKinstry, K. K. & Strutt, T. M. Expanding roles for CD4(+) T cells in immunity to viruses. *Nat Rev Immunol* **12**, 136-148, doi:10.1038/nri3152 (2012).
33 Janeway, C. A., Travers, P., Walport, M. & Shlomchik, M. J. in *Immunobiology 5th Edition. The Immune System in Health and Disease* Ch. 9, (Garland Publishing, 2001).
34 Tierney, R. J., Steven, N., Young, L. S. & Rickinson, A. B. Epstein-Barr virus latency in blood mononuclear cells: analysis of viral gene transcription during primary infection and in the carrier state. *J Virol* **68**, 7374-7385 (1994).
35 Levitskaya, J. *et al.* Inhibition of antigen processing by the internal repeat region of the Epstein-Barr virus nuclear antigen-1. *Nature* **375**, 685-688, doi:10.1038/375685a0 (1995).
36 Yates, J. L., Warren, N. & Sugden, B. Stable replication of plasmids derived from Epstein-Barr virus in various mammalian cells. *Nature* **313**, 812-815 (1985).
37 Murat, P. *et al.* G-quadruplexes regulate Epstein-Barr virus-encoded nuclear antigen 1 mRNA translation. *Nat Chem Biol* **10**, 358-364, doi:10.1038/nchembio.1479 (2014).
38 Paludan, C. *et al.* Endogenous MHC class II processing of a viral nuclear antigen after autophagy. *Science* **307**, 593-596, doi:10.1126/science.1104904 (2005).
39 Ling, P. D., Hsieh, J. J., Ruf, I. K., Rawlins, D. R. & Hayward, S. D. EBNA-2 upregulation of Epstein-Barr virus latency promoters and the cellular CD23 promoter utilizes a common targeting intermediate, CBF1. *J Virol* **68**, 5375-5383 (1994).
40 Robertson, E. S. *et al.* Epstein-Barr virus nuclear protein 3C modulates transcription through interaction with the sequence-specific DNA-binding protein J kappa. *J Virol* **69**, 3108-3116 (1995).
41 Parker, G. A. *et al.* Epstein-Barr virus nuclear antigen (EBNA)3C is an immortalizing oncoprotein with similar properties to adenovirus E1A and papillomavirus E7. *Oncogene* **13**, 2541-2549 (1996).
42 Radkov, S. A. *et al.* Epstein-Barr virus nuclear antigen 3C interacts with histone deacetylase to repress transcription. *J Virol* **73**, 5688-5697 (1999).
43 Kilger, E., Kieser, A., Baumann, M. & Hammerschmidt, W. Epstein-Barr virus-mediated B-cell proliferation is dependent upon latent membrane

protein 1, which simulates an activated CD40 receptor. *EMBO J* **17**, 1700-1709, doi:10.1093/emboj/17.6.1700 (1998).

44 Caldwell, R. G., Wilson, J. B., Anderson, S. J. & Longnecker, R. Epstein-Barr virus LMP2A drives B cell development and survival in the absence of normal B cell receptor signals. *Immunity* **9**, 405-411 (1998).

45 Rowe, M., Niedobitek, G. & Young, L. S. Epstein-Barr virus gene expression in post-transplant lymphoproliferative disorders. *Springer Semin Immunopathol* **20**, 389-403 (1998).

46 Rooney, C. M., Rowe, D. T., Ragot, T. & Farrell, P. J. The spliced BZLF1 gene of Epstein-Barr virus (EBV) transactivates an early EBV promoter and induces the virus productive cycle. *J Virol* **63**, 3109-3116 (1989).

47 Martorelli, D. *et al.* Role of CD4+ cytotoxic T lymphocytes in the control of viral diseases and cancer. *Int Rev Immunol* **29**, 371-402, doi:10.3109/08830185.2010.489658 (2010).

48 Adhikary, D. *et al.* Immunodominance of lytic cycle antigens in Epstein-Barr virus-specific CD4+ T cell preparations for therapy. *PLoS One* **2**, e583, doi:10.1371/journal.pone.0000583 (2007).

49 Tan, L. C. *et al.* A re-evaluation of the frequency of CD8+ T cells specific for EBV in healthy virus carriers. *J Immunol* **162**, 1827-1835 (1999).

50 Long, H. M. *et al.* CD4+ T-cell responses to Epstein-Barr virus (EBV) latent-cycle antigens and the recognition of EBV-transformed lymphoblastoid cell lines. *J Virol* **79**, 4896-4907, doi:10.1128/JVI.79.8.4896-4907.2005 (2005).

51 Sparks-Thissen, R. L., Braaten, D. C., Kreher, S., Speck, S. H. & Virgin, H. W. t. An optimized CD4 T-cell response can control productive and latent gammaherpesvirus infection. *J Virol* **78**, 6827-6835, doi:10.1128/JVI.78.13.6827-6835.2004 (2004).

52 Christensen, J. P., Cardin, R. D., Branum, K. C. & Doherty, P. C. CD4(+) T cell-mediated control of a gamma-herpesvirus in B cell-deficient mice is mediated by IFN-gamma. *Proc Natl Acad Sci U S A* **96**, 5135-5140 (1999).

53 Merlo, A. *et al.* Virus-specific cytotoxic CD4+ T cells for the treatment of EBV-related tumors. *J Immunol* **184**, 5895-5902, doi:10.4049/jimmunol.0902850 (2010).

54 Appay, V. *et al.* Characterization of CD4(+) CTLs ex vivo. *J Immunol* **168**, 5954-5958 (2002).

55 Walton, S., Mandaric, S. & Oxenius, A. CD4 T cell responses in latent and chronic viral infections. *Front Immunol* **4**, 105, doi:10.3389/fimmu.2013.00105 (2013).

56 Sun, Q., Burton, R. L. & Lucas, K. G. Cytokine production and cytolytic mechanism of CD4(+) cytotoxic T lymphocytes in ex vivo expanded therapeutic Epstein-Barr virus-specific T-cell cultures. *Blood* **99**, 3302-3309 (2002).

57 Marshall, N. B. & Swain, S. L. Cytotoxic CD4 T cells in antiviral immunity. *J Biomed Biotechnol* **2011**, 954602, doi:10.1155/2011/954602 (2011).

58 Nikiforow, S., Bottomly, K., Miller, G. & Munz, C. Cytolytic CD4(+)-T-cell clones reactive to EBNA1 inhibit Epstein-Barr virus-induced B-cell proliferation. *J Virol* **77**, 12088-12104 (2003).

59 Heller, K. N., Gurer, C. & Munz, C. Virus-specific CD4+ T cells: ready for direct attack. *The Journal of experimental medicine* **203**, 805-808, doi:10.1084/jem.20060215 (2006).

60 Adhikary, D. *et al.* Control of Epstein-Barr virus infection in vitro by T helper cells specific for virion glycoproteins. *The Journal of experimental medicine* **203**, 995-1006, doi:10.1084/jem.20051287 (2006).

61 Taylor, G. S. *et al.* A role for intercellular antigen transfer in the recognition of EBV-transformed B cell lines by EBV nuclear antigen-specific CD4+ T cells. *J Immunol* **177**, 3746-3756 (2006).

62 Brady, G., MacArthur, G. J. & Farrell, P. J. Epstein-Barr virus and Burkitt lymphoma. *J Clin Pathol* **60**, 1397-1402, doi:10.1136/jcp.2007.047977 (2007).

63 Neri, A. *et al.* Epstein-Barr virus infection precedes clonal expansion in Burkitt's and acquired immunodeficiency syndrome-associated lymphoma. *Blood* **77**, 1092-1095 (1991).

64 Lombardi, L., Newcomb, E. W. & Dalla-Favera, R. Pathogenesis of Burkitt lymphoma: expression of an activated c-myc oncogene causes the tumorigenic conversion of EBV-infected human B lymphoblasts. *Cell* **49**, 161-170 (1987).

65 Harris, R. S., Croom-Carter, D. S., Rickinson, A. B. & Neuberger, M. S. Epstein-Barr virus and the somatic hypermutation of immunoglobulin genes in Burkitt's lymphoma cells. *J Virol* **75**, 10488-10492, doi:10.1128/JVI.75.21.10488-10492.2001 (2001).

66 Rowe, M. *et al.* Differences in B cell growth phenotype reflect novel patterns of Epstein-Barr virus latent gene expression in Burkitt's lymphoma cells. *EMBO J* **6**, 2743-2751 (1987).

67 Hammerschmidt, W. & Sugden, B. Epstein-Barr virus sustains Burkitt's lymphomas and Hodgkin's disease. *Trends Mol Med* **10**, 331-336, doi:10.1016/j.molmed.2004.05.006 (2004).

68 Kuppers, R. The biology of Hodgkin's lymphoma. *Nat Rev Cancer* **9**, 15-27, doi:10.1038/nrc2542 (2009).

69 Deacon, E. M. *et al.* Epstein-Barr virus and Hodgkin's disease: transcriptional analysis of virus latency in the malignant cells. *The Journal of experimental medicine* **177**, 339-349 (1993).

70 Kanzler, H., Kuppers, R., Hansmann, M. L. & Rajewsky, K. Hodgkin and Reed-Sternberg cells in Hodgkin's disease represent the outgrowth of a dominant tumor clone derived from (crippled) germinal center B cells. *The Journal of experimental medicine* **184**, 1495-1505 (1996).

71 Hjalgrim, H. *et al.* Characteristics of Hodgkin's lymphoma after infectious mononucleosis. *N Engl J Med* **349**, 1324-1332, doi:10.1056/NEJMoa023141 (2003).

72 Barrett, A. J. in *Hematopoietic Stem Cell Transplantation in Clinical Practice* (eds J. Treleaven & A. J. Barrett) Ch. 2, 9-21 (Elsevier Ltd., 2009).

73 Jenq, R. R. & van den Brink, M. R. Allogeneic haematopoietic stem cell transplantation: individualized stem cell and immune therapy of cancer. *Nat Rev Cancer* **10**, 213-221, doi:10.1038/nrc2804 (2010).

74 Blazar, B. R., Murphy, W. J. & Abedi, M. Advances in graft-versus-host disease biology and therapy. *Nat Rev Immunol* **12**, 443-458, doi:10.1038/nri3212 (2012).

75 Kolb, H. J. Graft-versus-leukemia effects of transplantation and donor lymphocytes. *Blood* **112**, 4371-4383, doi:10.1182/blood-2008-03-077974 (2008).

76 Moss, P. & Rickinson, A. Cellular immunotherapy for viral infection after HSC transplantation. *Nat Rev Immunol* **5**, 9-20, doi:10.1038/nri1526 (2005).

77 Seggewiss, R. & Einsele, H. Immune reconstitution after allogeneic transplantation and expanding options for immunomodulation: an update. *Blood* **115**, 3861-3868, doi:10.1182/blood-2009-12-234096 (2010).

78 Kroll, J., Li, S., Levi, M. & Weinberg, A. Lytic and latent EBV gene expression in transplant recipients with and without post-transplant lymphoproliferative disorder. *J Clin Virol* **52**, 231-235, doi:10.1016/j.jcv.2011.06.013 (2011).

79 Babcock, G. J., Decker, L. L., Freeman, R. B. & Thorley-Lawson, D. A. Epstein-barr virus-infected resting memory B cells, not proliferating lymphoblasts, accumulate in the peripheral blood of immunosuppressed patients. *The Journal of experimental medicine* **190**, 567-576 (1999).

80 Paya, C. V. *et al.* Epstein-Barr virus-induced posttransplant lymphoproliferative disorders. ASTS/ASTP EBV-PTLD Task Force and The Mayo Clinic Organized International Consensus Development Meeting. *Transplantation* **68**, 1517-1525 (1999).

81 Swerdlow, S. H., Webber, S. A., Chadburn, A. & Ferry, J. in *WHO Classification of Tumours of Haematopoietic and Lymphoid Tissue* (IARC Press, 2008).

82 Meij, P. *et al.* Impaired recovery of Epstein-Barr virus (EBV)--specific CD8+ T lymphocytes after partially T-depleted allogeneic stem cell transplantation may identify patients at very high risk for progressive EBV reactivation and lymphoproliferative disease. *Blood* **101**, 4290-4297, doi:10.1182/blood-2002-10-3001 (2003).

83 Swinnen, L. J. *et al.* Prospective study of sequential reduction in immunosuppression, interferon alpha-2B, and chemotherapy for posttransplantation lymphoproliferative disorder. *Transplantation* **86**, 215-222, doi:10.1097/TP.0b013e3181761659 (2008).

84 Timms, J. M. *et al.* Target cells of Epstein-Barr-virus (EBV)-positive post-transplant lymphoproliferative disease: similarities to EBV-positive Hodgkin's lymphoma. *Lancet* **361**, 217-223, doi:10.1016/S0140-6736(03)12271-4 (2003).

85 Cesarman, E. *et al.* BCL-6 gene mutations in posttransplantation lymphoproliferative disorders predict response to therapy and clinical outcome. *Blood* **92**, 2294-2302 (1998).

86 Kuehnle, I. *et al.* CD20 monoclonal antibody (rituximab) for therapy of Epstein-Barr virus lymphoma after hemopoietic stem-cell transplantation. *Blood* **95**, 1502-1505 (2000).

87 Suzan, F., Ammor, M. & Ribrag, V. Fatal reactivation of cytomegalovirus infection after use of rituximab for a post-transplantation lymphoproliferative disorder. *N Engl J Med* **345**, 1000, doi:10.1056/NEJM200109273451315 (2001).

88 Kimby, E. Tolerability and safety of rituximab (MabThera). *Cancer Treat Rev* **31**, 456-473, doi:10.1016/j.ctrv.2005.05.007 (2005).

89 Savoldo, B. *et al.* Cellular immunity to Epstein-Barr virus in liver transplant recipients treated with rituximab for post-transplant lymphoproliferative disease. *Am J Transplant* **5**, 566-572, doi:10.1111/j.1600-6143.2004.00693.x (2005).

90 Abu-Elmagd, K. M. *et al.* Lymphoproliferative disorders and de novo malignancies in intestinal and multivisceral recipients: improved outcomes with new outlooks. *Transplantation* **88**, 926-934, doi:10.1097/TP.0b013e3181b7509c (2009).

91 Papadopoulos, E. B. *et al.* Infusions of donor leukocytes to treat Epstein-Barr virus-associated lymphoproliferative disorders after allogeneic bone marrow transplantation. *N Engl J Med* **330**, 1185-1191, doi:10.1056/NEJM199404283301703 (1994).

92 Heslop, H. E., Brenner, M. K. & Rooney, C. M. Donor T cells to treat EBV-associated lymphoma. *N Engl J Med* **331**, 679-680, doi:10.1056/NEJM199409083311017 (1994).

93 Tao, Q., Yang, J., Huang, H., Swinnen, L. J. & Ambinder, R. F. Conservation of Epstein-Barr virus cytotoxic T-cell epitopes in posttransplant lymphomas: implications for immune therapy. *Am J Pathol* **160**, 1839-1845, doi:10.1016/S0002-9440(10)61130-3 (2002).

94 Wilkie, G. M. *et al.* Establishment and characterization of a bank of cytotoxic T lymphocytes for immunotherapy of epstein-barr virus-associated diseases. *J Immunother* **27**, 309-316 (2004).

95 Sili, U. *et al.* Production of good manufacturing practice-grade cytotoxic T lymphocytes specific for Epstein-Barr virus, cytomegalovirus and adenovirus to prevent or treat viral infections post-allogeneic hematopoietic stem cell transplant. *Cytotherapy* **14**, 7-11, doi:10.3109/14653249.2011.636963 (2012).

96 Desombere, I. *et al.* The interferon gamma secretion assay: a reliable tool to study interferon gamma production at the single cell level. *Journal of immunological methods* **286**, 167-185, doi:10.1016/j.jim.2004.01.001 (2004).

97 Manz, R., Assenmacher, M., Pfluger, E., Miltenyi, S. & Radbruch, A. Analysis and sorting of live cells according to secreted molecules, relocated to a cell-surface affinity matrix. *Proc Natl Acad Sci U S A* **92**, 1921-1925 (1995).

98 Becker, C. *et al.* Adoptive tumor therapy with T lymphocytes enriched through an IFN-gamma capture assay. *Nat Med* **7**, 1159-1162, doi:10.1038/nm1001-1159 (2001).

99 Rauser, G. *et al.* Rapid generation of combined CMV-specific CD4+ and CD8+ T-cell lines for adoptive transfer into recipients of allogeneic stem

cell transplants. *Blood* **103**, 3565-3572, doi:10.1182/blood-2003-09-3056 (2004).

100 European Conference on Infection in Leukemia (ECIL) guidelines 2011. *http://www.ebmt.org/Contents/Resources/Library/ECIL/Pages/ECIL.aspx*.

101 Herr, W. *et al.* Identification of naturally processed and HLA-presented Epstein-Barr virus peptides recognized by CD4(+) or CD8(+) T lymphocytes from human blood. *Proc Natl Acad Sci U S A* **96**, 12033-12038 (1999).

102 Ghosh, S. K., Perrine, S. P. & Faller, D. V. Advances in Virus-Directed Therapeutics against Epstein-Barr Virus-Associated Malignancies. *Adv Virol* **2012**, 509296, doi:10.1155/2012/509296 (2012).

103 Ghosh, S. K., Perrine, S. P., Williams, R. M. & Faller, D. V. Histone deacetylase inhibitors are potent inducers of gene expression in latent EBV and sensitize lymphoma cells to nucleoside antiviral agents. *Blood* **119**, 1008-1017, doi:10.1182/blood-2011-06-362434 (2012).

104 Klebanoff, C. A., Gattinoni, L. & Restifo, N. P. Sorting through subsets: which T-cell populations mediate highly effective adoptive immunotherapy? *J Immunother* **35**, 651-660, doi:10.1097/CJI.0b013e31827806e6 (2012).

105 Gattinoni, L. *et al.* A human memory T cell subset with stem cell-like properties. *Nat Med* **17**, 1290-1297, doi:10.1038/nm.2446 (2011).

106 Terakura, S. *et al.* Generation of CD19-chimeric antigen receptor modified CD8+ T cells derived from virus-specific central memory T cells. *Blood* **119**, 72-82, doi:10.1182/blood-2011-07-366419 (2012).

Acknowledgements

First and foremost, I would like to express my sincere gratitude to my thesis supervisors, PD Dr. Nina Khanna and Prof. Regine Landmann, for giving me the opportunity to work at the Infection Biology lab and for their invaluable guidance on my scientific pathway, which helped me to develop not only as a researcher but also as a person. I would also like to thank Prof. Manuel Battegay for the scientific discussions.

I am very grateful to the lab members and external researchers, who helped me in preparations of my studies and with whom I shared a lot of great moments.

Many thanks to my amazing friends (especially PK) and family for their inestimable support.

Thank you, AD, for the life-long Przygoda.

Curriculum Vitae

Name: Justyna Nowakowska
Date of birth: 02.02.1986
Place of birth: Babice, Poland
Nationality: Polish
e-mail: justyna.nowakowska@unibas.ch

Education

2010-2014 PhD in Microbiology
Thesis supervisor: PD Dr. Nina Khanna and Prof. Regine Landmann
Infection Biology, University and University Hospital of Basel, Basel, Switzerland

2009-2010 MSc fellowship
Section of Medical Protein Chemistry, Department of Laboratory Medicine, Skåne University Hospital, Lund University, Malmö, Sweden

2005-2010 MSc in Biotechnology (specialization: medical biotechnology)
Thesis supervisor: Dr. Krzysztof Guzik
Thesis co-supervisor: Prof. Anna Blom
Thesis title: *Investigation into Role of Novel Complement Inhibitors, Thioredoxin and Thioredoxin80*
Department of Immunology, Faculty of Biochemistry, Biophysics and Biotechnology, Jagiellonian University, Cracow, Poland

Conferences and awards

2013 4th Thesinge Biofilm Meeting - Back to biofilms, Thesinge, Netherlands
Assessing the activity of antimicrobial coatings (oral presentation)

2012 European Congress of Clinical Microbiology and Infectious Diseases, London, United Kingdom

Serrulatane EN4, a new antimicrobial compound exerts potent activity against adherent biofilm-forming bacteria in vitro (poster)

2012 Club de Pathologie Infectieuse, Bern, Switzerland
Serrulatane EN4, a New Antimicrobial Compound?
(oral presentation)

2011 eCells & Materials Conference, Davos, Switzerland
Serrulatane EN4, a New Antimicrobial Compound?
(oral presentation)
Student RMS Foundation Award

Publications and protocols

- Nowakowska J., Stuehler C., Egli A., Battegay M., Rauser G., Bantug G.R *et al*. T cells specific for different latent and lytic viral proteins efficiently control Epstein-Barr virus-transformed B cells - *manuscript accepted in Cytotherapy*
- Nowakowska J., Landmann R., Khanna N. Foreign body infection models to study host-pathogen response and antimicrobial tolerance of bacterial biofilm (Review) - *manuscript submitted* (2014)
- Nowakowska J., Landmann R., Khanna N. Macromolecular Biosynthesis Assay for Evaluation of Influence of an Antimicrobial on the Synthesis of Macromolecules. *Bio-Protocol online* (2013)
- Nowakowska J., Griesser H. J., Textor M., Landmann R., Khanna N. Antimicrobial properties of 8-hydroxyserrulat-14-en-19-oic acid for treatment of implant-associated infections. *Antimicrob Agents Chemother.* 57(1), 333-42 (2013)
- King B., Nowakowska J., Karsten C. M., Köhl J., Renström E., Blom A. M. Truncated and full-length thioredoxin-1 have opposing activating and inhibitory properties for human complement with relevance to endothelial surfaces. *J Immunol.* 188(8), 4103-12 (2012)